Preparation of Atlas of Greenhouse Gases (Carbon Dioxide, Methane, and Nitrous Oxide) Over Pakistan: Emissions, Sources, and Sinks

Hiba Ahmed

Reg # 00000205115

A thesis submitted in partial fulfillment of requirements for the degree of

Master of Sciences

In

Environmental Sciences

INSTITUTE OF ENVIRONMENTAL SCIENCES AND ENGINEERING (IESE)

SCHOOL OF CIVIL AND ENVIRONMENTAL ENGINEERING (SCEE)

NATIONAL UNIVERSITY OF SCIENCE AND TECHNOLOGY (NUST) ISLAMABAD

(2021)

THESIS ACCEPTANCE CERTIFICATE

It is certified that the final copy of MS thesis written by Ms. Hiba Ahmed, Registration No. 00000205115 of IESE (SCEE) has been vetted by undersigned, found complete in all aspects as per NUST Statues/Regulations, is free of plagiarism, errors, and mistakes and is accepted as partial fulfilment for award of MS degree. It is further certified that necessary amendments as pointed out by GEC members have also been incorporated in the said thesis.

Signature with stamp: _____

Name of Supervisor: Dr. M. Fahim Khokhar (HoD, Professor, IESE, SCEE, NUST)

Date: _____

Signature of HoD with stamp: _____

Date: _____

Countersign by:

Signature (Dean/ Principal): _____

Date: _____

CERTIFICATE

It is certified that the contents and form of the thesis entitled

"Preparation of Atlas of Greenhouse Gases (Carbon Dioxide, Methane, and Nitrous Oxide) Over Pakistan: Emissions, Sources, and Sinks"

Submitted by:

Hiba Ahmed

have been found satisfactory for the requirement of the degree.

Supervisor: _____

Dr. Muhammad Fahim Khokhar

Professor

IESE, SCEE, NUST

Member: _____

Dr. Zeeshan Ali Khan

Assistant Professor

IESE, SCEE, NUST

Member: _____

Dr. Sofia Baig

Assistant Professor

IESE, SCEE, NUST

I dedicate this thesis to my parents.

Acknowledgements

I would like to acknowledge the support and constructive criticism of my supervisor Dr. M. Fahim Khokar, his kind guidance enabled me to complete this research study successfully. I would also like to show my gratitude to GEC members, Dr. Zeeshan Ali Khan and Dr. Sofia Baig for their assistance. I am forever indebted to my family for their unwavering support in all the endeavors I take up. Last but not the least my friends, and CCARGO colleagues.

Table of Contents

Abstract _____ *12*

CHAPTER 1 : INTRODUCTION _____ **13**

1.1. GLOBAL WARMING _____ 13
1.2. GREENHOUSE EFFECT & GREENHOUSE GASES _____ 13
1.3. CARBON DIOXIDE _____ 15
1.4. METHANE _____ 17
1.5. NITROUS OXIDE _____ 19
1.6. SITUATION IN PAKISTAN _____ 21
1.7. OBJECTIVES OF THE STUDY _____ 24

CHAPTER 2 : LITERATURE REVIEW _____ **25**

CHAPTER 3 : METHODOLOGY _____ **28**

3.1. STUDY AREA _____ 28
3.2. GREENHOUSE GASES (GHGS) _____ 28
3.3. GENERAL METHODOLOGY _____ 29
3.3.1. Satellite Data Retrieval _____ *29*
3.3.2. Inventory Data Retrieval _____ *30*
3.3.3. Software and Models _____ *31*
3.3.4. Meteorological Data _____ *31*
3.3.5. Probable Sources of Greenhouse Gases _____ *32*
3.3.6. NDVI _____ *32*
3.3.7. Other Variables _____ *32*
3.4. CARBON DIOXIDE _____ 32
3.5. METHANE _____ 34
3.6. NITROUS OXIDE _____ 34

CHAPTER 4 : RESULTS AND DISCUSSION _____ **35**

4.1. CARBON DIOXIDE _____ 35
4.1.1. Atmospheric Profile over Pakistan – AIRS _____ *35*
4.1.1.1. Yearly maps _____ 35
4.1.1.2. Annual concentration trend _____ 37
4.1.1.3. Monthly concentration trend _____ 38
4.1.1.4. Maxima and Minima _____ 39
4.1.1.5. Seasonal Cycles _____ 41
4.1.1.6. SCIAMACHY data – Comparison with AIRS _____ 46

4.1.2. ARIMA Model Forecasting *47*
4.1.3. Inventories: Sectoral emissions' data *47*
4.1.3.1. Selection of the inventory 47
4.1.3.2. CEDS 05x05 48
4.1.4. Sectoral data of development/industrial activities in Pakistan (Sources) – Regression Analysis with Inventory data *49*
4.1.5. Statistical analysis of Satellite-based emissions with various factors *50*
4.1.6. NDVI *52*
4.2. METHANE 53
4.2.1. Atmospheric Profile over Pakistan – AIRS *53*
4.2.1.1. Yearly maps 54
4.2.1.2. Rice Season Maps 56
4.2.1.3. Annual Concentration Trend 58
4.2.1.4. Monthly Concentration Trend 59
4.2.1.5. Increase in Maxima and Minima 61
4.2.1.6. Seasonal Cycles 62
4.2.1.7. Rice Season Trends 64
4.2.2. ARIMA Model Forecasting *65*
4.2.3. Inventories: Sectoral emissions' data *66*
4.2.3.1. Selection of the Inventory 66
4.2.3.2. Edgar v 4.3.2 (01x01) 67
4.2.4. Sectoral data of development/industrial activities in Pakistan – Regression Analysis with Inventory data 68
4.2.5. Statistical analysis of Satellite-based emissions with various factors *69*
4.2.6. NDVI as a measure of sink *70*
4.2.7. Temperature with Seasonal Cycle of Methane *71*
4.3. NITROUS OXIDE 72
4.3.1. Inventories: Sectoral emissions' data *72*
4.3.1.1. Selection of Inventory 72
CHAPTER 5 : CONCLUSION & RECOMMENDATIONS 75
REFERENCES 77

List of Abbreviations

ESA	European Space Agency
GCISC	Global Change Impact Studies Centre
GDP	Gross Domestic Product
GHGs	Greenhouse Gases
GOSAT	Greenhouse gases Observing Satellite
GWP	Global Warming Potential
HDF	Hierarchical Data Format
INDCs	Intended Nationally Determined Contributions
IPCC	Inter-government Panel on Climate Change
MoCC	Ministry of Climate Change
NDVI	Normalized Difference Vegetation Index
PBS	Pakistan Bureau of Statistics
PMD	Pakistan Meteorological Department
ppb	Parts per billion
ppm	Parts per million
Tg	Terra-gram
UNEP	United Nations Environment Programme
WHO	World Health Organization

List of Figures

Figure 1.1: Carbon Cycle (Britannica Encyclopedia 2012) 16
Figure 1.2: Methane Cycle (Britannica Encyclopedia 2012) 19
Figure 1.3: Nitrogen Cycle 21
Figure 1.4: GHG Emission Category in Pakistan (Mir et al., 2017) 23
Figure 3.1: General Methodology 29
Figure 4.1: Annual Maps of CO_2 (ppm) over Pakistan – 2002 - 2016 36
Figure 4.2: Annual CO_2 Trend over Pakistan – 2002 - 2016 37
Figure 4.3: Difference between Maximum and Minimum CO_2 37
Figure 4.4: CO_2 Monthly Trend (2002-2016) 39
Figure 4.5: Combined Increase in Minima and Maxima 40
Figure 4.6: Maximum and Minimum Monthly CO_2 (2002-2016) 40
Figure 4.7: Monthly CO_2 over Pakistan (2002 – 2016) 41
Figure 4.8: Winter Increase (WI) 42
Figure 4.9: Summer Decrease (SD) 42
Figure 4.10: Net Annual and Cumulative Effect of WI and SD 43
Figure 4.11: Seasonal Cycle of CO_2 within a year 44
Figure 4.12: Seasonal Trend of CO_2 (2002 - 2016) 45
Figure 4.13: Season wise Annual Trends of CO_2 (2002-2016) 46
Figure 4.14: Comparison between AIRS and SCIAMACHY data 46
Figure 4.15: ARIMA Model Forecast - 2030 47
Figure 4.16: Comparison of Inventories with GCISC Inventory 48
Figure 4.17: CO_2 Emissions - CEDS 05x05 48
Figure 4.18: CEDS and AIRS Data Comparison (2002 - 2014) 49
Figure 4.21: Annual Maps of CH_4 (ppbv) over Pakistan (2009 – 2018) 55
Figure 4.22: Methane Mean Concentrations (ppbv) in Rice Season over Pakistan (2009 - 2020) 57
Figure 4.23: Annual CH_4 concentration trend over Pakistan (2009 - 2020) 58

Figure 4.24: Difference between Maximum and Minimum Concentration of CH_4 (2009 - 2020) 58
Figure 4.25: CH_4 Monthly Trend over Pakistan (Jun 2009 - April 2021) 59
Figure 4.26: Difference between Monthly CH_4 concentrations 60
Figure 4.27: Combined Maxima and Minima of CH_4 concentrations (2009 - 2018) 61
Figure 4.28: Seasonal Cycle of CH_4 within a year 62
Figure 4.29: Seasonal Variation of CH_4 Concentration over Pakistan (2009-2020) 62
Figure 4.30: Seasonal Trend over the Years 2009-2020 63
Figure 4.31: Rice Season Trend (July-Nov) 2009-2020 64
Figure 4.32: Comparison between Yearly Means and Rice Season (2009 - 2020) 64
Figure 4.33: SCIAMACHY and GOSAT 's methane concentration (2003 - 2020) 65
Figure 4.34: ARIMDA Model Forecasting for Methane Conc. (25 years' forecasting) – (4,2,2) 66
Figure 4.35: Inventories' data Comparison 67
Figure 4.36: EDGAR v4.3.2 - Methane Emissions 67
Figure 4.37: Combined satellite and inventory data (Methane) 68
Figure 4.38: Methane Seasonal Cycle vs NDVI seasonal cycle 70
Figure 4.39: Inventories' data Comparison 72
Figure 4.40: Nitrous Oxide Emissions - Edgar v4.3.2 73

List of Tables

Table 1: Lifetime and GWPs of GHGs 28
Table 2: R-values – CEDS Emissions Sectors and Sectoral Activity Data (2002 – 2014) 50
Table 3: R-values of Emissions and Concentrations with Multiple Factors (Yearly means) 51
Table 4: R-values – PBS data and Edgar Emission Sectors 68
Table 5:R-values of Satellite and Inventory data with multiple factors 69
Table 6: R-values – PBS data and Edgar Emission Sectors 73
Table 7: R-values of Inventory data with multiple factors 74

Abstract

The increasing concentrations of greenhouse gases (GHGs) in earth's atmosphere are of a great concern due to climate change and subsequent consequences including global warming. The anthropogenic activities have increased the atmospheric concentrations of GHGs abnormally. Pakistan a developing country, is among the most affected countries by the adverse impacts of climate change. To study the GHGs' patterns with their sources and sinks is a mandatory step towards climate change adaptation and mitigation. This study emphasis on the monitoring and analysis of three GHGs: Carbon dioxide (CO_2), Methane (CH_4), and Nitrous Oxide (N_2O) in Pakistan. The satellite driven data and emission inventories' data are used to observe atmospheric concentrations and potential emissions' sources, respectively. Forest cover data and NDVIs are used as proxy for sinks. ARIMA model is used to forecast atmospheric concentrations of GHGs till 2050. The results showed increasing trend in both GHGs' emissions, and atmospheric concentrations in Pakistan. The forecast model predicts 38% (84 years forecast) and 33% (82 years forecast) increase of carbon dioxide and methane emissions, respectively. Carbon dioxide emissions mainly come from energy, industry, transport, and residential sectors. Loss of forests, the sink of carbon dioxide, have also contributed to its increased concentrations. Agriculture, waste, fuel, and residential sectors are primarily responsible for methane emissions. Nitrous oxide predominantly comes from agriculture, industry, residence, and waste sector. Expanding population and development activities are the reason behind emissions from these sectors. The results of NDVI as a measure of sink do not provide significant results. Overall, the emissions, and atmospheric concentrations of GHGs have been increased significantly, and are predicted to rise further if no preventive measures are taken.

Chapter 1 : Introduction

1.1. Global warming

The phenomenon of global warming has become more evident and observable during the last decade and its impacts on earth, and life are no more avoidable. It is one of the worst elements of climate change that affects the entire human population and the vulnerable nations experience severest consequences. Global warming is mainly driven by the altered atmospheric composition due to the anthropogenic activities that emit large amounts of unwanted gases including greenhouse gases (GHGs) in the atmosphere and cause destruction to the natural sinks of many gases. The greenhouse gases trap the heat around the earth and consequently increase the earth's average temperature.("IPCC, 2014," n.d.) Exploring the behavior and concentration patterns of the greenhouse gases in the atmosphere and investigating their natural and artificial sources and the sinks is important to find out the mitigation options by reducing sources and emissions, and by growing sinks and therefore it becomes the first step towards combating climate change.

1.2. Greenhouse effect & greenhouse gases

Earth's atmosphere starting from ground level to the space gradually becomes less concentrated and is divided into different layers. The two adjacent layers from ground are the troposphere and the stratosphere. The troposphere is the layer where mostly all weathers occur. The atmosphere contains different gases like Nitrogen (~78%), Oxygen (~21%) , Argon (~1%) including carbon dioxide, methane, ozone and nitrous oxide as trace gases with less than 1% concentration by volume. Water vapor, the main greenhouse gas, is also a major constituent of atmosphere at about up to 3% of volume depending on the location. (Brimblecombe, 1996) The small portion of the greenhouse gases is one of the reasons of life present on earth. These gases have the ability to trap infrared radiations that cause the "greenhouse effect". The back scattered longwave radiations from earth surface go up in the space and some of these radiations is trapped by the gases we call greenhouse gases. The undisturbed greenhouse effect caused by this small portion of gases remains our earth warm and livable. But the problem arises, when the natural balance of the greenhouse gases in the atmosphere is disrupted, and the unwanted greenhouse effect due to the excessive concentrations of these gases causes the increase in earth's average temperature by trapping more infrared radiations (Kirk-Davidoff, 2018) This increased greenhouse effect has already caused earth's average temperature to rise about 1.1 degree Celsius since 1880. ("NASA GISS, 2019)

The disrupted greenhouse effect that has resulted in the global warming is the major cause of changing climate. The increased concentrations of greenhouse gases do not only affect the earth's average temperature, but also have caused glacier melting and sea level rise, change in the precipitation patterns and disturbed water budget all around the globe, extreme events, loss of biodiversity and decreased human mortality. ("AR5 IPCC.) The impact of higher levels of greenhouse gases is not small, but very huge, widespread, and long-term. The natural systems are totally being interrupted by the impact of these gases; and therefore, the life on earth is at a major risk. (Al-Ghussain, 2019)

The greenhouse gases were in balance in the atmosphere before human-induced emissions of these gases started entering the atmosphere. The anthropogenic emissions are the sole reason of the higher concentrations of these GHGs in our atmosphere. The emissions got triggered after industrial revolution that took place in 1960s. Though, the emissions were not zero in the pre-industrial era, but after 1960s the emissions of greenhouse gases became exponential and global warming and climate change became more prominent and observable with the passage of time.

The greenhouse gases defined by The Kyoto Protocol are the carbon dioxide (CO_2), methane (CH_4), nitrous oxide (N_2O), chlorofluorocarbons (CFCs), hydrofluorocarbons (HFCs), perfluorocarbons (PFCs) and sulphur hexafluoride (SF_6). These gases behave differently in the atmosphere and possess different capacities to trap the longwave radiation. The role of each gas in the atmosphere, and impact on climate is different depending upon the physical and chemical properties of these gases. The ability of causing greenhouse effect is described by the Global Warming Potential (GWP). The GWP is the ability of a gas to trap heat and cause radiative forcing over a selected time horizon compared to that of the reference gas i.e. carbon dioxide. The global warming potential also depends on the life cycle of the gas in the atmosphere. (IPCC, 2014) The GWP of the carbon dioxide is 1 and compared to that the GWP of methane over 20-year time horizon is 84, and nitrous oxides is 264. The GWP helps us understand that how a small amount of a gas can has widespread impacts if added into the atmosphere. The GWP of different gases is given in table 1. Carbon dioxide, methane and nitrous oxide are the main greenhouse gases in the atmosphere since these three gases are directly attributed to the human activities.

1.3. Carbon Dioxide

Carbon dioxide is a colorless and odorless gas and is about 0.04 % by volume in our atmosphere. Its GWP over time horizon 20 and 100 is one as it is the reference gas. It is highly persistent gas as its lifetime is about 100 years. There exists a natural carbon cycle where carbon circulates among soil, ocean, atmosphere, animals and plants that act as either a source, sink or both. This natural cycle balances the global carbon budget. The human activities influence this natural cycle by adding sources i.e. emitters and reducing or removing the sinks or their ability to capture carbon.

1.3.1. Sources

The main anthropogenic source of carbon dioxide is the fossil fuel burning in different industrial and development activities. The energy sector, transportation, and industries utilize fossil fuels and their combustion releases high amounts of carbon dioxide that is added into the atmosphere. Besides these emissions, the human activities also influence the natural sinks that capture and remove carbon from the atmosphere. The deforestation reduces the forests that take up the excessive carbon dioxide and cleans the air. The higher atmospheric concentrations of carbon dioxide also influence the ability of oceans to absorb CO_2 and their quality by increasing acidification that also highly affects the marine population. Similarly, the soil capture of carbon dioxide is also reduced due to the expanding human activities. (Al-Ghussain, 2019; Field and Raupach, 2012; Keenan and Williams, 2018)

1.3.2. Sinks

The removal of carbon dioxide from the atmosphere by any procedure, entity or a region, either natural or manmade, is termed as sink of carbon dioxide. Carbon sequestrations is the process to remove carbon from the atmosphere. The natural sinks of carbon dioxide are plants, ocean, and soil. Plants and algae (phytoplankton) found in ocean take up carbon dioxide for the process of photosynthesis. Photosynthesis is the process where carbon dioxide is utilized to form food and energy.

$$CO_2 + H_2O + \text{energy} \rightarrow C_6H_{12}O_6 + O_2$$

Carbon dioxide is also taken up by the oceans. It is dissolved in the surface of ocean water to form carbonic acid. Oceans cover almost 71% of earth's surface, therefore, they are a great sink of carbon. The phenomenon of climate change is also expressed as ocean acidification. Where, ocean water is becoming more acid and pH is decreasing. The acidification also affects ocean ecosystem adversely.

$$CO_2 + H_2O \rightarrow H_2CO_3$$

Another sink of carbon dioxide is rainwater deposition. Carbon dioxide reacts with rainwater to form carbonic acid that reacts with rocks and bicarbonate ions (HCO_{3^-}) are formed. These bicarbonate ions reach oceans through groundwater and streams and are used to produce calcium carbonate by marine organisms. Carbon present in organic matter is deposited in soils to eventually form fossil fuels.

There are some artificial sinks of carbon dioxide as well. Some procedures focus on enhancing the capacity or efficiency of natural sinks. Some of them include afforestation, ocean fertilization, carbon farming etc. The other procedures directly capture and store carbon in earth's surface that include geological sequestration, ocean sequestration etc.

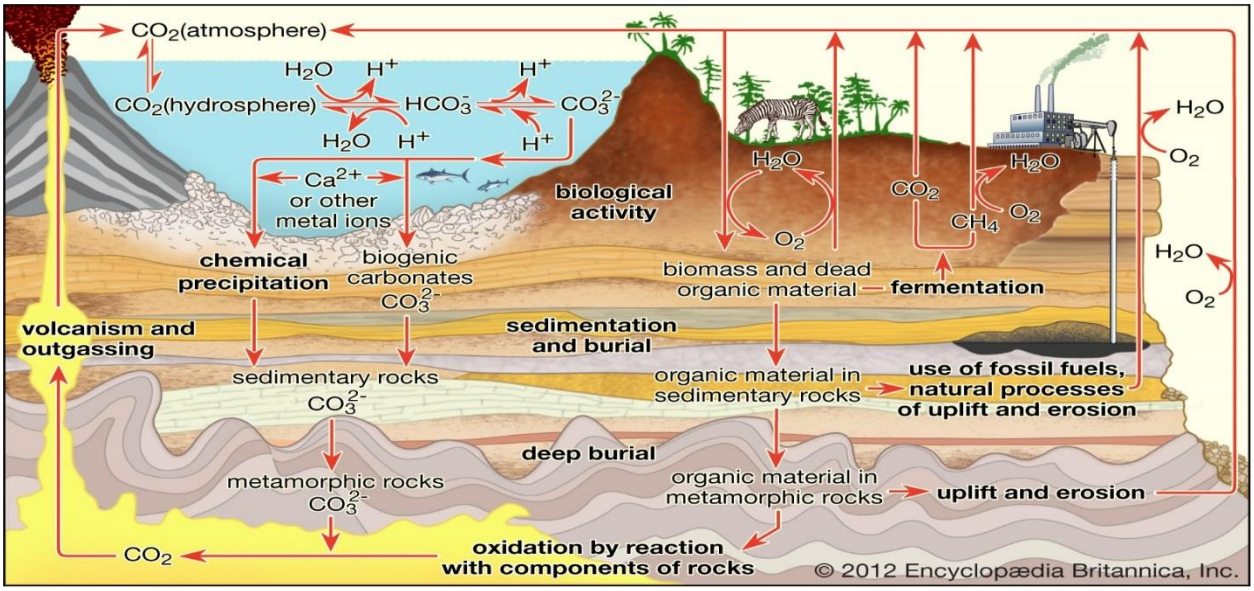

Figure 1.1: Carbon Cycle (Britannica Encyclopedia 2012)

1.4. Methane

Methane is a colorless, odorless and flammable gas and is about ~0.00017 % by volume in our atmosphere. Its GWP over time horizon 20 is 84, and 28 for 100-year time horizon. It is because it is not as persistent as carbon dioxide and its lifetime is about 10 years. Methane natural cycle, like carbon, without human intervention is balanced. Wetlands, bacteria on organic matter decay, volcanoes, methane hydrates of the oceans etc are some if its natural sources. Whereas the natural sinks include atmosphere where OH^- radical reacts with it and forms carbon dioxide and water vapour, and soils. The anthropogenic activities are adding more methane in the atmosphere than the capacity of sinks to remove. These anthropogenic sources include cultivation of rice, farming of livestock, fossil fuel combustion like coal and natural gas, biomass burning, and organic matter decay in landfills. (Al-Ghussain, 2019; Heilig, 1994; Reay et al., 2010) The concentration of methane in pre-industrial era were about ~700 ppb, and it has reached to ~1870 ppb in 2019.

1.4.1. Sources

Methane's emissions are distributed in natural and anthropogenic sources almost equally. (IPCC, 2001) Methanogenesis, the microbial activity, is the major natural process that emit emissions in waterlogged soils or wetlands. The emission depends on various factor like temperature, water level, soil type etc. Organic carbon in the waterlogged areas becomes anaerobic (the absence of oxygen) and therefore microbial mineralization occur. During the summer season, when water level decreases due to drying up, the methane emissions also reduces as oxygen level increases in soil. Human activities also affect wetland emissions by water drainage and land use changes. The wetland emissions can be controlled if water level is managed by proper drainage system.

Termites also produce methane as a result of their digestion process depending upon their species. Though each termite produces a minute amount of CH_4, but the effect of all termites all around the world can be substantial.

Oceans are also responsible for methane natural emissions. In oceans the methane is also produced by methanogenic bacteria. The oceanic emissions are increased when anthropogenic run-off from rivers, drainage, sewage etc enters the ocean and increases its nutrients level that produce ideal conditions for methanogenesis. Clathrates also known as methane hydrates are deposits in deep

ocean sediments and in polar areas that releases methane when conditions of temperature and pressure are changed. Global warming leading to increased sea temperature can cause exponential emission of methane from these hydrates eventually causing greater warming.

Landfills and rice cultivation are among anthropogenic sources of methane emissions. Both provide ideal conditions for methanogenesis i.e. lots of nutrient level and absence of oxygen. In rice cultivation, the rice paddies are waterlogged for about four months.

Livestock methane emission is also a kind of anthropogenic source of methane. The guts of ruminant livestock produce methane as a result of methanogenic bacteria. The amount of methane produced by livestock strongly depend on the composition of their feed. Agricultural and municipal waste due to high organic carbon content produce large amounts of methane as well when they meet anaerobic conditions.

Biomass burning is also responsible for emitting large amounts of methane.

1.4.2. Sinks

The most important methane sink is the removal of CH_4 in the troposphere by hydroxyl (OH^-) radicals that accounts for 88% of the total sinks. The other two are the stratospheric destruction and soil oxidation by bacteria. The soils except methane producing like rice paddies and wetlands act as sink when soil aerobic bacteria use methane as a source of carbon by oxidation. The removal of methane by OH radical is also beneficial in other way as the reaction leads to the ozone formation as well.

$$CH_4 + OH \rightarrow CH_3 + H_2O$$

The reaction initially produces methyl and water. A chain of reactions occur afterwards that produce water vapor and carbon dioxide. The other methane sinks can be the chemical oxidation by atmospheric chlorine and chlorine of sea water surfaces. Although the anthropogenic activities have a relatively less impact on methane sink processes but the emission of other atmospheric pollutants like NO_x can affect the OH level in the atmosphere, thus decreasing the capacity of atmosphere to remove methane.

The artificial methane sinks include the exploitation of the process of biological oxidation of methane in the hotspot areas like landfills. Methanotrophs (aerobic bacteria that use methane by oxidation) can limit the release of methane in the atmosphere. The common example is the covering of landfill by the soil cover which contains methanotrophs that oxidize emitted methane from the landfill.

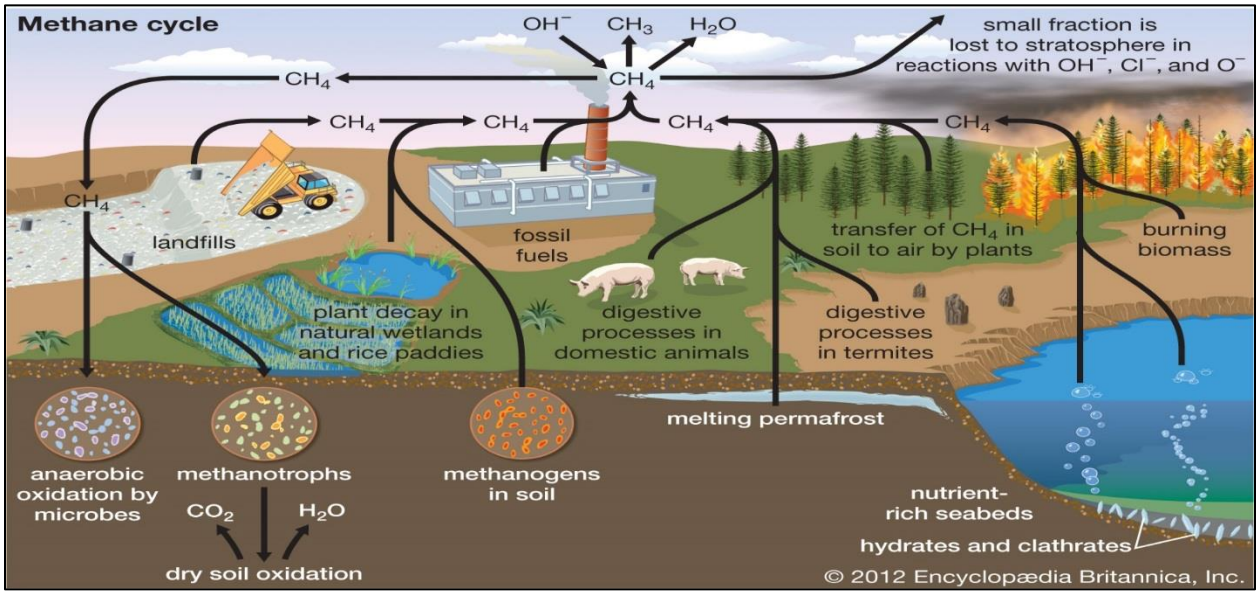

Figure 1.2: Methane Cycle (Britannica Encyclopedia 2012)

1.5. Nitrous Oxide

Nitrous oxide is a colorless, non-flammable gas with a light odor. It is ~ 0.000031 % by volume in the atmosphere. It is a very important component of the earth's systems as it plays a major role in natural nitrogen cycle, stratosphere's chemistry and earth's radiation balance. It acts as a source for stratospheric nitric oxide to decompose ozone layer. Its GWP is a lot more than that of CO_2 and CH_4 that makes it very significant in global warming. Its GWP for 20 years is 264 relative to the CO_2 and for 100 years is 265.("AR5 IPCC) It is because its lifetime is 121, more persistent than carbon dioxide making it more harmful even if its emissions are less. The natural sources of nitrous oxide are oceans, soils, forests and grasslands. Its sinks include soils and stratospheric photolysis. Other than these sources, the anthropogenic sources are the industrial like nitric acid production, fertilizers' production, soil cultivation, biomass burning, fossil fuel combustion, and

animal manure decay. (Al-Ghussain, 2019; Smith, 2010) It's pre-industrial concentrations were ~270 ppb ("TAR Climate Change 2001,IPCC) that has reached to ~330.1 ppb in 2018. (WDCGG)

1.5.1. Sources

The oceans are a source of nitrous oxide emissions. The microbial activity of oceanic surface adds nitrous oxide to the atmosphere. The particles in ocean surface make anaerobic conditions for denitrification. In this process, the microbes use nitrate instead of oxygen for energy and produce nitrogen gas. The chain of reactions includes production of nitrous oxide in the middle of the reactions that is released to the atmosphere when go unused. It is also produced as a by-product of nitrification in the ocean. The sewage, agricultural runoff and other nitrogen containing waters enter the rivers, coastal waters making them ideal for denitrification, and therefore produce nitrous oxide. Anthropogenic activities also lead to the increased amount of reactive nitrogen to the surface waters that also results in N_2O emissions.

In atmosphere, oxidation of ammonia (NH_3) causes the emission of N_2O. The livestock farming releases NH_3 in the atmosphere. Use of agricultural fertilizers and other chemicals are also an important source of atmospheric ammonia. Soils also release nitrous oxide in the atmosphere by microbial activities. Using animal waste as fertilizer can also cause nitrous oxide emissions if poorly managed. An indirect emission of nitrous oxide is by the runoff from agricultural areas and in the form of leaching. The large quantities of nitrogen go into the waterways like rivers, streams, drainage lines etc. that produces nitrous oxide when the water is exposed to the air. Another indirect emitter is the volatilization of NH_3 and its deposition on other soils. Food waste and sewage, that are nitrogen-rich, have caused increased emissions of indirect N_2O.

Another source of nitrogen in the atmosphere is the biomass burning, mainly as a result of anthropogenic activities. Incomplete combustion produces large amounts of nitrous oxide. This burning can be the forests or grass land burning, wood burning for domestic or commercial use, and the crop residue burning.

In industries, production of nitric acid is the main cause if industrial leakages of nitrous oxide. Nitric acid, an important factor in nitrogen fertilizers, is produces by the oxidation of ammonia, during which the emissions occur. Another industrial emission includes nylon manufacturing

process that use nitrogen-based acid. Nitrous oxide is also emitted into the atmosphere through transport sector. The use of fossil fuel and catalytic converter used in cars are the responsible factors for its emissions.

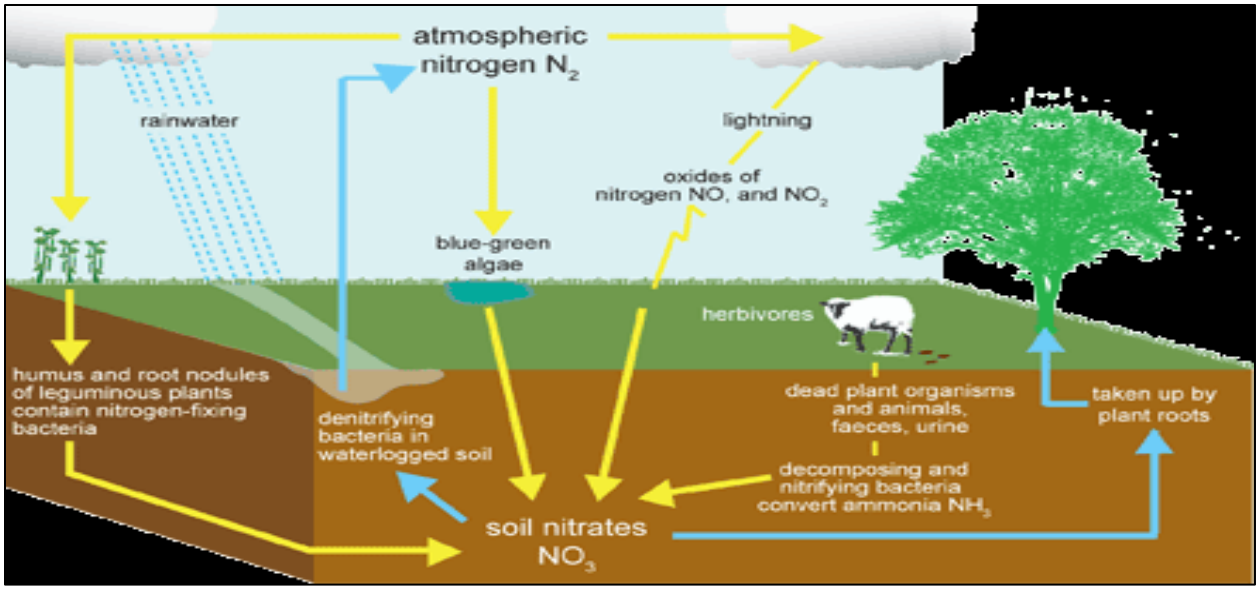

Figure 1.3: Nitrogen Cycle

1.5.2. Sinks

Nitrous oxide is removed from the atmosphere in the stratosphere layer that lies above troposphere. It is removed by the direct photolysis by sunlight. A small amount is also removed by the chemical reaction with the excited oxygen atom O(1D).

Soils also act as an important sink of atmospheric nitrous oxide. Denitrification by bacteria in soils produce nitrogen gas from nitrous oxide. But since the soils are also an emitter, so the net flux is what that matters. There are many factors that affect soil uptake of nitrous oxide including nitrogen content, water content, pH and temperature. Similarly, the surface water bodies like oceans also uptake N_2O besides being the emitter.

1.6. Situation in Pakistan

Pakistan is located in South Asia, and is the fifth most populous country in the world with ~213 million population. (PBS, 2019) It is the world's 33rd largest country by area with a diverse geography and climate. The diversity includes coastal areas, plains, desserts, glacial mountains,

plateaus, forests and hills. The climate, therefore, also varies with tropical, temperate, arid states. The major seasons are winter, spring, monsoon and post-monsoon. A variety of flora and fauna exists in Pakistan due this diversity. (Chaudhry, 2017; Heiden, 2011) Almost 5% of the land of Pakistan is under forest cover.

The average mean temperature of Pakistan has faced ~0.5 degree rise during the last 5 decades. The heatwaves incidents have also increased is previous years. Sea level rise and change in the precipitation patterns are also the few climate change consequences Pakistan has seen. (Chaudhry, 2017) Other extreme events like glacial outburst, droughts, floods etc have also been observed in Pakistan, making Pakistan the 5th most vulnerable country according to German Watch's long-term Climate Risk Index – 2020. The greenhouse gases' emissions distribution in Pakistan is as follows; 54% Carbon dioxide, 36% methane, 9% nitrous oxide and 1% other gases. Pakistan contributes to 0.8% of total global greenhouse gas budget as calculated with per capita income. Energy consumption is the major cause of GHG emissions. (Hussain et al., 2019)

Pakistan made its first ever climate policy in February 2013 that focuses on reducing GHG emissions and adopting low-carbon technologies. (Hussain et al., 2019) Pakistan also submitted INDCs after COP21 in 2015 and ratified The Paris Agreement on November 2016. According to the INDC, Pakistan has to reduce 20% of the emissions projected to 2030. (Chaudhry, 2017) The National Climate Change Policy was then passed by the ministry of climate change (MoCC) in 2012 as a legal framework for climate change issues. (Mir et al., 2017)

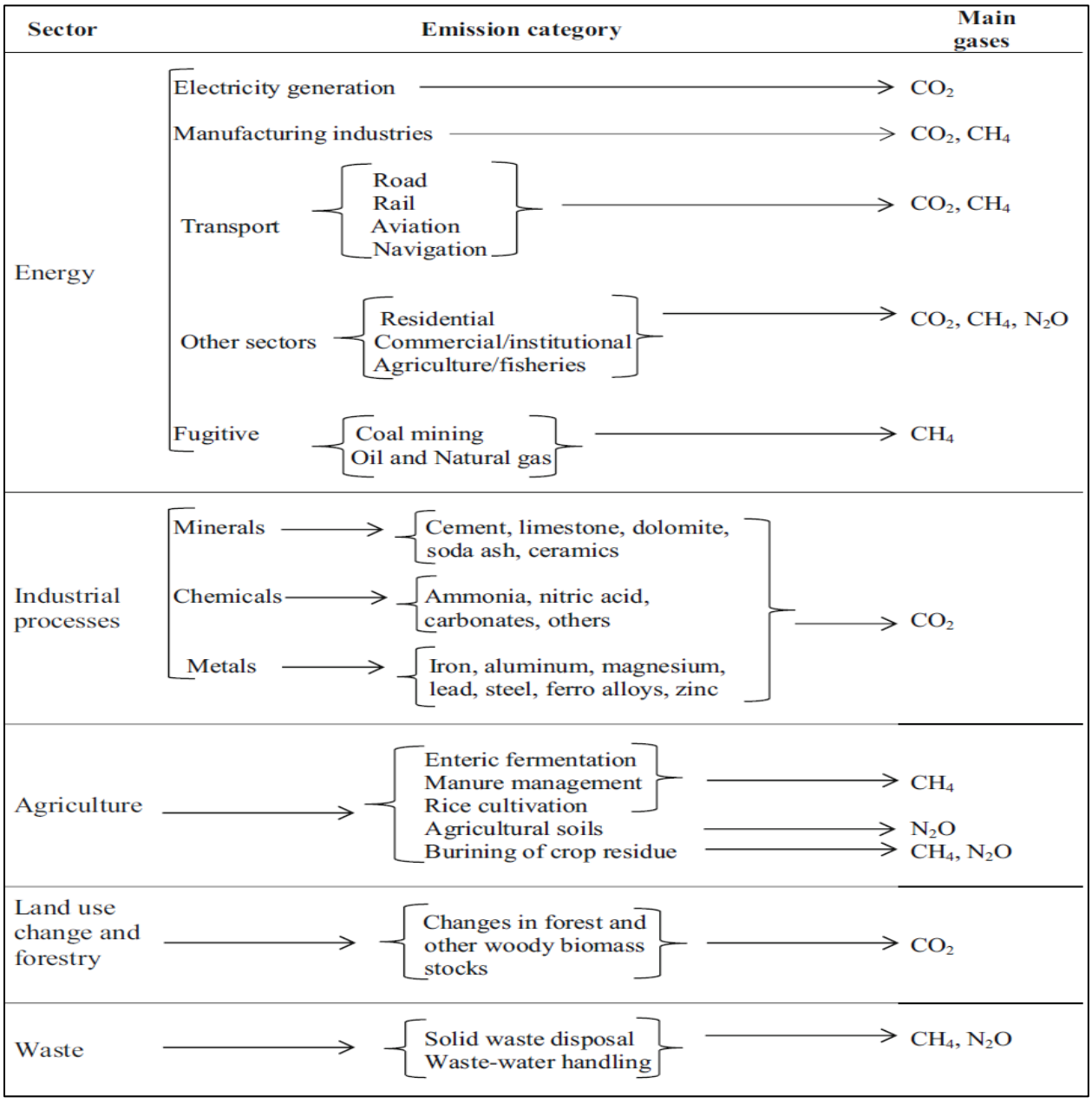

Figure 1.4: GHG Emission Category in Pakistan (Mir et al., 2017)

Pakistan is placed at 135th position on the basis of per capita GHG emissions, its per capita GHG emission is 2.06 Gt. In 2012, estimated total GHGs emission is 369 Gt-eq. Major sources for carbon dioxide include energy and biomass emission, whereas enteric fermentation, and oil and natural gas emissions leads the methane emissions. In case of nitrous oxide most of the emissions in the country are caused due to Transport and when agriculture residue is burnt. (INDC PAKISTAN)

Today's world is facing serious environmental issue: one of the most critical environmental issues is deteriorating air quality. Especially, air quality in various urban cities is alarmingly dangerous. Such circumstances demand continuous monitoring of air quality. Hence, continuous efforts are being made globally to monitor and improve air quality. W.H.O. and United Nations Environmental Programme (UNEP) worked together to monitor air quality. They initiated a progamme Global Environmental Monitoring System/Air (GEMS/Air) in 1970. As the severity of GHG emissions associated with global warming and its impacts has been increased, the worldwide efforts to measure, monitor and study these GHGs have also increased. There are several international organizations that are studying GHGs, their emissions and providing guidance, tools, and education to measure and manage these gases, e.g. GHG Protocol. The Paris Agreement is also a major step forward to cope with GHG induced climate change.

1.7. Objectives of the study

The objectives of this study are:

1. To observe the current and historical patterns of atmospheric concentrations of greenhouse gases over Pakistan.
2. To quantify the sources and sinks of these GHGs in Pakistan and by relating the atmospheric concentrations to potential sources' and sinks' data of Pakistan.

Chapter 2 : Literature Review

Mir et al., 2017 developed an inventory for the year 2012 for Pakistan using IPCC Tier 1 methodology and discussed the sectoral emissions' results in his paper. 367 Tg CO_2eq total GHG emissions are estimated in his paper. He also compared the results with historical data describing that the emissions have been increased over the years and are subjected to rise in future given growing development in Pakistan. Study done by USAID suggests Energy and agriculture sectors are leading the Pakistan's GHG emission, contributing to 87% of the total emissions of the country. From 1990 to 2012 annual increase in GHE is 2.9%, Overall, Pakistan GHE increase during this time period (1990-2012) is 89%. (Boden et al., 2015) Biggest sources contributing in energy sectors are the electricity and transportation whereas in agriculture sector 54% of emissions are caused by enteric fermentation making it the biggest source of GHE in this sector.

A Chinese team studied spatial and temporal variations of CO_2 (using GOSAT) in China during 2009–2016, and the factors influencing those changes. Seasonal cycle was observed in China that is controlled by NDVI. Human activity and biomass burning were found to be the main sources of CO_2 emissions. (Lv et al., 2020) A recent study examined global trends and drivers of greenhouse gas emissions by sector from 1990 to 2018. It found that decarbonization in energy systems has occurred in Europe and North America due to shift to renewables. By contrast, in rapidly industrializing regions, emissions are growing in the industry, buildings and transport sectors, particularly in Eastern Asia, Southern Asia and South-East Asia. (Lamb et al., 2021)

Rajab et. al. used AIRS data to map CO_2 measurements over Indonesia. He used AIRS Aqua level 3 monthly product for hi study. He demonstrated that the CO_2 levels were highest above industrial and populated urban areas. The emissions peaked twice a year; the natural peak that was observed from February to April, the dry season (the biomass burning), and the second peak was observed in wet season that is from July to September, due to forest fires of Indonesia. The correlation was also observed between less precipitation in dry season and CO_2 emissions. (Rajab et al., 2009) Mossa et. al. monitored the Iraq's tropospheric CO_2 for year 2010-2011. His results showed the highest concertation in the month of March, and lowest in September. The hotspot regions of CO_2 were congested urban and industrial areas. (Mossa et al., 2012) A study over Pakistan used AIRS data to monitor CO_2 and CH_4 profiles over Pakistan. The results showed the substantial increased of these gases over the years. (Mahmood et al., 2016)

SCIAMCHY was used for a research to map CO_2 distribution over Peninsular, Malaysia. The results effectively detected the regions with highest and lowest concentrations. (Tan et al., 2012) Similarly, a Chinese study successfully used SCIAMCHY data to analyze spatiotemporal variations of CO_2 over China. The results were strongly correlated to anthropogenic emissions, meteorological data, and terrestrial ecosystem. (Wang et al., 2011)

A study compared the GOSAT, AIRS and SCIAMACHY data for CO_2. The results showed that SCIAMACHY data had limitations over the ocean, GOSAT lacked the good coverage for global scale but ocean detection was good for CO_2, whereas AIRS came out to be the most efficient to present CO_2 distribution and changes over the globe. (Zhang et al., 2015)

A regional case study over Pakistan and neighboring countries has employed AIRS and inventory data to monitor CO_2. Th major anthropogenic emission sources in this region were industrial activities, road transport, crop waste burning and energy production. The higher CO_2 concentrations were found over the congested urban areas. The seasonal variations showed spring maximum. (ul-Haq et al., 2017)

An Iranian research has been done using GOSAT methane retrievals for spatiotemporal analysis. Land surface temperature (LST), humidity, NDVI and other factors had been correlated with CH_4 concentrations. The correlations with LST and temperature were positive. (Mousavi and Falahatkar, 2020) Another study titled. "Comparison between global rice paddy field mapping and methane flux data from GOSAT" found a positive relation between inventory and GOSAT results. (Jonai and Takeuchi, 2014) A ground data comparison with GOSAT for CO_2 was done by (Zhang et al., 2015), and it came out that the GOSAT data values are smaller than the ground values by 5-10 ppm.

There are several research papers where GOSAT has been used to monitor methane seasonal cycle. An Indian paper found out that the transport and chemistry dominate in the lower troposphere and thus the formation of the XCH4 seasonal cycle is not consistent with the seasonal cycle of local emissions. Distinct seasonal variations of XCH4 have been observed over the northern (north of 15◦ N) and southern (south of 15◦ N) parts of India, corresponding to the peak during the southwestern monsoon (July–September) and early autumn (October–December) seasons, respectively. According to their analysis, it is governed by both the heterogeneous distributions of

surface emissions and a contribution of the partial CH4 column in the upper troposphere. (Chandra et al., 2017) An Iranian research also showed the seasonal cycle of CH4 that peaks in October starting from June. (Mousavi and Falahatkar, 2020) A study revealed that the methane atmospheric concentrations is primarily driven by large scale CH4 flux signals advected into the local area rather than from local emission, indicating that variations in XCH4 do not simply translate to variations in the underlying rice paddy emissions. (Zeng et al., 2021) This explains the shift in GOSAT seasonal cycle of our results. Several other studies also showed the methane seasonal cycle with peak in October. (Jonai and Takeuchi, 2014; Kivimäki et al., 2019; Parker et al., 2011) A Chinese paper discussed the probable causes of high concentrations in winter when the rice paddies are weak. The atmospheric accumulation of methane due to the regional topography was assumed. (Qin et al., 2015)

Sentinal Tropomi data for CH_4 is available from 2019 and onwards. Several recent studies have used its data for CH_4 monitoring.(Hu et al., 2018; Lorente et al., 2021; Schneising et al., 2019; Varon et al., 2021)

(Malik et al., 2020) used ARIMA model to forecast CO_2 emissions from energy consumption in Pakistan. Emissions were projected to 2030 and results showed the various scenarios that under what conditions Pakistan can achieve its targets as presented in NDCs. There are several other studies that have used ARIMA model to predict GHGs, energy consumption etc. (Hopali and Cakmak, 2020; Nyoni and Bonga, 2019; Ozturk and Ozturk, 2018; Sen et al., 2016)

Many studies assessed the correlation between GHGs and NDVI. (Guo et al., 2013) found the R^2 value 0.76 with $P < 0.01$ between XCH_4 and NDVI, and 0.76 R^2 with $P < 0.01$ between XCO_2 and NDVI. (Choi et al., 2013) showed in his study a negative correlation between NDVI and CO_2.

Chapter 3 : Methodology

3.1. Study Area

The study area of this research is Pakistan with coordinates of 30.3753° N and 69.3451° E. It is considered as a developing country. Pakistan's GDP is 320 billion US dollars (1196.60 US dollars Per capita) in 2019, according to world bank data and it depends on agriculture, industry and services. (World Bank, 2019) It is the 6th most populated country globally, and its climate is arid to semi-arid mainly. Pakistan contributes a very little in world's greenhouse gas budget i.e. less than 1% annually but is among the most affected countries due to climate change. It is prone to natural disasters like floods, earthquakes, droughts, landslides etc. that can drastically affect economy. The changed temperature and precipitation patterns in Pakistan have been observed and future projection of temperature are expected to rise the global averages with negative impacts on agriculture sector, water resources distribution and human wellbeing. The coastal areas esp. the largest city of Pakistan, Karachi can be threatened by rise in sea level and salinity of coastal areas. (Climate Risk Profile USAID 2017)

3.2. Greenhouse Gases (GHGs)

There are main six greenhouse gases that are most abundant in earth's atmosphere. These are Water vapor (H_2O), Carbon dioxide (CO_2), Methane (CH_4), Nitrous oxide (N_2O), Ozone (O_3), Sulfur hexafluoride (SF_6), Chlorofluorocarbons (CFCs), Hydrofluorocarbons (includes HCFCs and HFCs). We selected three greenhouse gases for our study i.e.

- Carbon dioxide (CO_2)
- Methane (CH_4)
- Nitrous oxide (N_2O)

Table 1: Lifetime and GWPs of GHGs

Gas	*Lifetime (Years)*	*Global Warming Potential (GWP)*	
		20-year time horizon	*100-year time horizon*
Carbon dioxide (CO_2)	30-100	1	1
Methane (CH_4)	12	84	28
Nitrous oxide (N_2O)	121	264	265

3.3. General Methodology

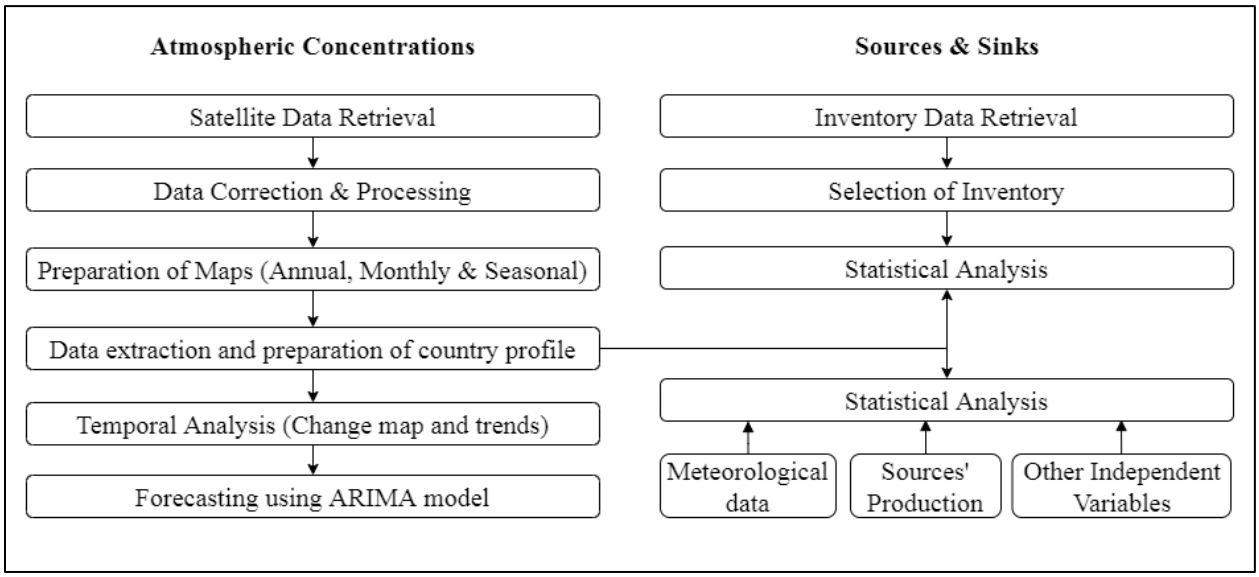

Figure 3.1: General Methodology

The fig 3.1 shows the general methodology of this study. For GHG emissions, satellite observations were used. Emission inventories' data was utilized for source identification. Locally produced data by government agencies, meteorological parameters, and various other independent variables were also used to find the possible correlation among these variables and the atmospheric concentrations and emissions of greenhouse gases. The following topics will elaborate this general methodology.

3.3.1. Satellite Data Retrieval

International Earth Observing System (EOS) of NASA has a multi-disciplinary mission, Aqua, that focuses on earth's water cycle systems and its relation to changes in earth system. It has six instruments including AIRS (atmospheric infrared sounder) that provided mid-tropospheric carbon dioxide concentrations with 13.5 km nadir horizontal, 1 km vertical resolution and >2 ppm accuracy. It was originally set to have water vapor and temperature profiles with spectral resolution of 2378 bands.

The carbon dioxide data has been retrieved from AIRS AQUA.

Greenhouse gases Observing Satellite (GOSAT) is JAXA mission and as name indicates it studies the greenhouse gases mainly carbon dioxide and methane. The TANSO-FTS (Thermal and Near infrared Sensor for carbon Observation - Fourier Transform Spectrometer) is the instrument that measures their global distributions on a 3-day cycle. The instrument has high spectral resolution with VIS, SWIR, MWIR, and TIR ranges. The data is available from 2009 and onwards.

The Sentinel-5, a joint mission by ESA and Netherlands, is dedicated to observing atmospheric elements. The Sentinal-5 missions has a satellite with TROPOMI (Tropospheric Monitoring Instrument). With high spatial and temporal resolution, the instrument is designated to record air quality, ozone, UV radiation, and to monitor and forecast climate. Its resolution is very high as compared to older missions i.e. 7x3 kms. The SWIR band (2.3 um) is used to record methane measurements from the atmosphere.

Data for methane concentrations has been taken from GOSAT for year 2009 to 2018 and Sentinal-5 for year 2019 and 2020.

EnviSat (full form Environmental Satellite) is European Space Agency (ESA)'s satellite that studied and monitored earth's environment on different scales. This mission has been declared ended by ESA in 2012. But the datasets are still available and are used for historical datasets. SCIAMACHY (Scanning Imaging Absorption Spectrometer for Atmospheric Cartography) was an EnviSat's instrument designed to measure trace gases in troposphere and stratosphere including greenhouse gases.

Carbon dioxide and methane's historical profiles were obtained from EnviSat's SCIAMACHY that were later utilized in ARIMA model.

3.3.2. Inventory Data Retrieval

ECCAD (Emissions of atmospheric Compounds and Compilation of Ancillary Data) is the GEIA Global Emission Initiative data portal and is part of AERIS, the French data service for Atmosphere. Users can access various datasets of surface emissions of atmospheric compounds with different scales and resolutions. Different inventories were used to download the greenhouse gases' data as per their availability over Pakistan, and the most suitable one was ultimately selected. (Crippa et al., 2018; Hoesly et al., 2018)

GCISC (Global Change Impact Studies Centre) is a government institute that published an inventory report for year 2012. (Mir and Ijaz, 2016) This local inventory data issued by the government is assumed to be more reliable than the others and it was used to select the most suitable and consistent inventory from the ECCAD inventory's list. We chose those inventories from ECCAD whose data was close and corresponding to the GCISC's data.

3.3.3. Software and Models

A brief summary on the software, tools and models used for this research is given below.

- ArcGIS – is an ESRI's GIS software with different applications. ArcMap version 10.3.1 is used for the satellite data processing and mapping.
- XLSAT – is a statistics software that works on MS excel and provides wide range of data analysis and statistics tools.
- ARIMA – AutoRegressive Integrated Moving Average, is a forecasting algorithm that use the information of the past values from a time series to give the prediction of future scenarios of that time series.

  The ARIMA model is based on three terms, p, d, and q.

  a) The p is AR term i.e. number of autoregressive terms,
  b) q the MA term i.e. number of lagged forecast errors in the prediction equation, and,
  c) d is the difference required to make our time series stationary. The term d is taken 0 if series is already stationary, otherwise difference between the previous and the current is taken to make it stationary.

3.3.4. Meteorological Data

Meteorological data i.e. Precipitation and Temperature's monthly data was requested from Pakistan Meteorological department (PMD) to regress it with GHGs temporal profiles. (PMD - 2019) The regression analysis was carried out by keeping GHGs data as independent variables (x), and temperature and precipitation data as dependent variable (y) to find out the impact of changing concentrations of GHGs on precipitation and temperature over the years.

3.3.5. Probable Sources of Greenhouse Gases

Pakistan Bureau of Statistics (PBS) and Ministry of Finance publish their yearly reports. The reports consist of the data about production of goods (industrial and agriculture), manufacture and use of transport, energy production and consumption, and other economic related industries and departments. The greenhouse gas related possible sources like coal production and consumption for carbon dioxide etc were extracted from those reports with their historical timelines and was used for regression analysis with GHGs' concentration. This locally generated data can help us validate the global emission inventory data to some extent as well as give us the opportunity to identify the GHG sources where the inventory data is not available.

3.3.6. NDVI

NDVI (normalized difference vegetation index) is used in remote sensing to identify whether a certain location contains vegetation or not. The overall NDVI value over a city or a country can tell us that how much of the total area is covered with vegetation. The bands used to calculate NDVI are Near Infrared (NIR) and Red. The formula goes as follows;

$$\frac{NIR-Red}{NIR+Red} \quad \textit{Equation 3-1}$$

The images over Pakistan from NASA's Landsat mission that provides continuous space-based earth imagery was downloaded. Yearly averages over Pakistan were calculated after pre-processing and NDVI was computed. The activity provided us with individual NDVIs against each year. The NDVI time-series was also regressed with GHGs concentrations to see the impact of increase or decrease in vegetation cover on GHGs. The NDVI is used as measure of sink in our study.

3.3.7. Other Variables

Gross domestic production (GDP), population, forest cover, and some other variables were also taken from the World Bank's data portal. The idea of such variables like GDP was to relate the development activities with GHGs emissions, similarly population increase, or decrease can also be linked with increased or decreased GHG concentrations.

3.4. Carbon Dioxide

CO_2 data was downloaded from NASA's official site for data sets with the following URL https://CO_2.jpl.nasa.gov/#mission=AIRS. The date was selected from September 2002 to May

2017. The website allows user to customize their datasets according to their requirements before download. The coordinated for Pakistan were applied first from the global data. The option to generate Level 3 data from level 2 data was selected since it allows users to have a gridded product. The temporal resolution was set to monthly. The cell size in degrees was set to 1o latitude and 1o longitude. Then the files were downloaded in CSV format.

Initially, the files were filtered to eliminate missing values using MS Excel. The filtered monthly files were then mapped on ArcMap, georeferenced and clipped for the shapefile of Pakistan. Similarly, annual and seasonal maps were also generated. After the preparation of maps, mean, maximum, and minimum value from each map was extracted for statistical analysis and graphs were created using MS Excel.

The SCIAMACHY data was also processed in the similar way and a mean value from the monthly maps was extracted that was later used in comparison.

The ECCAD website with URL: https://eccad.aeris-data.fr/catalogue/; allows user to select the required inventory for desired gas by selecting the following attributes: 1) category of inventory e.g. anthropogenic, biomass burning, oceanic, 2) temporal coverage, 3) time resolution, and 4) grid size. We selected inventories that could provide the anthropogenic emissions or biomass burning emissions, maximum temporal coverage with latest years, and were global. Then the regional mask was applied to select the results for Pakistan. The resultant data is mainly be given in Tg yr-1 units with different downloading formats. We downloaded our data as .csv files for further processing. After the downloading, the data was filtered for gaps and unnecessary figures.

Once the datasheets were prepared, the trends were observed by making graphs using MS Excel and regression analysis was done by using XLSTAT. The ARIMA model from XLSTAT was used to forecast the CO_2 emissions for the coming years. The model parameters p, q, and d were kept 0 initially and were increased by 1 value gradually to find the fittest mode. On the basis of autocorrelation function (ACF) and Partial autocorrelation function (PACF) the p, d, and q were decided. Based on Pearson coefficient with value 0.999 and <0.0001 P-values, the most precise model was selected.

3.5. Methane

The following URL gives us the access to the GOSAT data products: https://data2.gosat.nies.go.jp/. The L3 global CH_4 distribution (SWIR) monthly data is available in HDF format. The files from June 2009 to November 2018 were downloaded. The files were opened in ArcMap and the missing data was eliminated. Then georeferencing were applied and the polygon covering area of Pakistan was cropped for each file. Google Earth Engine was used to extract TROPOMI data for year 2019 and 2020. The monthly, seasonal, and annual maps were then created. Mean, maximum, minimum values were also extracted from each map for further analysis.

The succeeding methods are similar to what has been described in previous section of carbon dioxide.

3.6. Nitrous Oxide

There were limitations in the availability of the satellite data for nitrous oxide. To study nitrous oxide, we used inventory data with other variables as mentioned above. This section is limited and is based on the inventory data.

Chapter 4 : Results and Discussions

The results include maps, graphs, scatter plots etc. for each GHG that are discussed in the following sections.

4.1. Carbon Dioxide

4.1.1. Atmospheric Profile over Pakistan – AIRS

This section presents the results of atmospheric concentration of carbon dioxide retrieved from the AIRS (atmospheric infrared sounder) satellite instrument.

4.1.1.1. Yearly maps

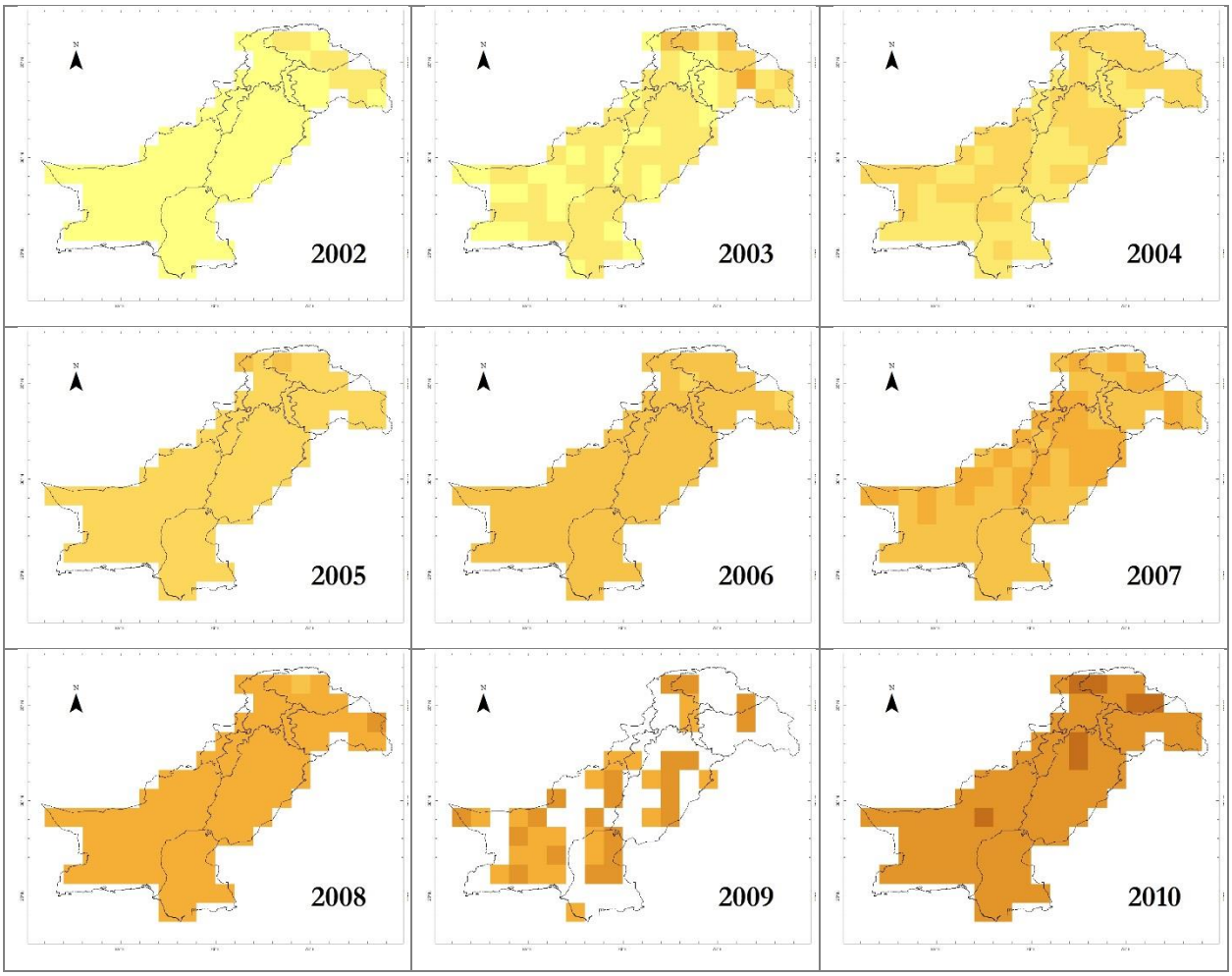

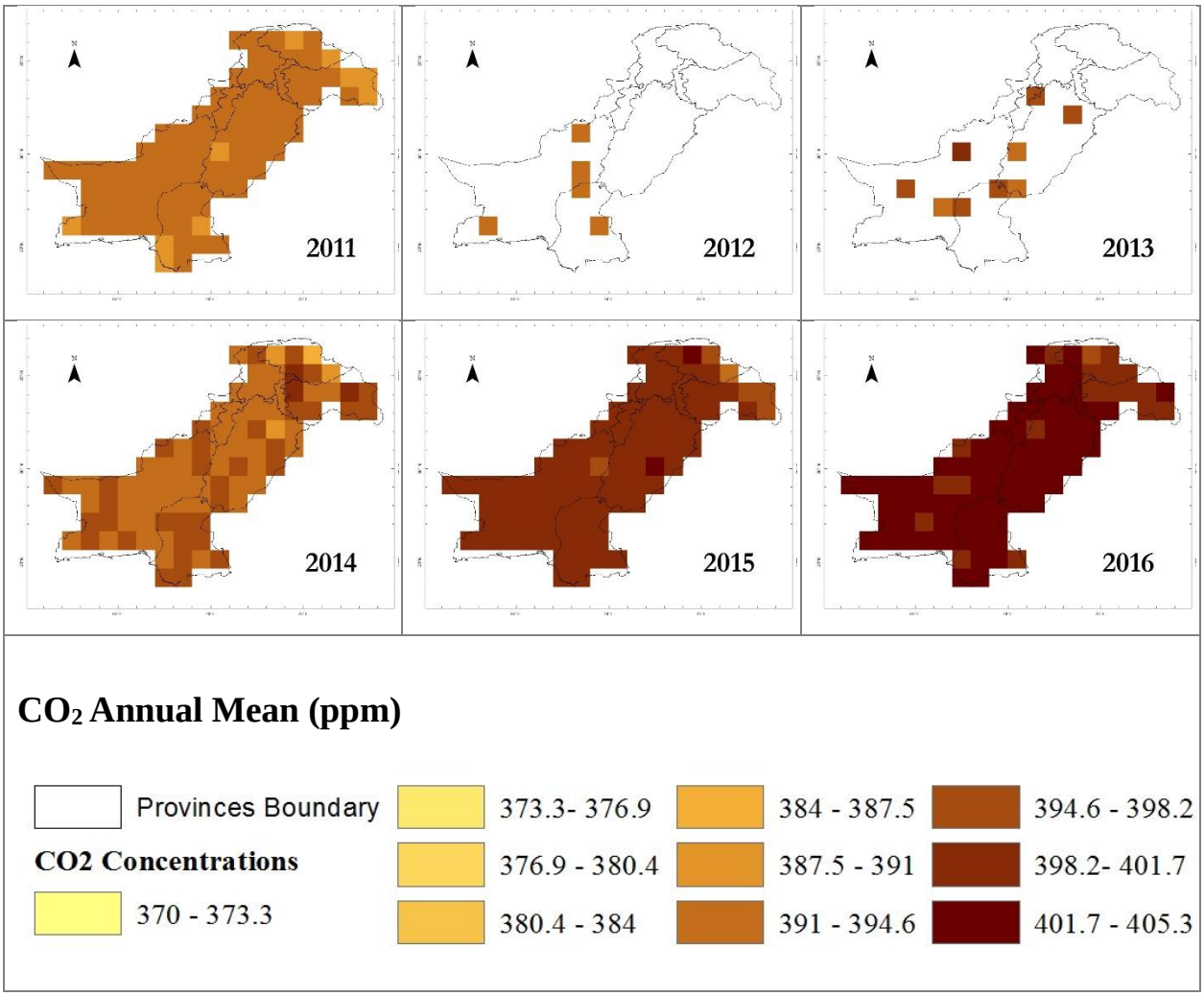

Figure 4.1: Annual Maps of CO_2 (ppm) over Pakistan – 2002 - 2016

The maps present the carbon dioxide concentrations over Pakistan from year 2002 to 2016. The color coding (as seen in legend) describes that the concentration has significantly increased from the minimum value of 369.97 ppm in 2002 to 397.7 ppm in 2016. In 2016, the maximum concentration of CO_2 observed was 405.21 ppm. It can also be seen in maps that the frequency of high and low mean concentrations (dark and light color tone respectively) has also changed over the years. The whole area of Pakistan had almost consistent concentrations in a year with slight variations.

The data points for year 2012 and 2013 are very limited and do not presents the whole country. Though the average value can be used for our analysis and visualization, but the values of maximum, minimum and difference between them would be largely affected due to this limitation.

This data gap shall be considered in maximum and minimum analysis while discussing the results in later sections.

4.1.1.2. Annual concentration trend

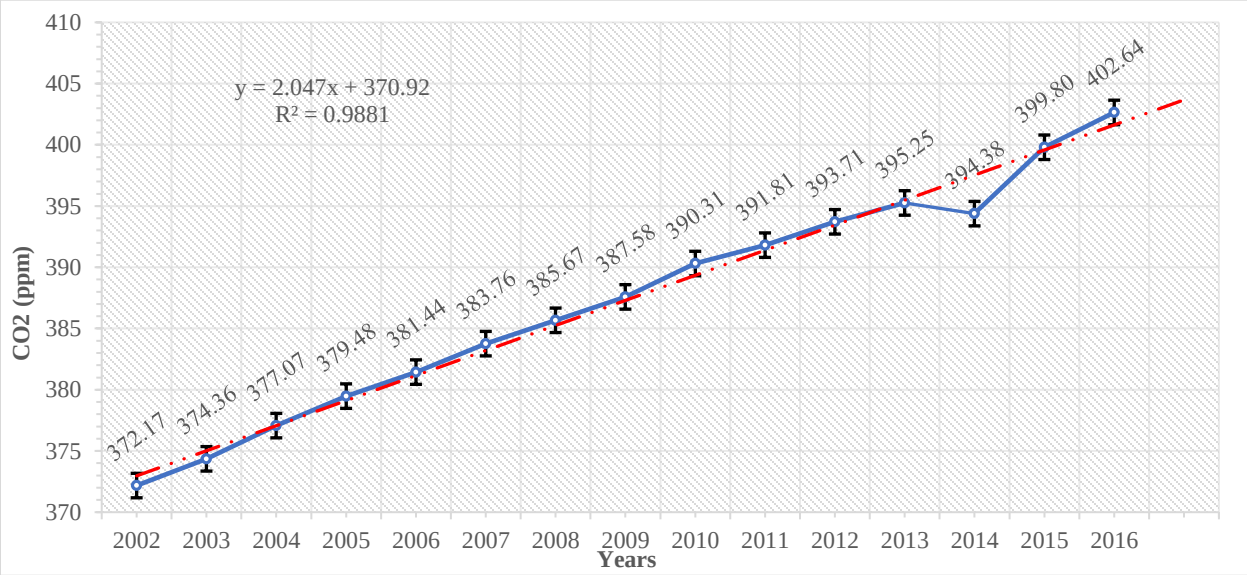

Figure 4.2: Annual CO_2 Trend over Pakistan – 2002 - 2016

The trend shows a linear increase of ~8.2% from the base year 2002 to 2016. In over 15 years, ~30.47 ppm increase in CO_2 levels has been observed.

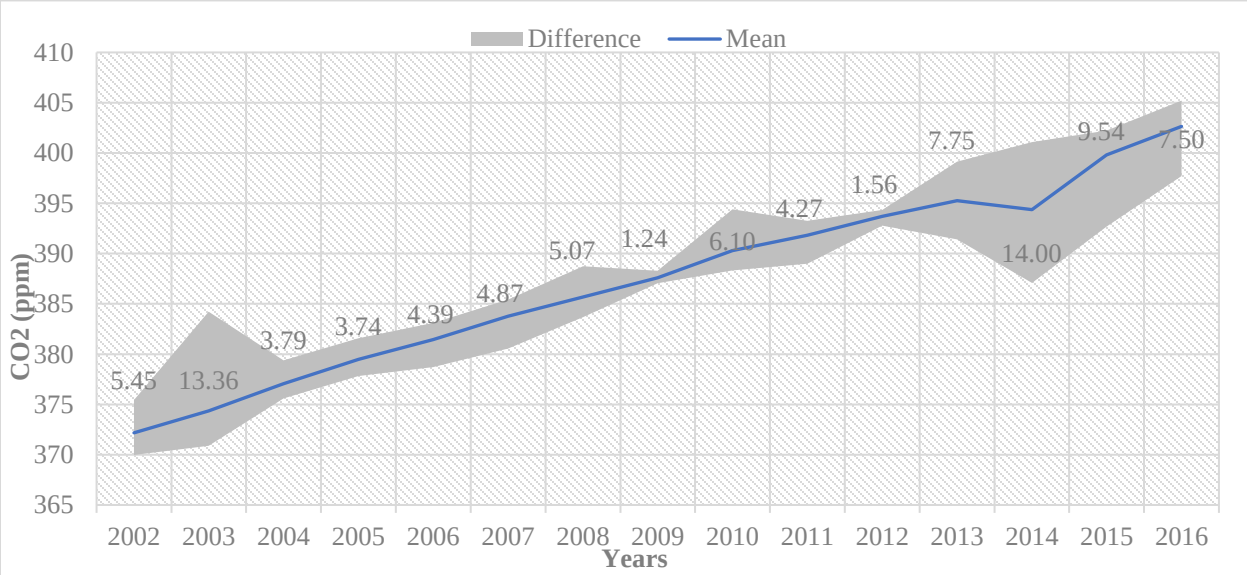

Figure 4.3: Difference between Maximum and Minimum CO_2

The figure shows the difference between maximum and minimum concentrations over Pakistan. The maximum difference observed is 14 ppm in 2014, and the minimum difference is 1.24 ppm in year 2009. In 2014, the maximum concentration observed was 401.098 and minimum was 387.09. While in 2009, the maximum concentration was 388.3 and the minimum concentration was 387.05.

4.1.1.3. Monthly concentration trend

The figure 4.4 below represents the monthly values (average) of CO_2 concentration from 2002 to 2016. The curve shown in figure is known as keeling curve that means the accumulation of CO_2 over the years from the baseline year that is 1958 as per Mauna Loa Observatory. The graph gives us the information about seasonal variation of concentrations. The peaks of the curve are called as maxima, and depths are called minima. The maxima and minima values are related to the minimum and maximum concentrations of CO_2 during winter and spring season respectively. The gaps indicate the missing data for several months over Pakistan.

The increase of concentrations from November to May and decrease in concentrations from May to November can be explained by the photosynthesis and respiration processes of plants. That is, photosynthesis dominates in plants in spring and summer, and respiration dominates during fall and winter season.

The graph shows that the curve usually peaks in the month of May and falls in the months of October-November. The curve fairly corresponds to the keeling curve of Mauna Loa Observatory.

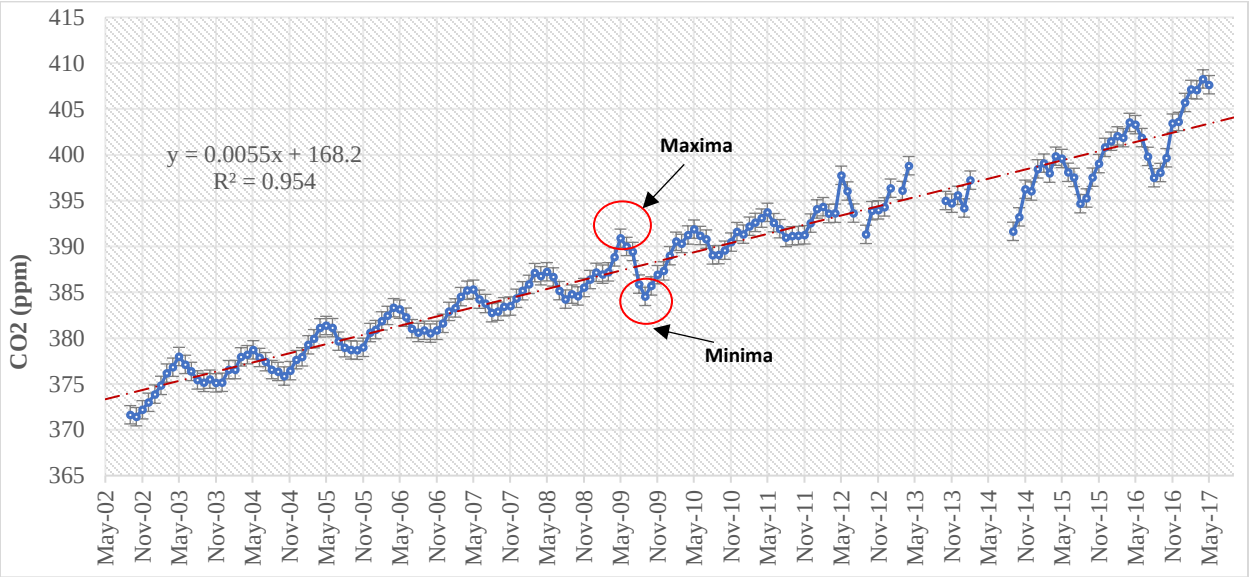

Figure 4.4: CO_2 Monthly Trend (2002-2016)

4.1.1.4. Maxima and Minima

The figures 4.5 shows the trend of maxima and minima from year 2002 to 2016. The maxima start from 375.43 ppm in 2002 and reaches the value of 405.21 in 2016. The absolute increase in maxima is 29.78 ppm over these 15 years.

Similarly, the minima value in 2002 was 369.97 ppm that goes up to 397.71 in 2016, with absolute increase of 27.74 ppm in these 15 years.

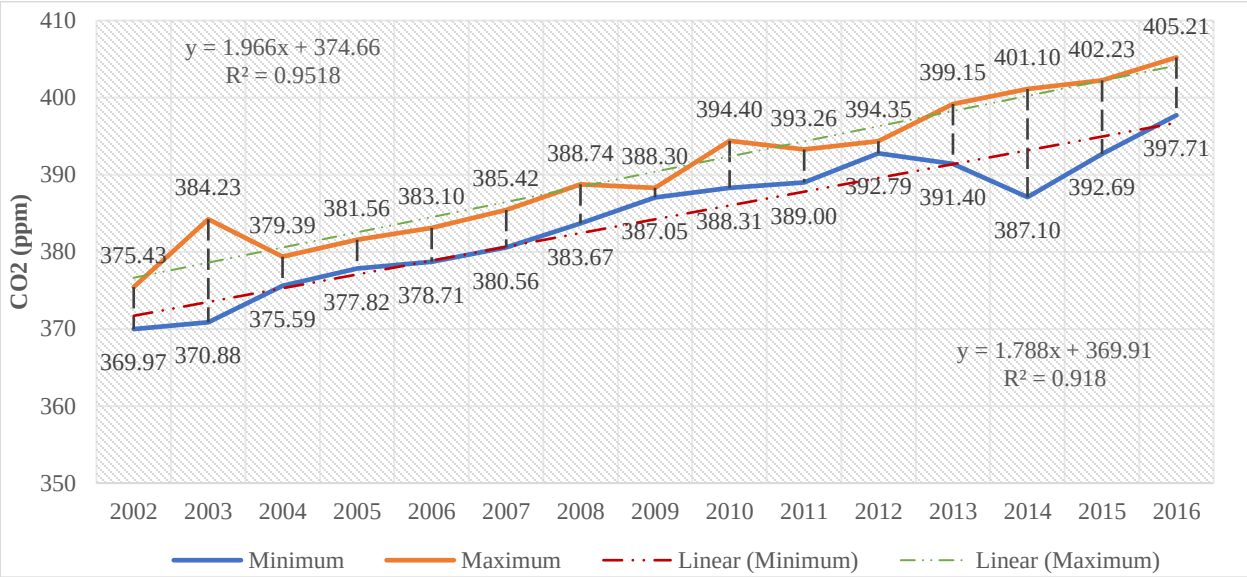

Figure 4.5: Combined Increase in Minima and Maxima

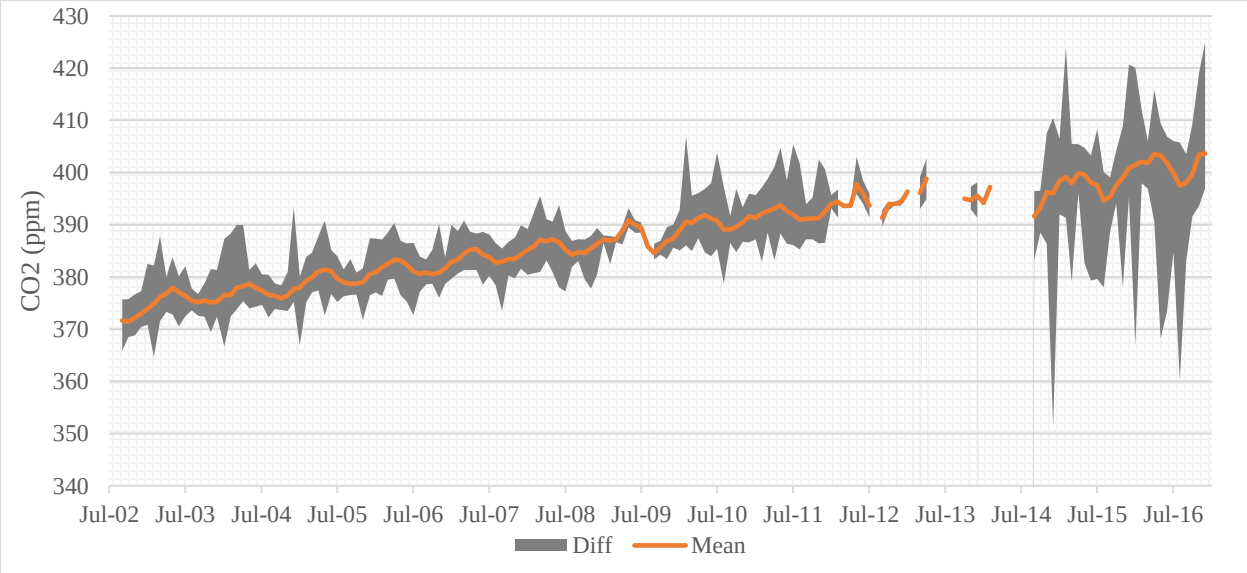

Figure 4.6: Maximum and Minimum Monthly CO_2 (2002-2016)

The figure 4.6 shows the difference in monthly concentrations of CO_2 from 2002 to 2016. The graph shows that the more variation has been occurred from end of 2014 and onwards. That indicates that either natural seasonal variations of CO_2 concentrations have altered due to seasonal shifts or addition of anthropogenic factors in natural cycles of CO_2 emissions and sinks.

4.1.1.5. Seasonal Cycles

The monthly cycle of CO_2 concentration shows the change in amplitude in winters and summers. Winter Increase (WI) represents that increase in concentrations of atmospheric CO_2 in winter season. However, Summer Decrease (SD) represents the decrease in atmospheric CO_2 in summer season. The 15 years' curve demonstrates the increase in the amplitudes with respect to WI and SD. (Fig 4.8, 4.9)

WI is calculated from minima of the previous year to the maxima of the following year. Whereas, SD is calculated from the maxima and minima of the same year.

$$WI = Y_{x+1\,(max)} - Y_{x\,(min)} \quad \textit{Equation 4-1}$$

$$SD = Y_{(min)} - Y_{(max)} \quad \textit{Equation 4-2}$$

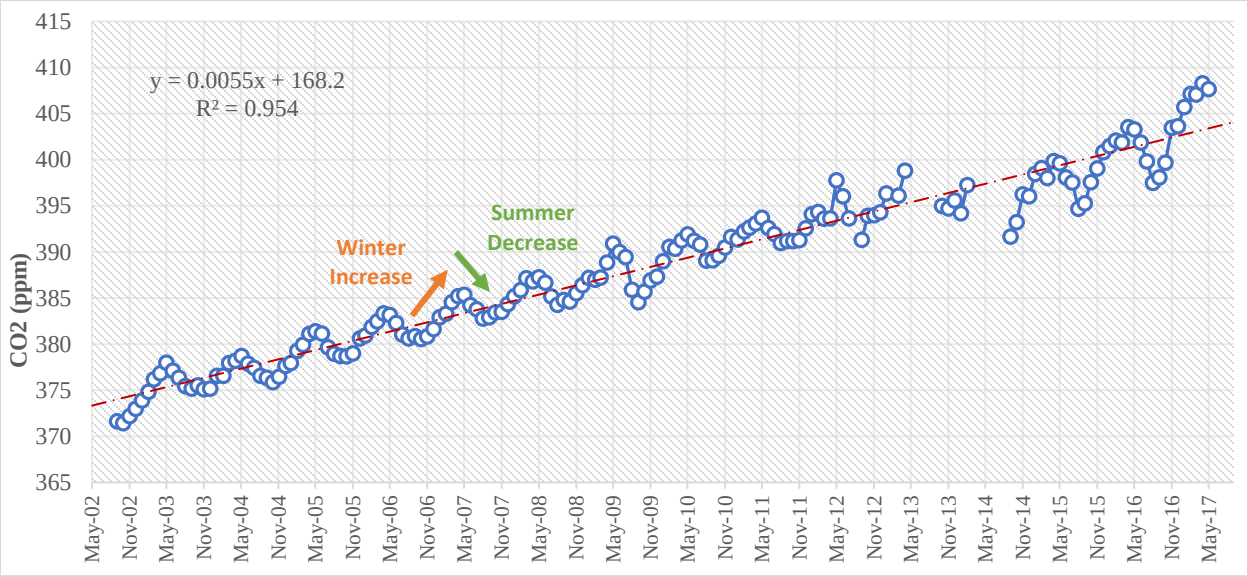

Figure 4.7: Monthly CO_2 over Pakistan (2002 – 2016)

The figures below (4.8 & 4.9) describes the increase and decrease in amplitudes of WI and SD. The WI in 2003 is 14.26 that drops in later years and increase again in year 2015 and 2016 with values of 15.13 and 12.52 respectively. The average increase during all years is 8.21. The SD in 2003 is -13.36 and becomes -7.50 in 2016. The results present an overall decrease with average value of -6.23.

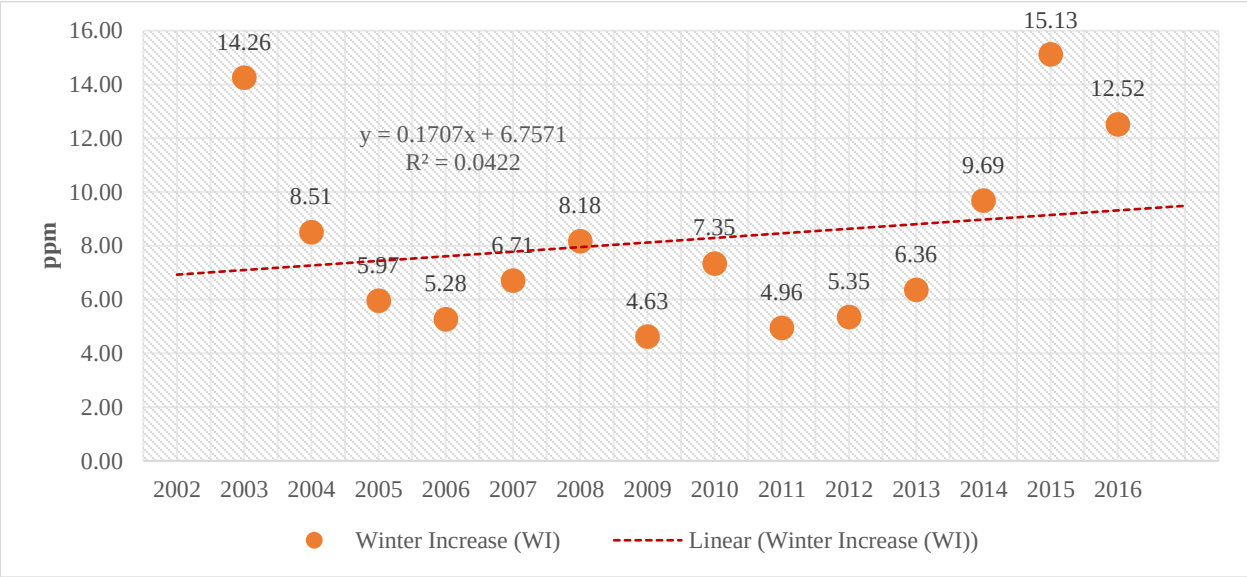

Figure 4.8: Winter Increase (WI)

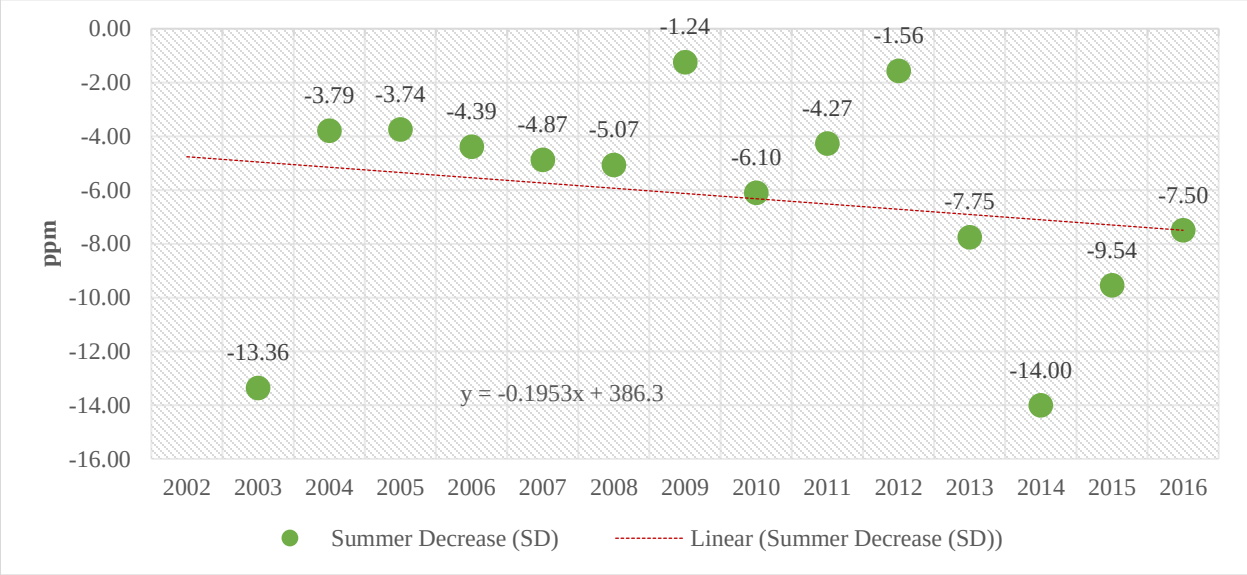

Figure 4.9: Summer Decrease (SD)

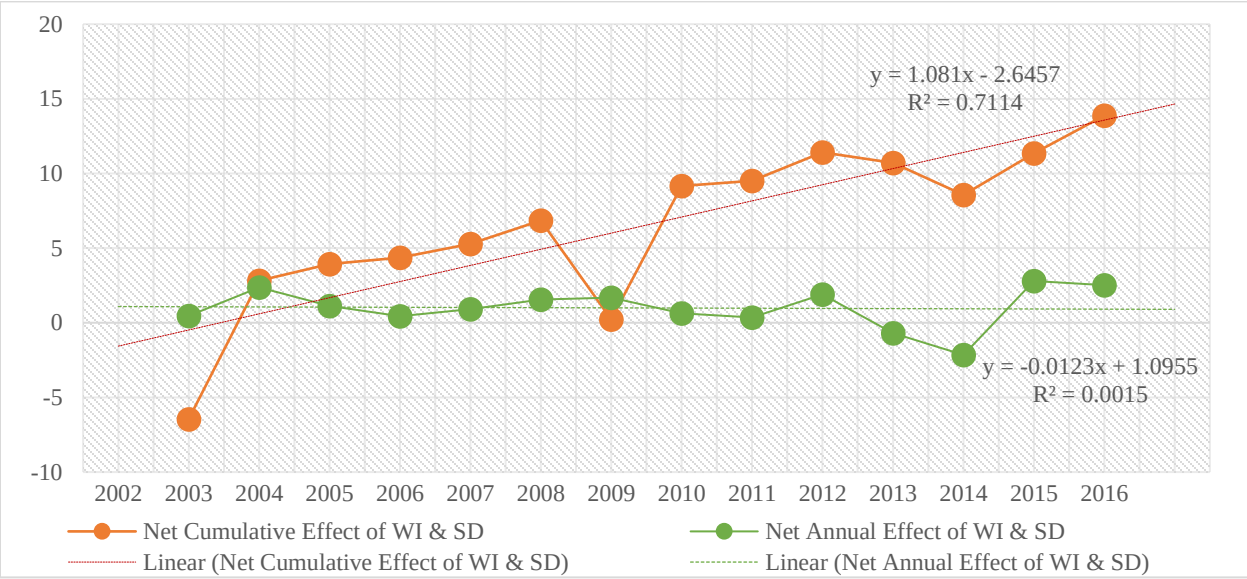

Figure 4.10: Net Annual and Cumulative Effect of WI and SD

The figure 4.10 shows the net annual and cumulative effect of WI and SD from 2002 to 2016. The increasing slope of cumulative net that doesn't correspond completely to our annual concentration trend refers to the addition of source or sink in addition to the natural wiggles. The slope of annual net shows an increasing trend, although a small. That also suggests the presence of external factor like fossil fuel emissions etc. in CO_2 concentrations over the years.

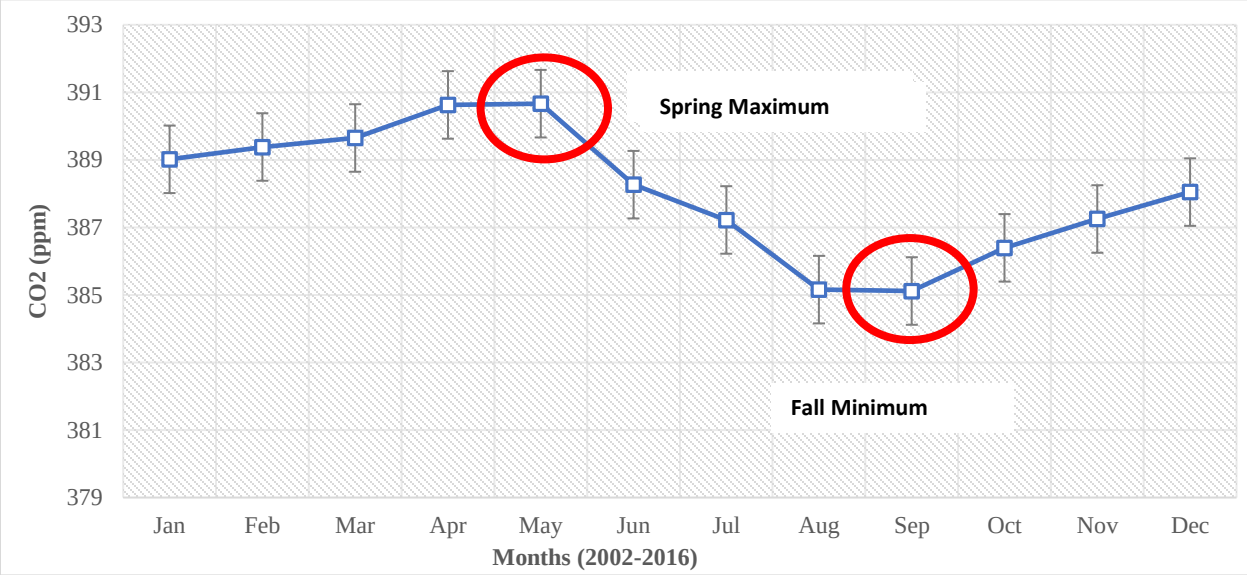

Figure 4.11: Seasonal Cycle of CO_2 within a year

Figure 4.11 explains the seasonal cycle of CO_2 concentration taken as averages of each individual month from 2002 to 2016. The curve conforms with the Keeling curve of Mauna Loa, Hawaii. The cycle shows a pattern where CO_2 concentrations decreases in summer and increase in winters. The concentration level peaks at the month of May, called Spring Maximum. After May, it starts decreasing and reaches its lowest point in September. The minimum level is called Fall Minimum. The mean CO_2 concentration is 390.66 in Spring Maxima, and 385.11 in Fall Minima. This cycle can be explained by the photosynthesis and respiration patterns of plants. The photosynthesis decreases in winter, and respiration increases. Thus, emitting more CO_2 in the atmosphere. In the contrast, in summers the photosynthesis increases as compared to respiration.

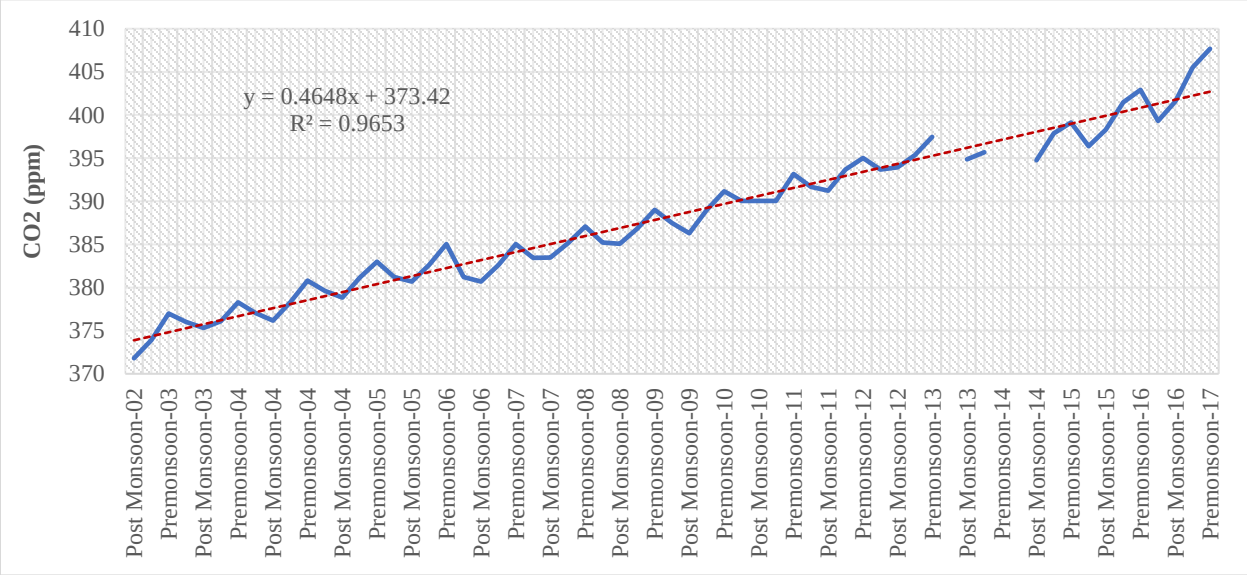

Figure 4.12: Seasonal Trend of CO_2 (2002 - 2016)

The seasonal trend of CO_2 shows represents CO_2 concentrations with respect to four seasons; Pre-monsoon (Spring), Monsoon, Post Monsoon, and Winter. The trend shows that the concentrations are highest in Pre-monsoon season, and lowest in Post-monsoon season. The concentrations have a continuous increasing pattern over the years. The trend is similar to the monthly trend described previously.

The bar chart below shows the increase in mean concentrations of CO_2 in four seasons from 2002 to 2016. The CO_2 concentrations have increased in all seasons in 15 years. The maximum concentration observed is in winter 2016. The post-monsoon season has faced maximum increase, whereas minimum increase has occurred in spring season.

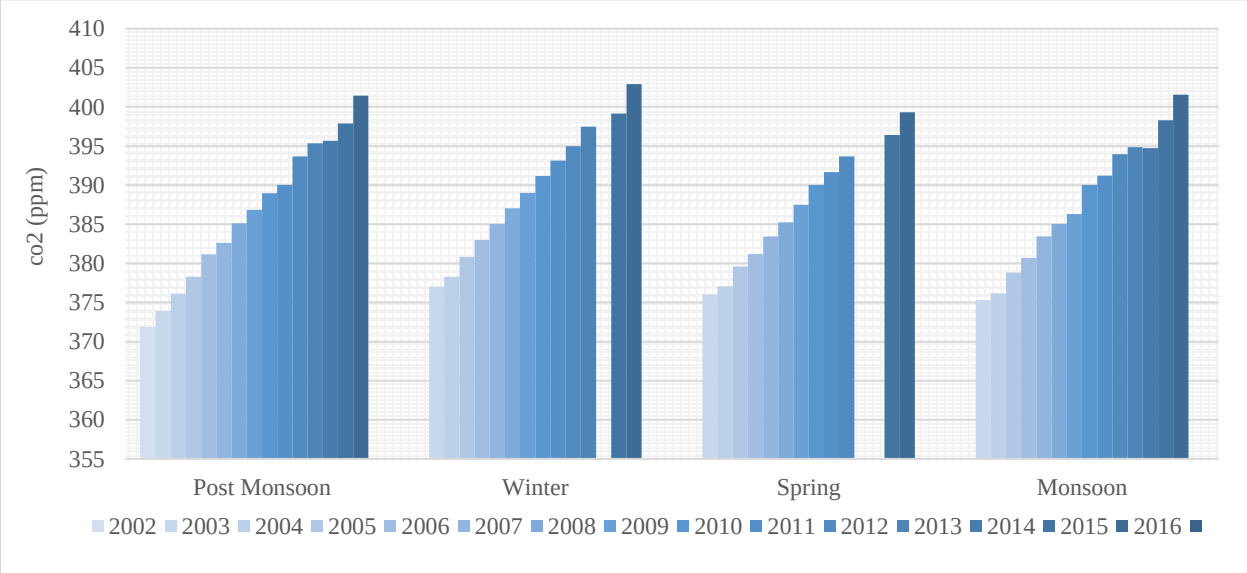

Figure 4.13: Season wise Annual Trends of CO_2 (2002-2016)

4.1.1.6. SCIAMACHY data – Comparison with AIRS

The AIRS data is also compared with SCIAMACHY observations. The SCIAMACHY data is available till 2012, so AIRS observations from 2002 to 2012 have been compared and correlated with them. It is observed that the data of both instruments have a similar trend but the SCIAMACHY data shows the higher concentrations of CO_2 than that of the AIRS. The regression analysis between these two shows the high correlation between them with R^2 value of 0.988.

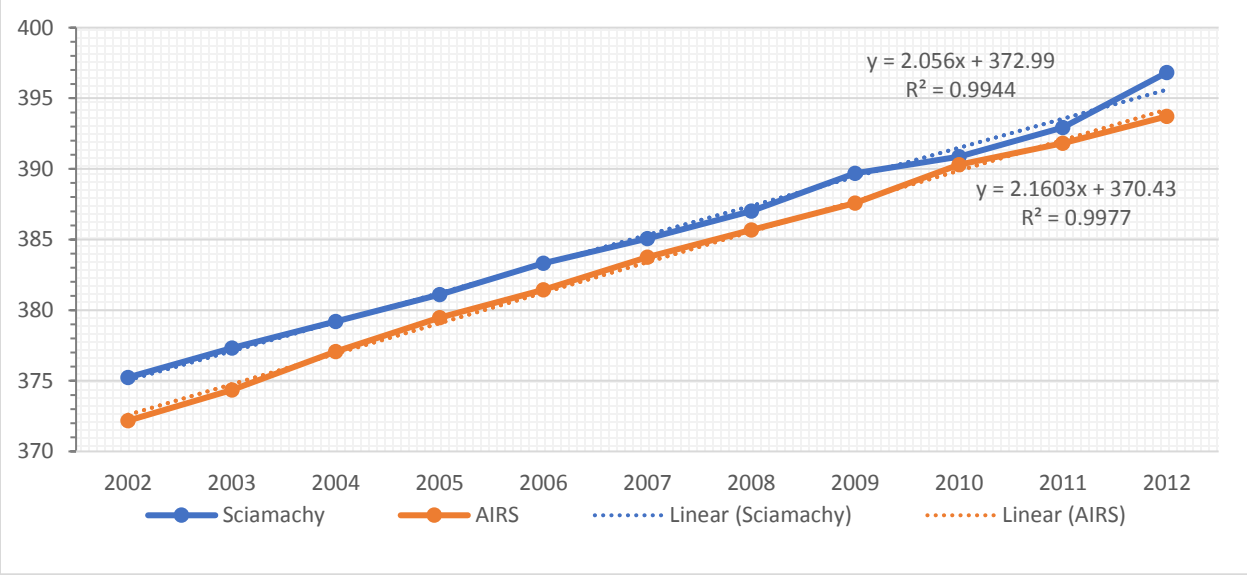

Figure 4.14: Comparison between AIRS and SCIAMACHY data

4.1.2. ARIMA Model Forecasting

To forecast CO_2 concentrations for the upcoming years, the ARIMA model has been used. The model parameters (p, d, q) were taken as (1, 2, 2). The difference of 2 was taken to make the model stationary. The CO_2 levels are forecasted to year 2100. The results show that the concentrations will increase up to 548.79 ppm in 2100 with 95 % confidence interval, that is 38.8% increase from year 2013.

To validate our results, the ARIMA forecasted observations from 2002 to 2016 are correlated with the actual observations. The R^2 value is 0.988 between them with significance level $\alpha = 0.05$.

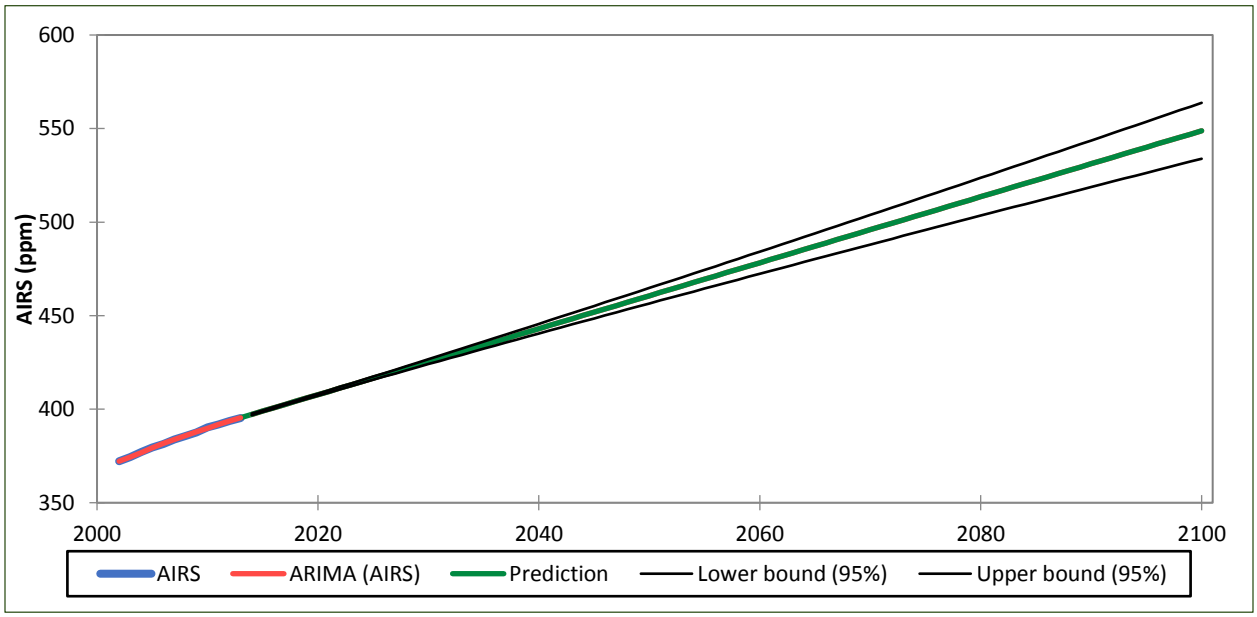

Figure 4.15: ARIMA Model Forecast – Year 2100

4.1.3. Emission Inventories: Sectoral emissions' data

4.1.3.1. Selection of the Emission Inventory

The data of multiple emission inventories were downloaded and compared with the locally produced emission data by the Global Change Impact Studies Centre (GCISC). Among REAS, EDGAR and CEDS, the GCISC inventory observations were strongly correlated with the CEDS. It was selected for further analysis. (Fig 16)

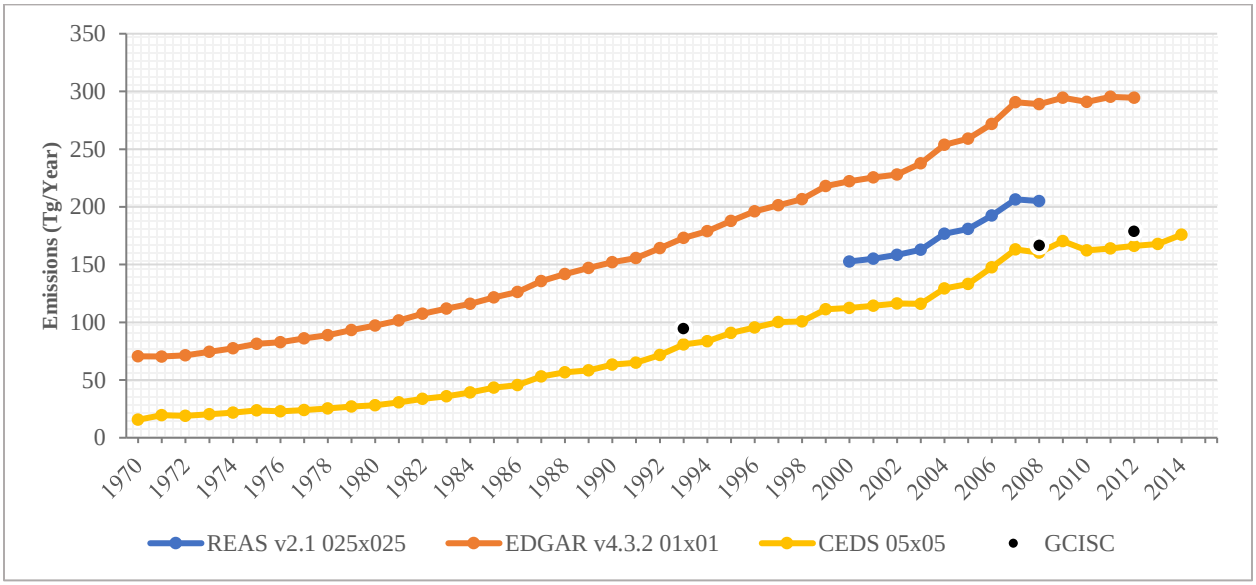

Figure 4.16: Comparison of Inventories with GCISC Inventory

4.1.3.2. CEDS

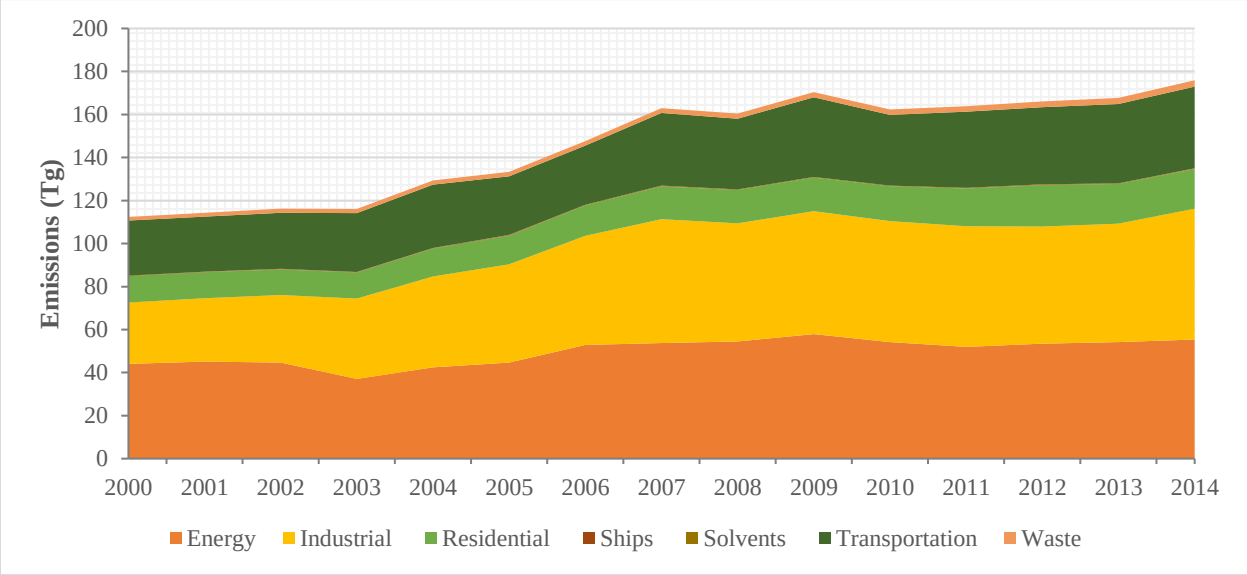

Figure 4.17: CO_2 Emissions - CEDS

The emissions from different sectors from year 2002 to 2014 are given in the figure 4.17. The stacked areas represent different sectors responsible for CO_2 emissions. The emissions are given in Tera-grams. The energy and industrial sectors are the most influential ones whereas, the emissions from ships and solvents are negligible. The other two sectors whose emissions are

significant are transportation and residential. The total emissions in 2000 are estimated to be ~110 Tg and in 2014 the emissions have increased to ~175 Tg.

Figure 4.18 represents the CO_2 emissions and atmospheric concentrations by CEDS and AIRS respectively. The pre-industrial earth's atmospheric CO_2 concentration was 280 ppm, and if we take 2000 as our baseline year, the earth's atmospheric concentration was 370 ppm. Atmospheric concentrations are not just emissions but accounts for the net CO_2 of carbon cycle.

The graph shows the increasing trend of both inventory and satellite observations. The inventory data shows the emissions of 0.116 Gt in 2002 and 0.176 Gt in 2014. Whereas, the satellite results show the ~372 ppm of CO_2 concentration in 2002, and ~397 ppm in 2014. The correlation between these two datasets have the R^2 value of 0.847.

The results reflect that the atmospheric concentrations of CO_2 over Pakistan are increasing as the emissions are also increasing due to development activities.

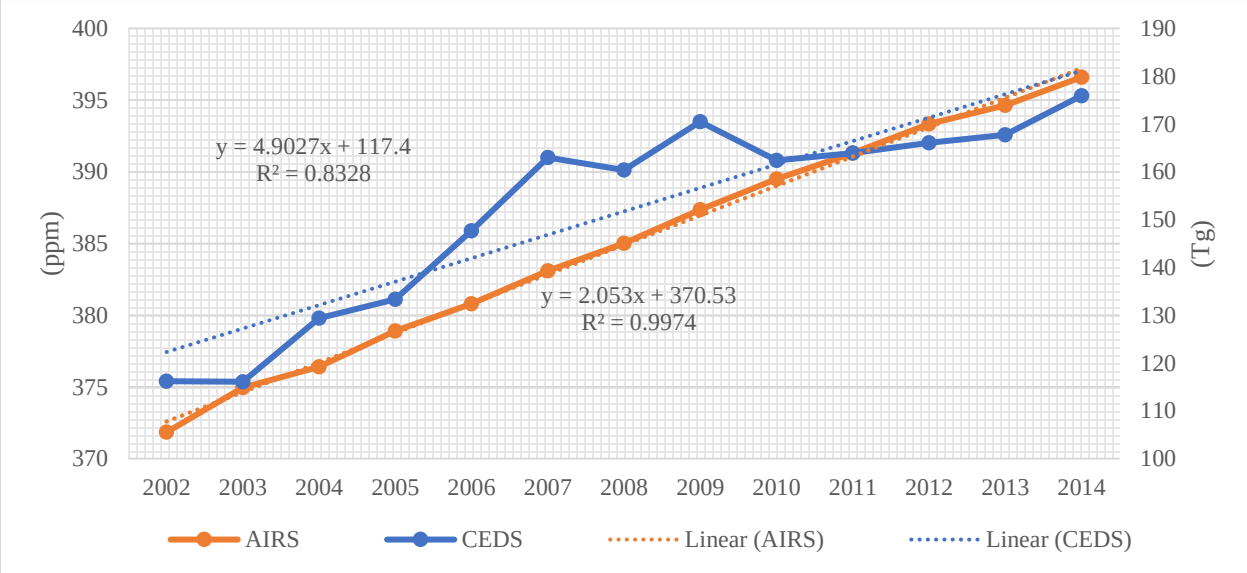

Figure 4.18: CEDS and AIRS Data Comparison (2002 - 2014)

4.1.4. Sectoral data of development/industrial activities in Pakistan (Sources) – Regression Analysis with Inventory data

The data of emissions sources like industrial activities, transportation, energy, agriculture and other sectors by Pakistan Bureau of Statistics (PBS) and other government institutes was compiled and correlated against inventory data. The inventory data that is given in categories, was correlated

with the relevant sectors' details, e.g. the energy sector of inventory was correlated with energy related activities of Pakistan like oil and gas consumption. The results gave us the idea about the data precision.

Table 2: R-values – CEDS Emissions Sectors and Sectoral Activity Data (2002 – 2014)

	CEDS Energy	*CEDS Industrial*	*CEDS Transport*	*CEDS Residential*
Oil consumption	**0.61** *(p<0.05)*	**0.64** *(p<0.05)*	-	-
Gas consumption	**0.85** *(p<0.05)*	**0.93** *(p<0.05)*	-	-
Electricity consumption	-	0.95	-	**0.92** *(p<0.05)*
Coal Consumption	0.72	0.73	-	0.48
Natural gas consumption	0.84	0.94	0.70	0.88
Petroleum products consumption	-0.21	-0.25	-0.53	-
Crude oil extraction	0.46	0.54	-	-
Minerals & Coal extraction	-	**0.89** *(p<0.05)*	-	-
Total fertilizer production	-	0.60	-	-
Sugar production	-	0.43	-	-
Cement production	-	0.91	-	-
Steel products	-	-0.61	-	-
Aviation	-	-	-0.14	-
Motor Vehicles	-	-	0.70	-

The results show that the overall emissions and sources do not possess good correlation between them. The most R-values are not significant with $p>0.05$. The emissions of CEDS energy sector only show a good correlation with gas consumption with R-values of 0.85. The CEDS industrial emissions show a good R-value of 0.93 with gas consumption, and 0.89 with minerals and coal extraction. The transport sector emissions and transport activities do not have a good correlation between them. The CEDS residential emissions' sector provided 0.92 R-values with electricity consumption. The results indicate that the inventory and sources' data are not completely corresponding to each other.

4.1.5. Statistical analysis of Satellite-based emissions with various factors

The table 3 below describes the correlation of CO_2 emissions (CEDS Inventory) and atmospheric concentrations (AIRS) with multiple factors. Both emissions and concentrations show the almost same results. Precipitation and temperature do not show any significant values of R. The GDP and

population show a good correlation with emissions (0.92 and 0.98 respectively) and concentrations (0.99 and 0.99 respectively).

Forest cover and NDVI are used as a measure of sink. For forest cover and NDVI, the residential sector emissions of CEDS were used since urbanization is directly linked to decreased forest cover and altered NDVI. The forest cover shows a strong negative correlation value i.e. -0.99 R for AIRS CO_2 concentrations and -0.98 R for CO_2 CEDS emissions. The forests are the sinks of carbon dioxide, and the negative relation shows that the shrinking forests have given rise to carbon dioxide emissions, and concentrations. Whereas, NDVI doesn't give the significant R-value with any of them, it may be due to the yearly means utilization where generic value for a whole year and for a whole region might not be enough to have good results.

Table 3: R-values of Emissions and Concentrations with Multiple Factors (Yearly means)

	AIRS CO_2 Concentrations	*CO_2 Emissions (CEDS)*
Mean Temperature	-0.006	0.387
Mean Precipitation	0.009	-0.187
GDP	**0.991** *(p<0.05)*	**0.925** *(p<0.05)*
Population	**0.993** *(p<0.05)*	**0.983** *(p<0.05)*
Forest Cover	**-0.992** *(p<0.05)*	**-0.984** *(p<0.05)*
Mean NDVI (>0.3)	-0.217	0.199

The yearly means of temperature and precipitation have not provided any useful information, but previously the seasonal and monthly analysis have shown a strong relation of temperature and precipitation with atmospheric concentrations of carbon dioxide. This implies that for such analysis of seasons' dependent factors, the yearly means instead of monthly and seasonal means, may give distorted results. It is inferred that the poor correlation values of NDVI are due to same reason since NDVI is also season dependent.

4.1.6. NDVI

NDVI was used as measure of sink for carbon dioxide. The R^2 value between AIRS concentration and NDVI came out to be 0.047. The poor value may be due to the annual means of both datasets, where they are unable to show a correlation between them. Another reason can be the dependence of both, atmospheric concentrations and NDVI, on various other factors. Quantification of sink may require models where sources, chemistry of carbon dioxide and other processes are given weightage.

NDVI was combined with seasonal cycle of CO_2 to portray their seasonal behavior and patterns with each other. Fig 4.19 show the combined graph of these two datasets.

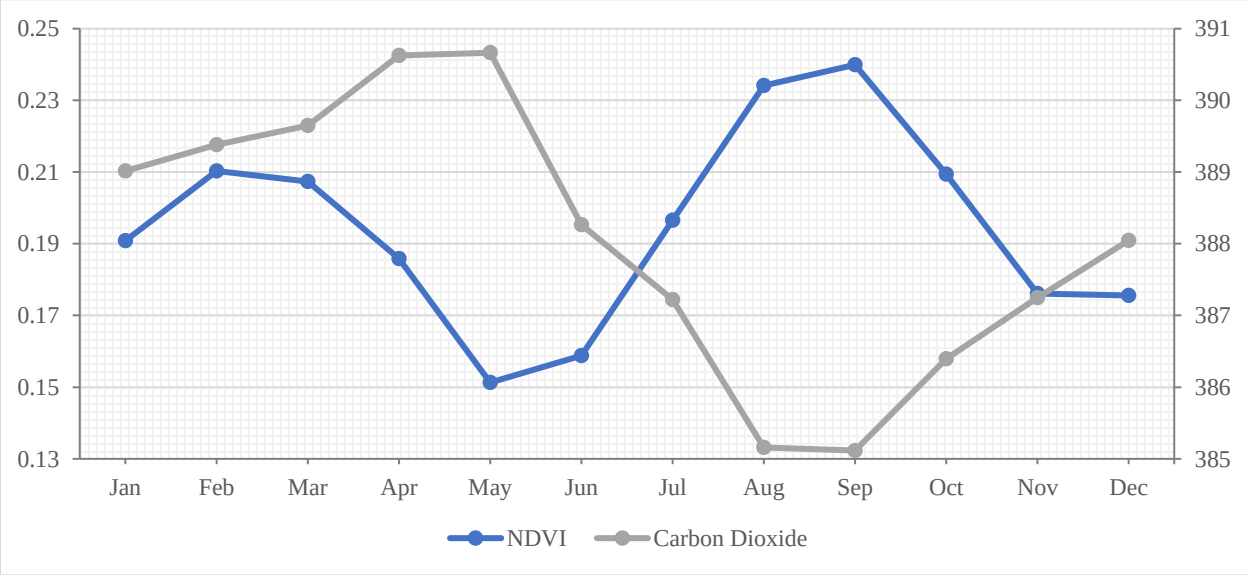

Figure 4.19: NDVI and Carbon dioxide's seasonal Cycles

The graph shows that the two cycles are opposite to each other. Carbon dioxide atmospheric concentration peaks when NDVI decreases and vice versa. It reflects that when NDVI is high the vegetation/forest uptake of carbon dioxide is also high, and atmospheric concentrations decrease.

The graph depicts a good behavior of forests and vegetation acting as a sink for carbon dioxide. But detailed study by modeling other factors with these results is important in order to properly estimate the capacity of forests to uptake carbon dioxide.

4.1.7. Temperature

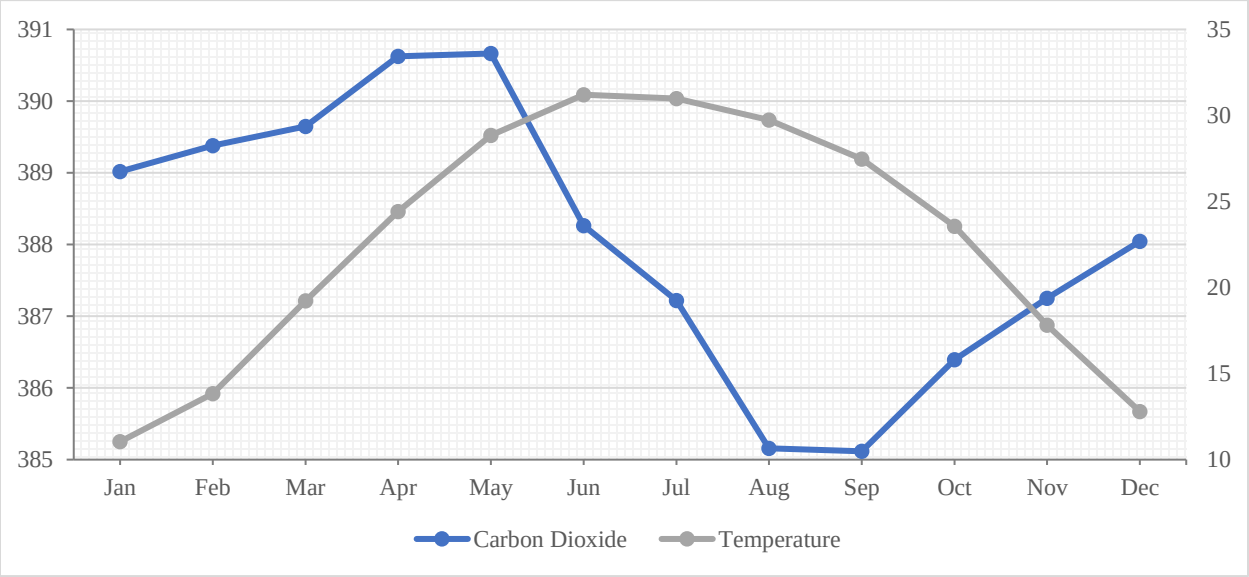

Figure 4.19a: Temperature and Carbon dioxide's seasonal Cycles

The carbon dioxide's atmospheric concentrations increase when the temperature rise and decrease when the temperature falls except in the months of fall and winter. In these seasons, dead plants and fallen leaves from the trees decay that release carbon dioxide. Respiration increases in these months combined with the decreased photosynthesis. These all phenomenon along with human induced emissions give rise to the atmospheric concentrations in winter. In peak summer, the photosynthesis increases that remove more carbon dioxide from the atmosphere, and consequently, the atmospheric concentrations of carbon dioxide are decreased.

4.2. Methane

4.2.1. Atmospheric Profile over Pakistan – AIRS

This section presents the results of atmospheric concentration of methane retrieved from the GOSAT (greenhouse gases observing satellite), and Sentinal-5's TROPOMI (Tropospheric Monitoring Instrument).

4.2.1.1. Yearly maps

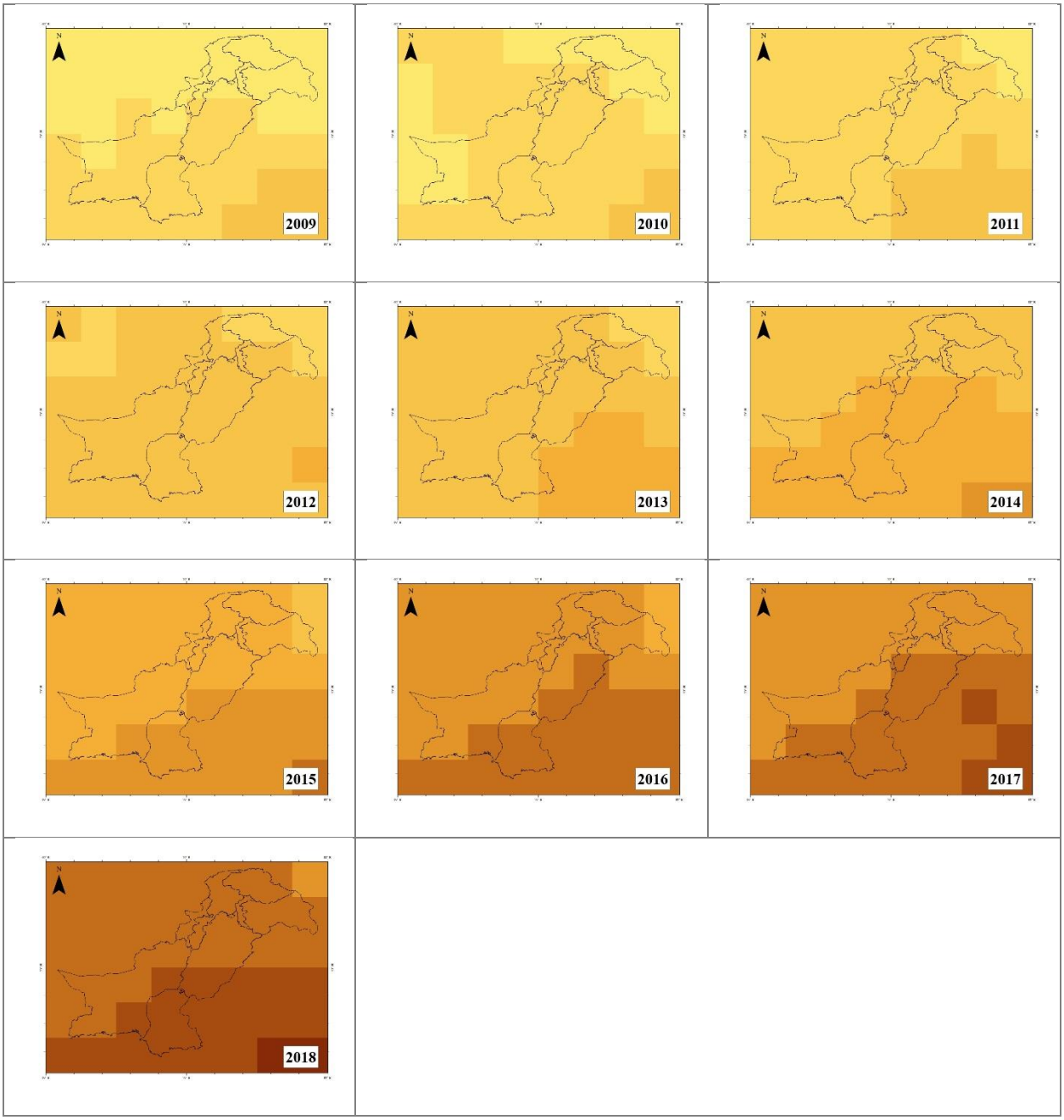

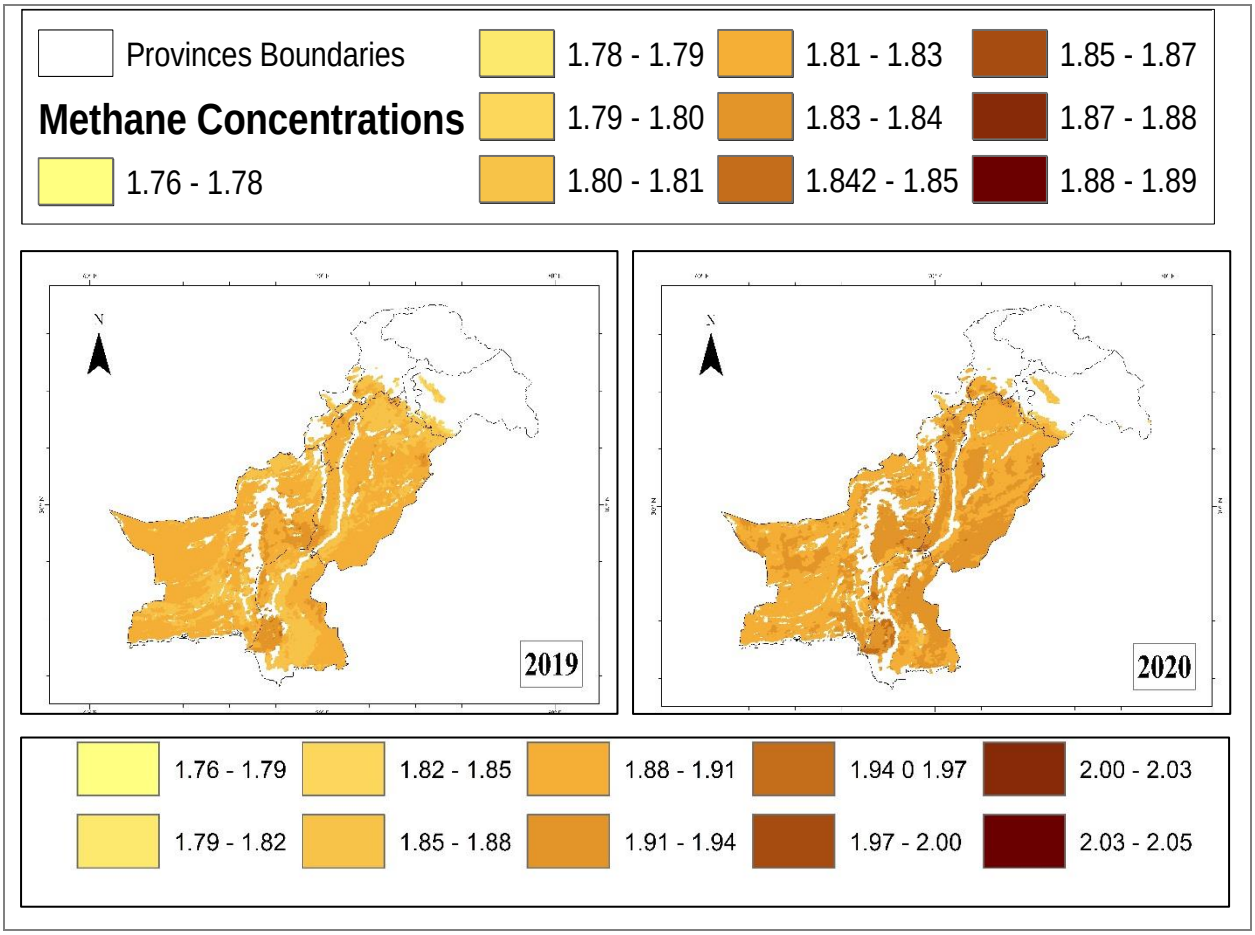

Figure 20: Annual Maps of CH_4 (ppbv) over Pakistan (2009 – 2018)

The maps in figure 24 show the atmospheric methane concentration over Pakistan from year 2009 to year 2020. The legends present the light color tone as low concentrations and dark tone as high concentrations. The minimum concentrations of methane have considerably increased from 1.78 ppbv in 2009 to 1.84 ppbv in 2018. Whereas maximum concentration in 2009 was 1.80 and in 2018 it becomes 1.87 ppbv. The year 2019 and 2020 maps are from sentinel-5 where methane observations exceed the GOSAT results. The different legend for Sentinal-5 shows the methane concentration in year 2019 are greater than 1.88 ppbv, larger than that of 2018. And in year 2020, the concentrations reached to 1.97 ppbv in east Pakistan regions. The overall increase of methane concentrations in year 2020 as compared to 2019, and previous GOSAT results is also obvious from the maps.

It can be observed from the maps that the increase in concentration is from the east side of Pakistan, where the India lies. The emissions from the agricultural zones (esp. rice) of Pakistan and India can explain this behavior.

4.2.1.2. Rice Season Maps

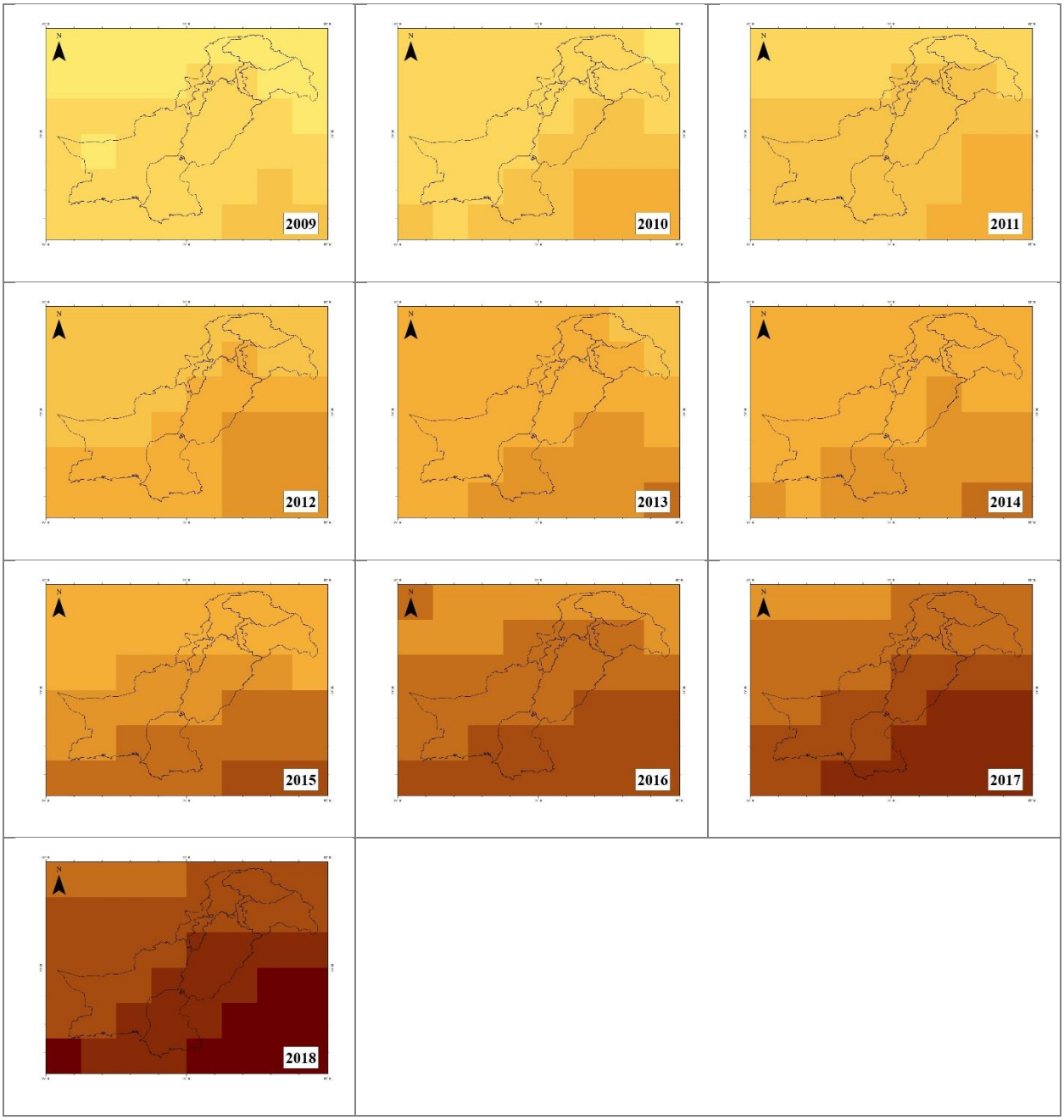

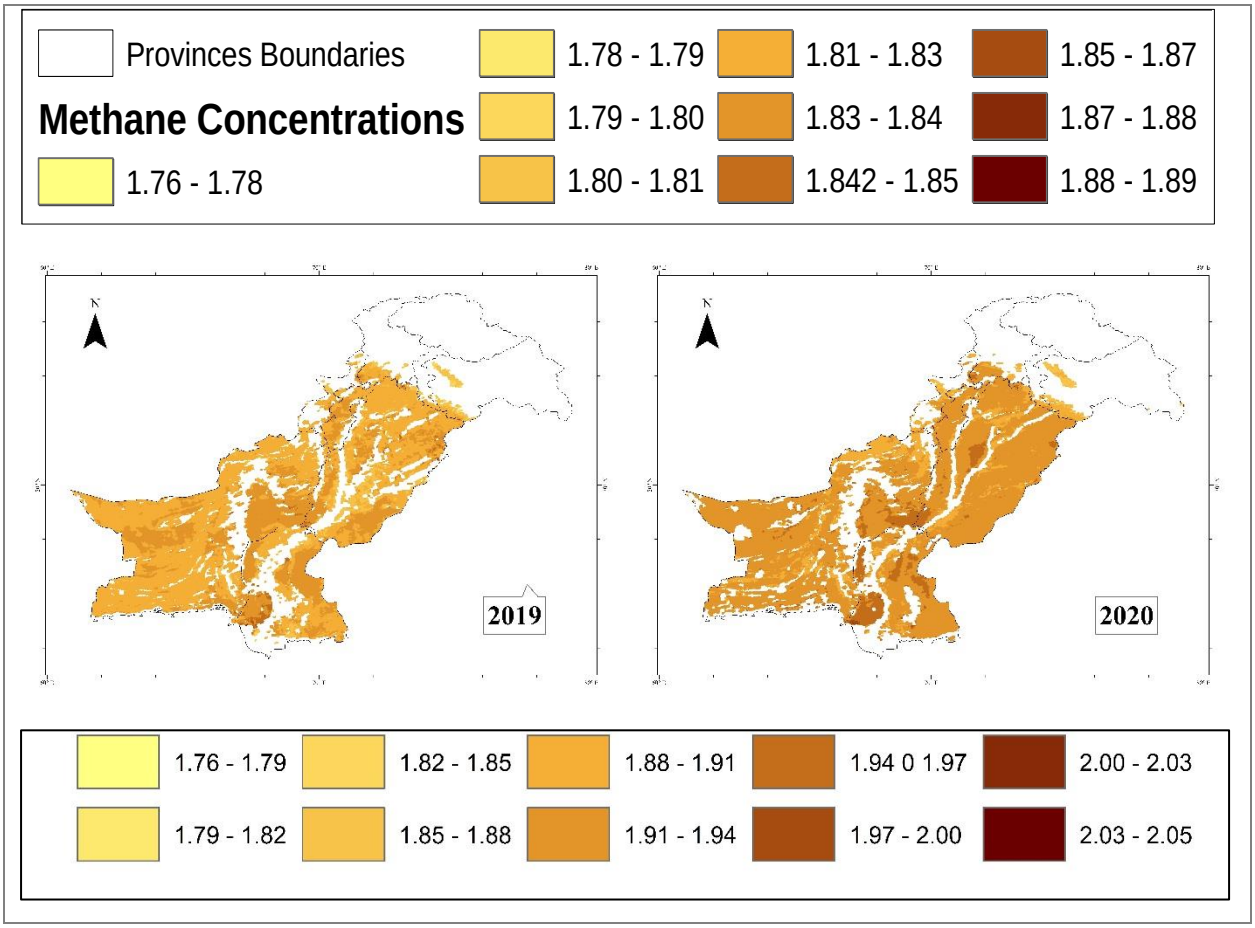

Figure 4.20: Methane Mean Concentrations (ppbv) in Rice Season over Pakistan (2009 - 2020)

The rice production is associated with methane emissions as the bacteria in flooded soil of rice fields produce large quantities of methane. The means of rice production months were calculated and mapped. The results showed the higher atmospheric CH_4 in the rice season than the annual mean concentrations. During the months of rice production, the minimum methane concentration in 2009 was 1.78 and maximum concentration was 1.80 ppbv. Whereas, in 2020, the minimum and maximum CH_4 concentrations were 1.79 and 2.02 ppbv respectively. Like annual mean maps, the south-east region of Pakistan, and India had the higher amount of CH_4 than the other regions. Indian methane emissions also influence Pakistan's atmospheric methane concentrations.

4.2.1.3. Annual Concentration Trend

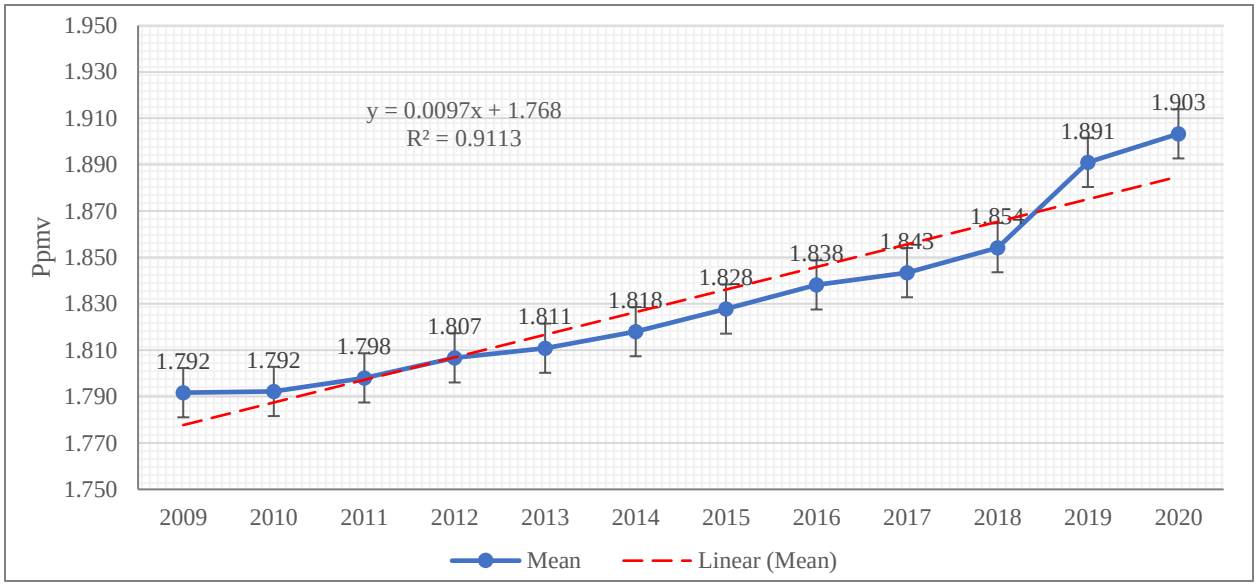

Figure 4.21: Annual CH_4 concentration trend over Pakistan (2009 - 2020)

The figure 4.21 shows an increasing annual CH_4 concentration trend over Pakistan from year 2009 to year 2020. It exhibits that the concentration has increased 0.111 ppb in 12 years; from 1.792 ppb in 2009 to 1.903 ppb in 2020. It accounts for ~6.2 % increase in these twelve years. The values in 2019 and 2020 are significantly high due to the different sensor. From 2009 to 2018, the rise is 0.062 ppb that is 3.4% increase from 2009.

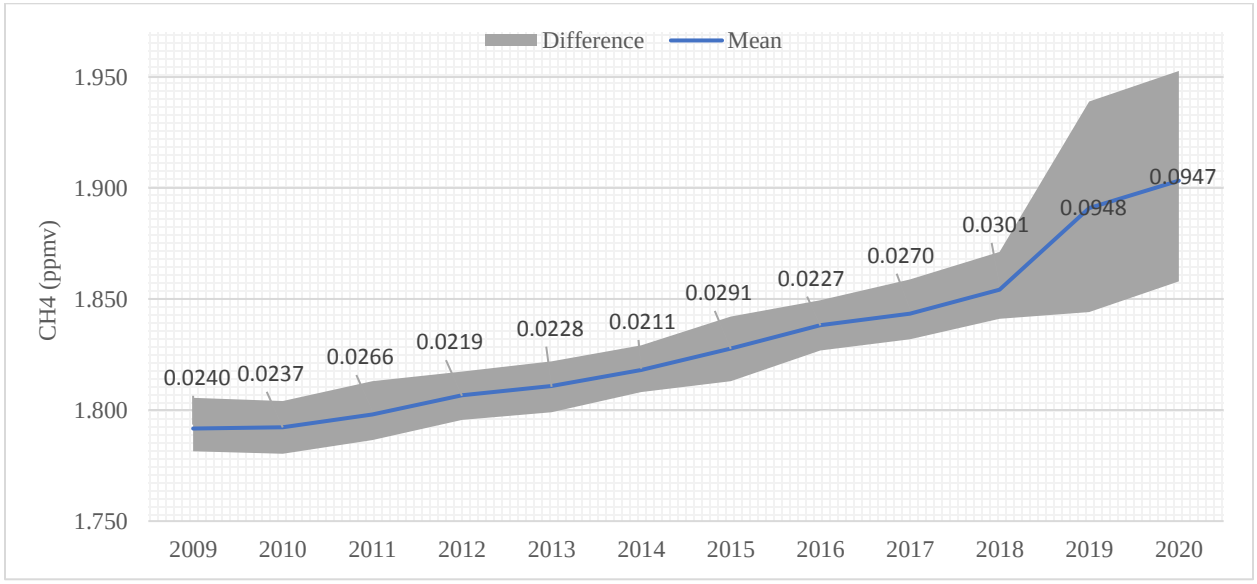

Figure 4.22: Difference between Maximum and Minimum Concentration of CH_4 (2009 - 2020)

The difference chart shows that the difference in maximum and minimum concentrations does not vary substantially in GOSAT data, whereas the year 2019 and 2020 observe large difference between maximum and minimum values. It is due to the high resolution of TROPOMI data. The maximum difference observed was in 2019 with 0.095 ppb, and the minimum difference was observed in 2014, with 0.0211 ppb.

4.2.1.4. Monthly Concentration Trend

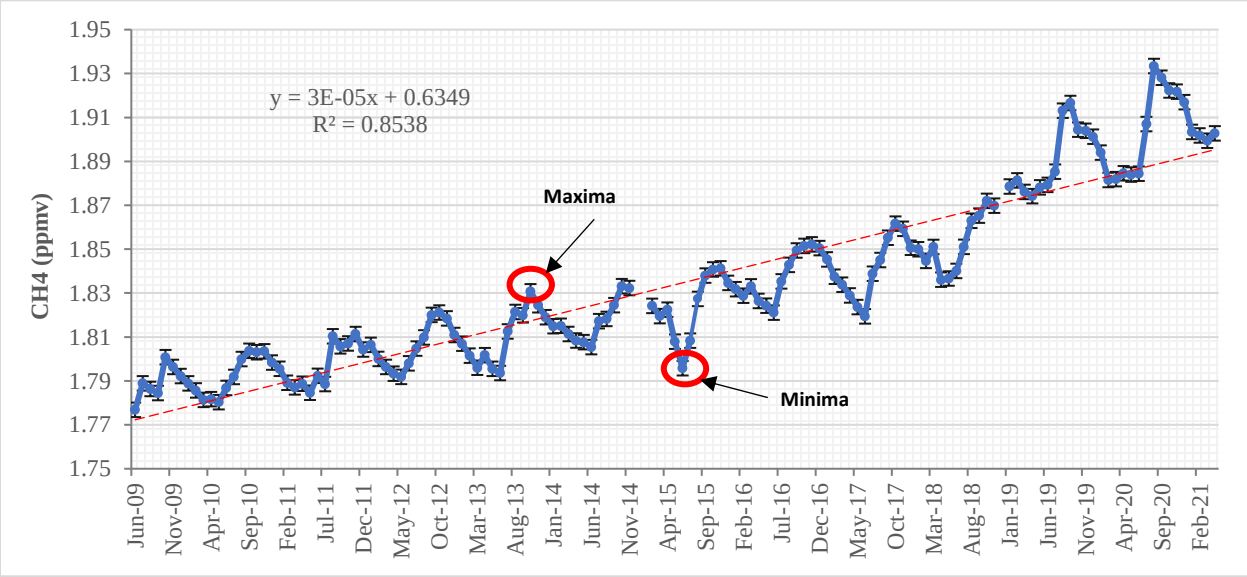

Figure 4.23: CH_4 Monthly Trend over Pakistan (Jun 2009 - April 2021)

Methane also exhibits monthly and seasonal cycle like carbon dioxide. The fig 4.23 illustrates the months with the highest and lowest concentrations of CH_4. The months of October and November are with highest concentrations that have increased over the years from 2009 to 2020. Whereas, the months of May and June are with the lowest concentrations in the monthly cycle, as mentioned in a study. (Javadinejad et al., 2019) But the GOSAT cycle doesn't follow the typical pattern of methane as demonstrated by other satellite (as mentioned in literature review). The sentinel observations (2019-2020) show the peak in August-September as per the typical monthly pattern due to rice season.

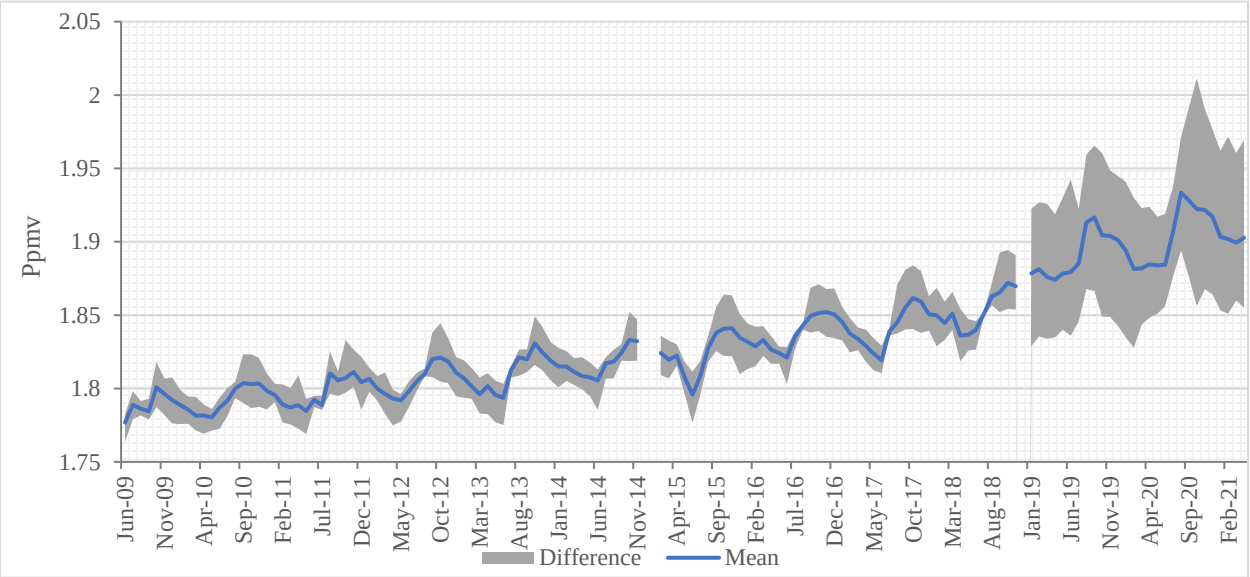

Figure 4.24: Difference between Monthly CH_4 concentrations

The monthly difference graph shows that the methane concentrations are not homogenous and consistent throughout the year. The difference between maximum and minimum methane concentrations is high in a few months, whereas the difference is negligible in the other months. The pattern of the difference is not the same from year 2009 to 2020. But the months of June, July, August, and September have the high frequency of minimum differences, though not consistent in all 12 years.

The homogeneity of methane concentrations in the months of minimum difference could be due to the seasonal patterns of temperature, and precipitation, so correlation among them was determined. The monsoon months' concentrations gave no significant R^2 values with temperature and precipitation in respective months.

4.2.1.5. Increase in Maxima and Minima

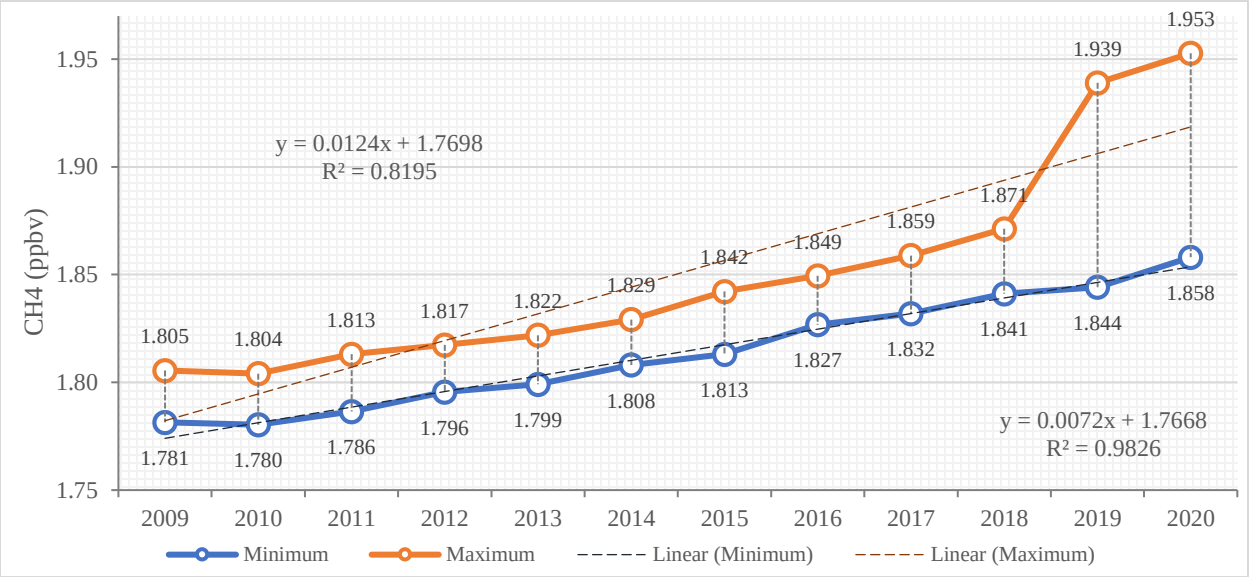

Figure 4.25: Combined Maxima and Minima of CH_4 concentrations (2009 - 2018)

The above figure (Fig. 4.25) represents the combined increase in maxima and minima of methane concentrations from 2009 to 2020. The maxima start from 1.80 ppb in 2009 and increases to the 1.95 ppbv in 2020, with the absolute increase of 0.15 ppbv in twelve years. 0.066 ppbv absolute increase from 2009 to 2018.

Similarly, the minima in 2009 is at 1.78 ppbv that reaches to 1.86 ppbv in 2020, with the absolute increase of 0.08 ppbv. 0.06 ppbv increase from 2009 to 2018. The figure also shows that the minima of Sentinel TROPOMI is in a good correspondence (almost linear) with the minima of GOSAT whereas, the maxima of both instruments have difference in their values.

4.2.1.6. Seasonal Cycles

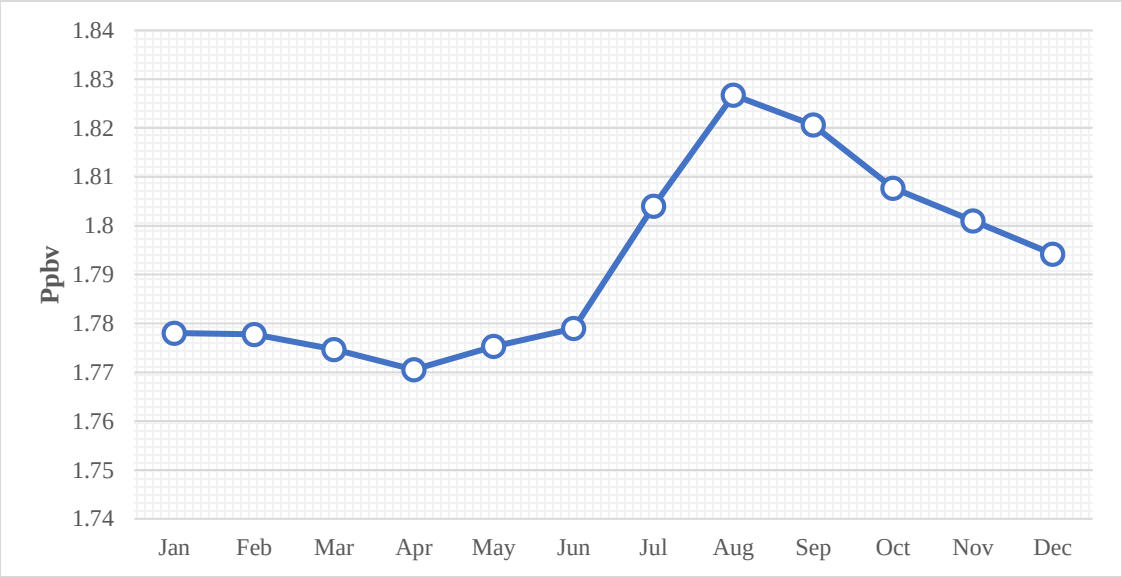

Figure 4.26: Seasonal Cycle of CH_4 within a year

The seasonal cycle of methane shows that the concentrations start to rise in the month of June and Peak in August. After August, the concentrations start decreasing till January and from January to June the pattern is almost constant. The methane cycle peaks in monsoon season whereas it lowers in post-monsoon and winter season. The reason behind it can be the rice season that is also from July to November in Pakistan.

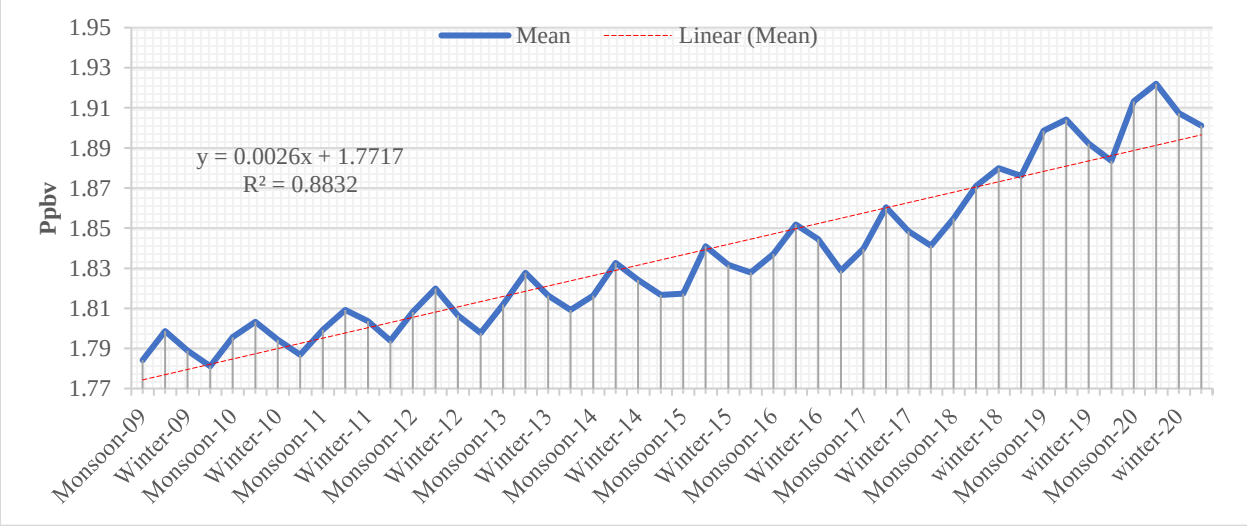

Figure 4.27: Seasonal Variation of CH_4 Concentration over Pakistan (2009-2020)

Fig. 4.27 represents seasonal variation of CH_4 over Pakistan from 2009-2020. It can be seen that each year the methane concentrations are at their maximum values in monsoon and post-monsoon season, whereas the concentrations are lower in winter and pre-monsoon period.

The bar chart below shows the increase in mean concentrations of methane in four seasons from 2009 to 2020. The CH_4 concentrations have increased in all seasons in 12 years. The maximum increase is observed in post-monsoon and minimum in pre-monsoon.

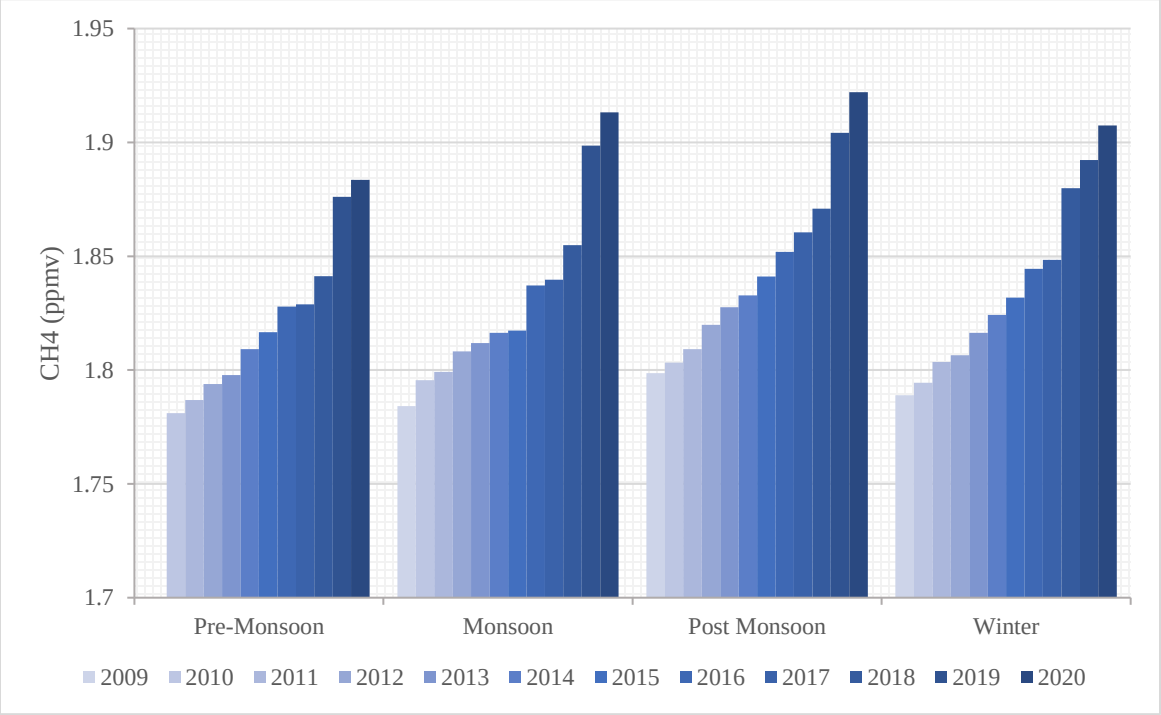

Figure 4.28: Seasonal Trend over the Years 2009-2020

4.2.1.7. Rice Season Trends

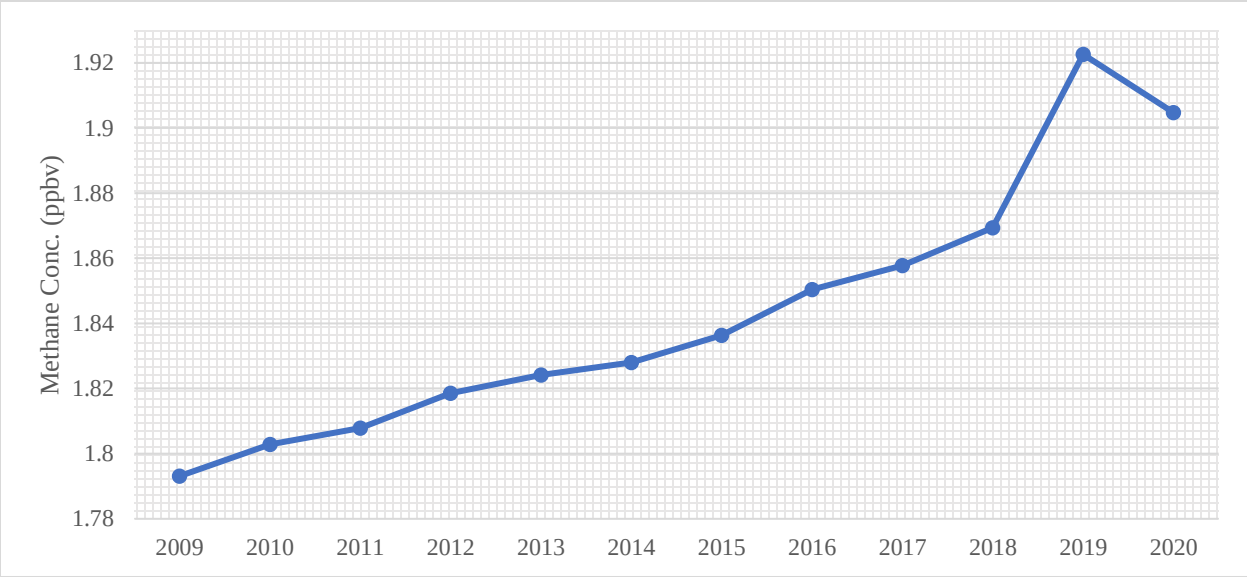

Figure 4.29: Rice Season Trend (July-Nov) 2009-2020

Fig. 4.30 presents the graph of CH_4 concentrations during the rice season in Pakistan, i.e. July to November, from 2009 to 2020. The concentration starts from 1.79 ppbv in 2009 and reaches to the level of 1.90 ppbv in 2020. The absolute increase is 0.11 in these 12 years. The highest value of 1.92 ppbv observed in year 2019. From 2009 to 2018, the increase is 0.076 ppbv, that is ~4% from 2009.

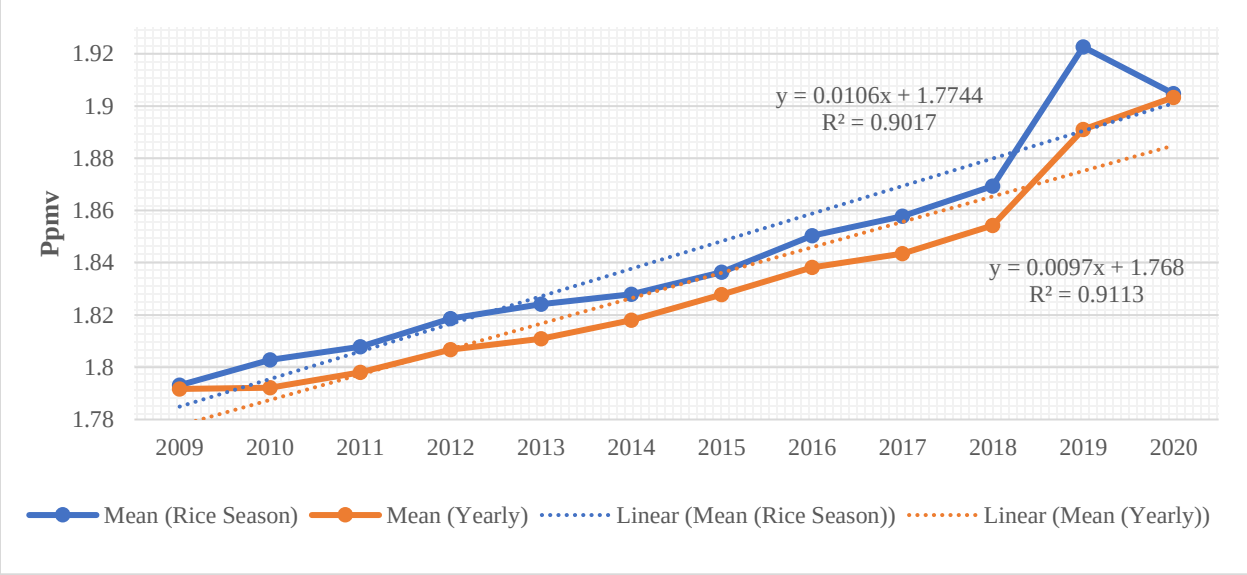

Figure 4.30: Comparison between Yearly Means and Rice Season (2009 - 2020)

There is a combined graph (figure 4.31) of methane concentrations in a year and in the rice season. The increasing trend is similar, and the methane values are high in the rice season.

4.2.2. ARIMA Model Forecasting

The SCIAMACHY's data was used to extend our data for forecasting purpose in addition to GOSAT data. Fig. 4.32 shows a good correspondence between these data sets. The GOSAT's data values are in a good correlation with SCIAMACHY's forecasted values over 2009 to 2018.

The Sentinel TROPOMI dataset had only values for two years with significant higher values than that of GOSAT's, and its inclusion in ARIMA model didn't provide results with high confidence levels and less bias. The Sentinel values haven't been used in our ARIMA model to have the forecasted values with less error.

To forecast CH_4 concentrations for the upcoming years, the ARIMA model has been used. The model parameters (p, d, q) were taken as (4, 2, 2). The difference of 2 was taken to make the model stationary. The CH_4 levels are forecasted to year 2100 (82 years from 2018). The results (fig. 4.33) show that the concentrations will increase up to 2.47 ± 0.086 ppb in 2100 with 95 % confidence interval, that is 33% rise from 2018.

To validate our results, the ARIMA forecasted observations are correlated with the actual observations. The R^2 value is 0.99 between them with significance level $\alpha = 0.05$.

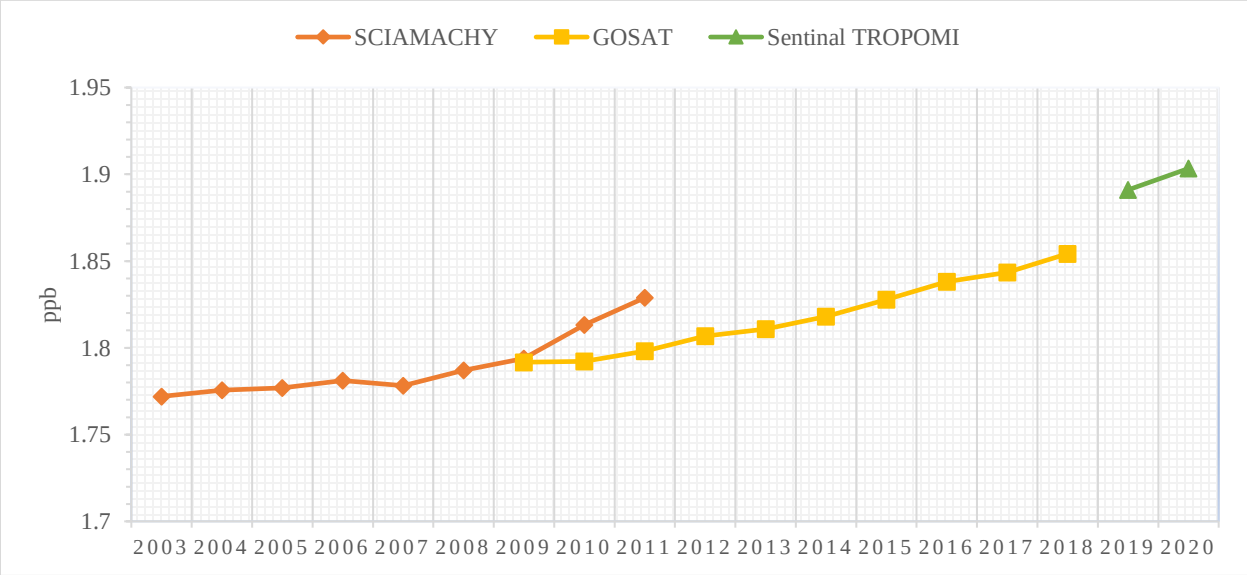

Figure 4.31: SCIAMACHY and GOSAT 's methane concentration (2003 - 2020)

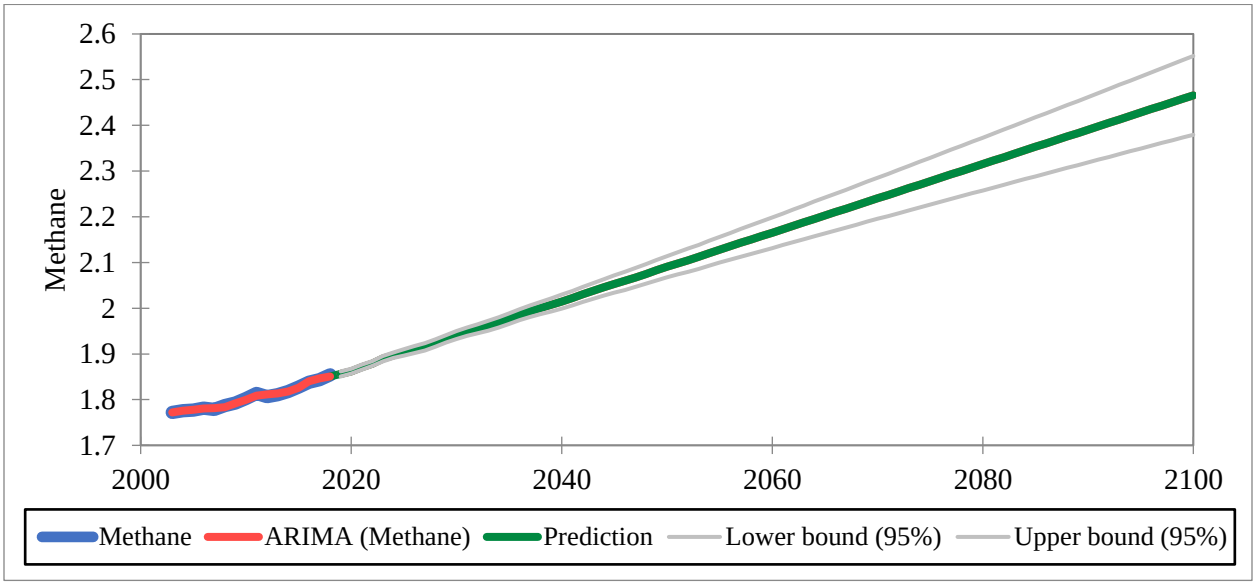

Figure 4.32: ARIMDA Model Forecasting for Methane Conc. (82 years' forecasting) – (4,2,2)

4.2.3. Emission Inventories: Sectoral emissions' data

4.2.3.1. Selection of the Emission Inventory

The data of multiple inventories were downloaded and compared with the locally produced data by the inventory of Global Change Impact Studies Centre (GCISC). Among REAS, EDGAR and CEDS, the GCISC inventory observations were in a good correlation with the EDGAR v4.3.2 and REAS 025x025. The REAS data was available for a shorter period than the EDGAR one. So, EDGAR v4.3.2 was selected for further analysis. (Fig 4.34)

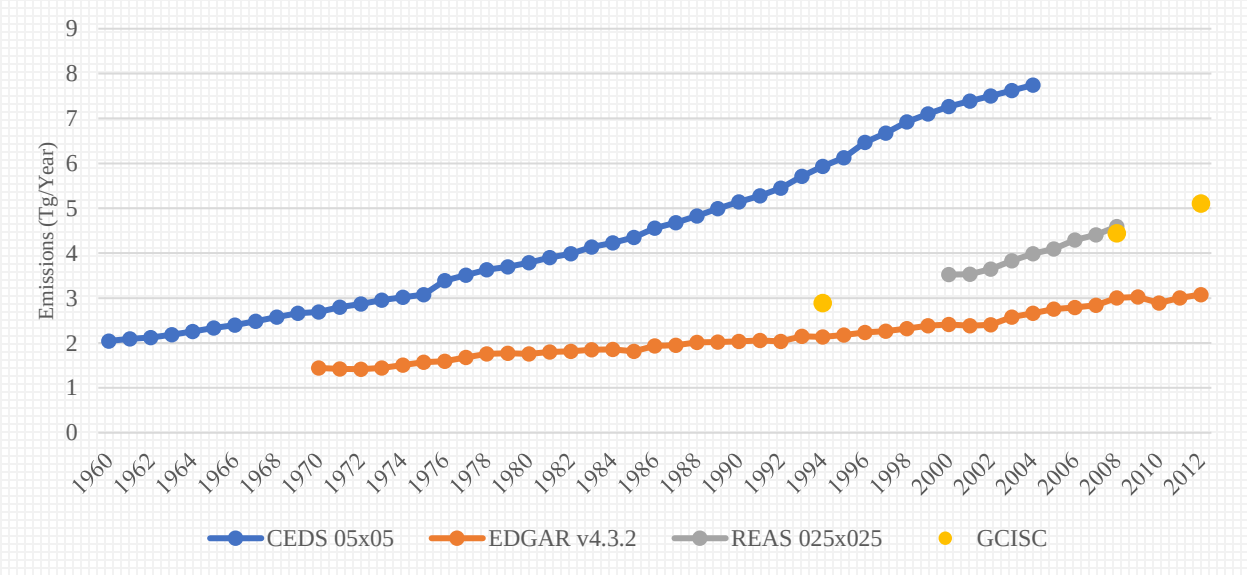

Figure 4.33: Inventories' data Comparison

4.2.3.2. Edgar v 4.3.2 (01x01)

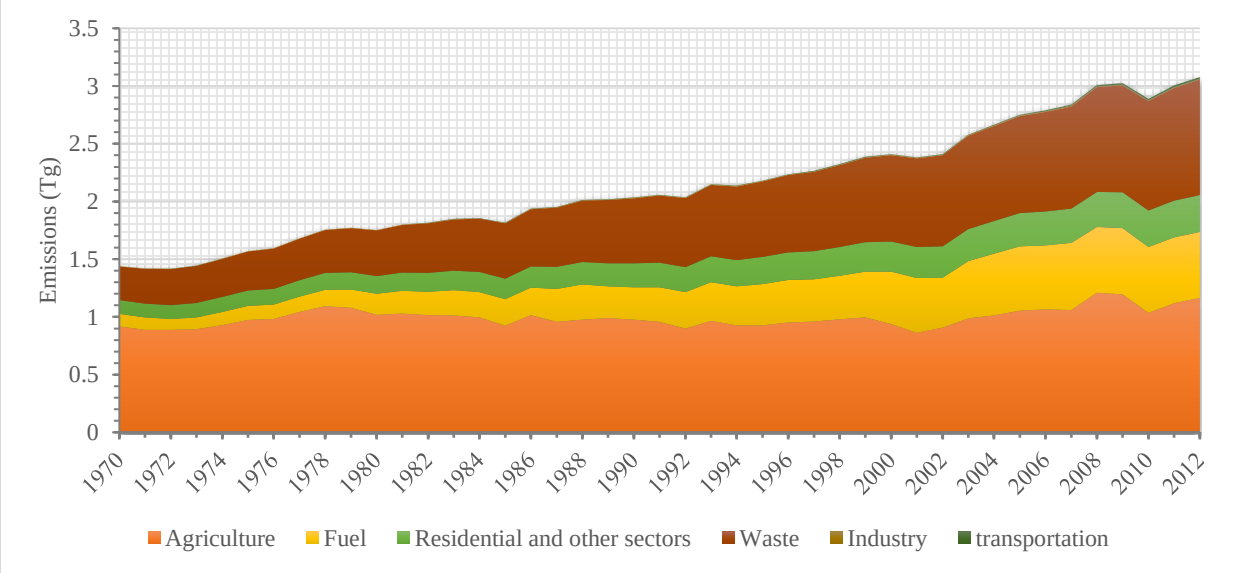

Figure 4.34: EDGAR v4.3.2 - Methane Emissions

Figure 4.35 is the stacked graph of sectoral emissions of methane by Edgar inventory v4.3.2. According to the results, agriculture sectoral is the most responsible for methane emissions then comes fuel, residential, and waste sector. The emissions from industries and transportation are not significant. The agricultural emissions are almost constant through all these years, whereas

emissions from waste, fuel, and residential have an increasing trend from 1.44 Tg in 1970 to 3.06 Tg in 2012.

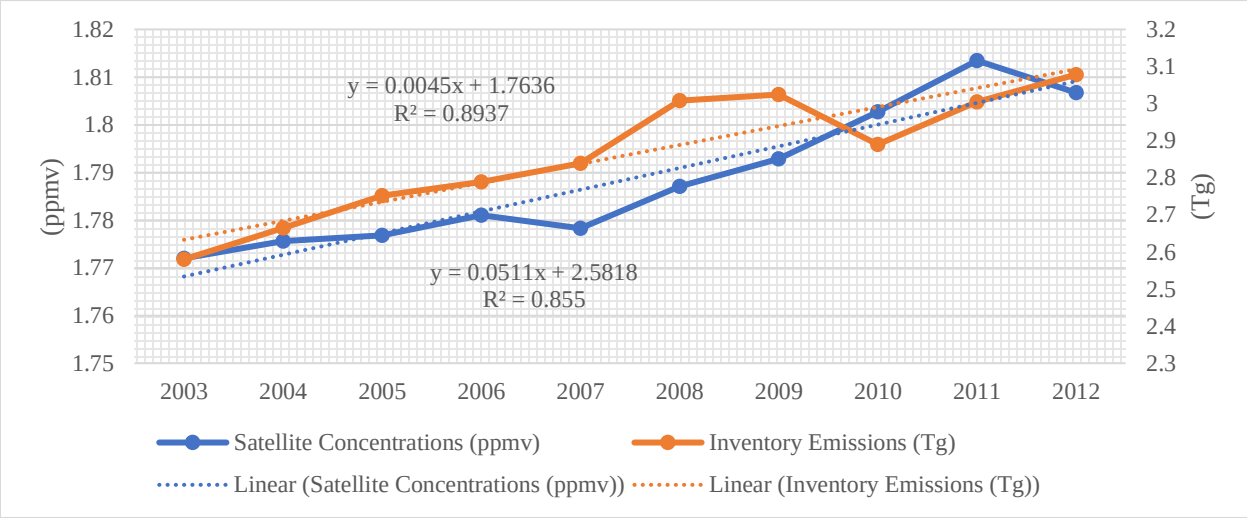

Figure 4.35: Combined satellite and inventory data (Methane)

Figure 4.36 is a combined graph of satellite monitored methane atmospheric concentration and methane inventory emissions. The trend of both, concentrations and emissions are rising till 2012. The R^2 value between these two datasets is 0.6473. The correlation value is not so high because atmospheric concentrations depend on other factors like the natural sources and sinks, chemistry of methane in the atmosphere, its lifecycle, and its reaction with the other gases, whereas emissions are the unit of anthropogenic addition of methane in the atmosphere.

4.2.4. Sectoral data of development/industrial activities in Pakistan – Regression Analysis with Inventory data

Table 4: R-values – PBS data and Edgar Emission Sectors

	Edgar Agriculture	Edgar Fuel	Edgar Residential	Edgar Industry	Edgar Waste	Edgar Transportation
Livestock	**0.83** *(p<0.05)*	-	-	-	**1** *(p<0.05)*	-
Crop Area	0.78	-	-	-	0.39	-
Rice Area	0.79	-	-	-	-	-
Rice Production	**0.93**	-	-	-	-	-

	(p<0.05)					
Gas Production	-	**0.96** *(p<0.05)*	-	-	-	-
Crude Oil Extraction	-	0.65	-	-	-	-
Gas Extraction	-	0.96	-	-	-	-
Gas Consumption	-	-	**0.87** *(p<0.05)*	-	-	**0.77** *(p<0.05)*
Mineral & Coal Extraction	-	-	-	**0.91** *(p<0.05)*	-	-

The table 4 correlates the data presented by Pakistan Bureau of Statistics (PBS) and Edgar's data. The correlation between different sectors is high. The correspondence between values suspects that the emission inventory has utilized the PBS data to estimate emissions. This can also explain the difference with satellite measured concentrations if studied more deeply. The waste sector and livestock give R-value of 1, that shows the one dataset has been used to derive other. The other R-values between different sectors are also good that represents the high correspondence between these two datasets.

4.2.5. Statistical analysis of Satellite-based emissions with various factors

Table 5:R-values of Satellite and Inventory data with multiple factors

	GOSAT CH_4 Concentrations	CH_4 Emissions (Edgar)
Rice Production (FAO)	0.80	**0.93** *(p<0.05)*
Mean Temperature	0.28	0.56
Mean Precipitation	-0.14	-0.11
GDP	**0.98** *(p<0.05)*	**0.94** *(p<0.05)*
Population	**0.99** *(p<0.05)*	**0.99** *(p<0.05)*
Mean NDVI (>0.3)	0.61	-0.61

Satellite driven atmospheric concentrations and inventory driven emissions of methane were also correlated with various factors to draw a relationship among them. The rice production statistics by FAO showed a good correlation with Edgar inventory emissions but poor correlation with satellite concentrations. Temperature and precipitation exhibit no correlation at all. Both may show

seasonal patterns with emissions and concentrations and a yearly mean fails to exhibit relation among them. For such analysis, use of monthly data may add to the results. Same goes with NDVI where correlation values are poor probably due to annual means. GDP and population show a strong correlation with both, emissions and concentrations. Increase in population and GDP represents the increased development activity and urbanization that play a major role in increase in emissions and concentrations of CH_4 in the atmosphere. The inventory data is based upon the development activities data, so the high correlation between them is suspected. The satellite observed methane concentrations are in a high correlation with GDP and population that validates the satellite data.

4.2.6. NDVI as a measure of sink

NDVI was also used as a measure of sink for methane. The R^2 values between satellite observations of methane concentrations and NDVI is 0.018. Since the forests and vegetation act as both source and sink, it is difficult to draw a relationship of NDVI as a sink, plus NDVI values' mean over yearly basis might not be enough to investigate the matter. Rice paddies and other methane emitting vegetations also undermine the role of soils acting as sink of methane. NDVI also depends on various factors, and its value might not be a good indication of soil uptake of methane.

Methane's seasonal cycle has been combined with NDVI seasonal cycle to study their seasonal pattern. Fig 4.37 explains their seasonality and variability of peaks between these two datasets.

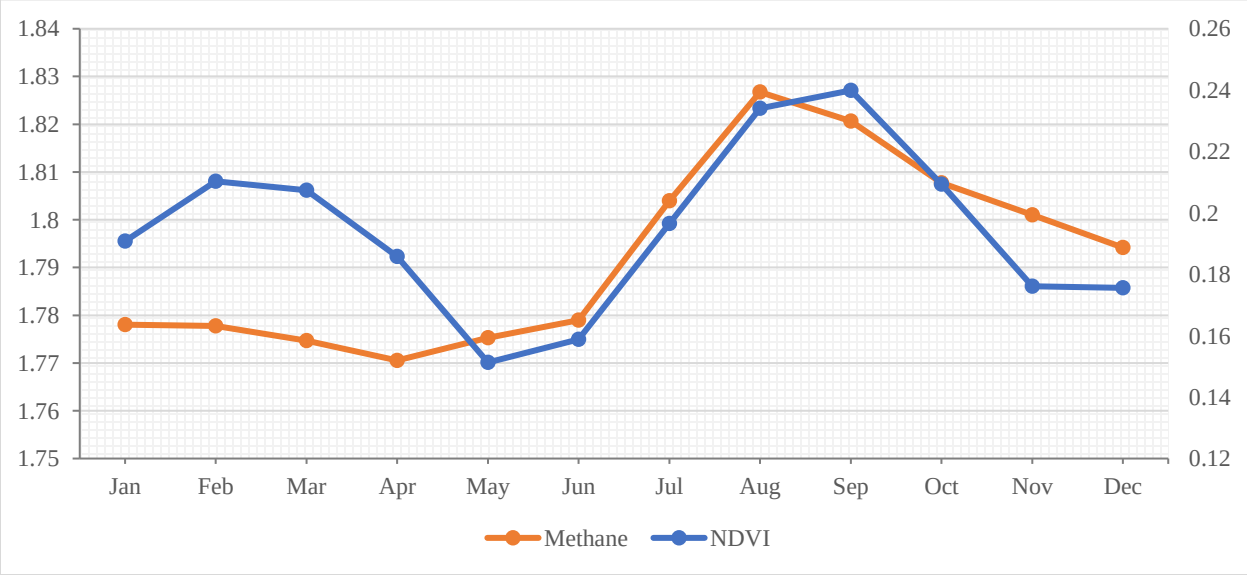

Figure 4.36: Methane Seasonal Cycle vs NDVI seasonal cycle

The both cycles show a similar trend, that starts to peak from June till August-September, and then declines till Summer. The behavior shows that the methane emission peaks when vegetation also increased, and similarly emissions decrease when NDVI starts decreasing as well. The behavior shows that the forests, vegetation and other plantation play a greater role in emitting methane than acting as a methane sink. The quantification of sink is difficult, and its role is undermined by the influence of methane emissions through soil sources. The study of such behavior may pose meaningful result for quantifying NDVI as sink if regions of rice paddies, wetlands etc. are excepted from the study area.

4.2.7. Temperature with Seasonal Cycle of Methane

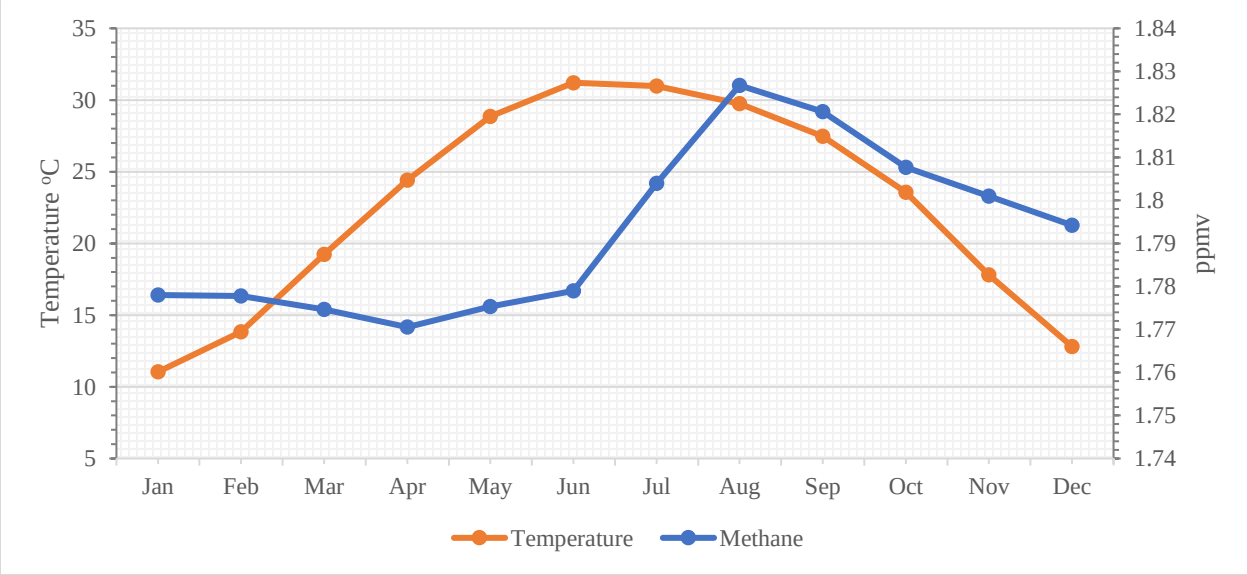

Figure 4.37: Temperature Seasonal Variation and Methane Seasonal Cycle

Figure 4.37 shows temperature and methane's seasonal cycles on different axis. The graph exhibits that the methane concentrations and temperature follow a similar pattern in most of year. From March, the both start increasing till monsoon. The temperature peaks in the month of June, whereas methane atmospheric concentrations peak in August. From August, both entities show a decreasing trend till January. The plot shows an impact of temperature on methane concentrations to some extent, but small-scale regional seasonality might provide better and comprehensive results instead of these country-wise means. (Gao et al., 2011)

4.3. Nitrous Oxide

4.3.1. Inventories: Sectoral emissions' data

4.3.1.1. Selection of Inventory

The data of multiple inventories were downloaded and compared with the locally produced data by the inventory of Global Change Impact Studies Centre (GCISC). Among GFAS, EDGAR and REAS, the GCISC inventory observations were in a good correlation (among 3) with the EDGAR v4.3.2. EDGAR v4.3.2 was selected for further analysis.

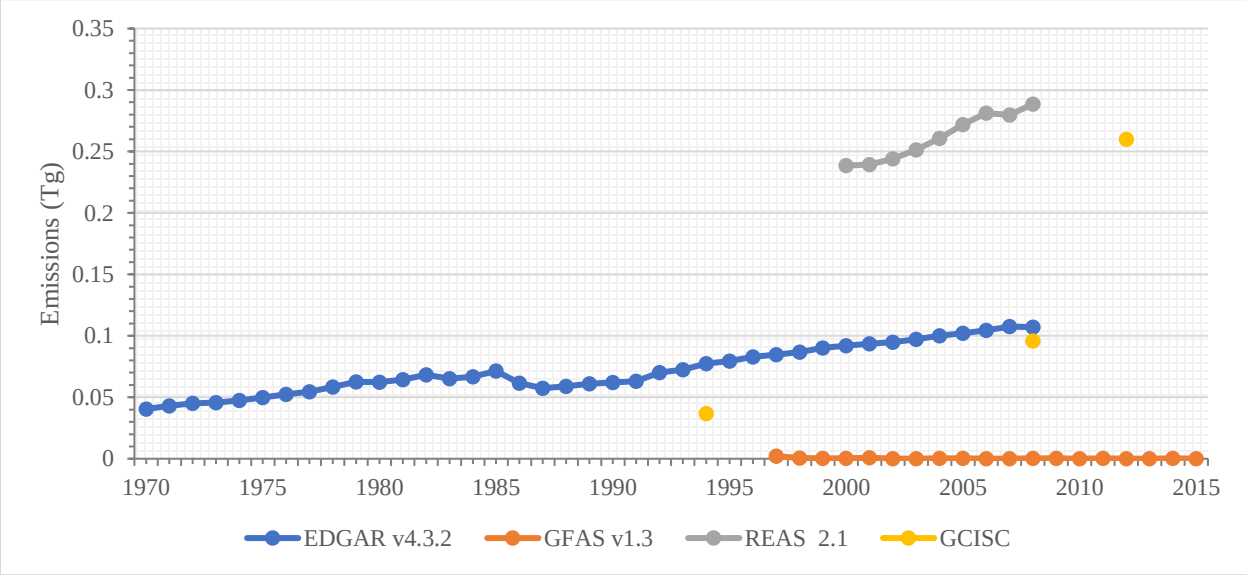

Figure 4.37: Inventories' data Comparison

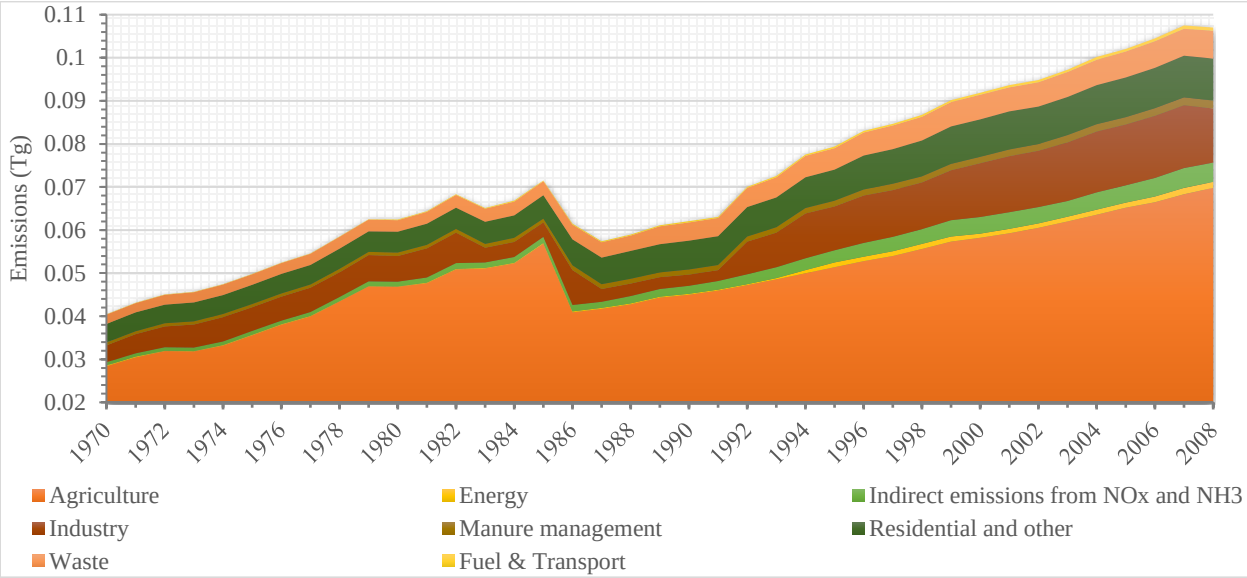

Figure 4.38: Nitrous Oxide Emissions - Edgar v4.3.2

Fig. 38 shows the stacked emissions of nitrous oxide by different sectors from 1970 to 2008. Agriculture sector is the most responsible for the N_2O emissions due to the use of nitrogen fertilizers. Then comes industrial emissions and residential emissions. Waste sector, animal manure and indirect emissions from NOx and NH_3 also play important role in nitrous oxide emissions. Energy sector, fuel and transport are the least responsible for nitrous oxide emissions in this case. The emissions were 0.04 Tg in 1970 that has reached upto 0.11 in 2008 that is 175% rise in nitrous oxide emissions since 1970. The absolute increase is 0.07 Tg in all these years.

Table 6: R-values – PBS data and Edgar Emission Sectors

	Edgar Agriculture	Edgar Energy	Edgar Transport	Edgar Industry	Edgar Manure Management
Nitrogen Fertilizers	0.82	-	-	-	-
Crop Area	**0.96** *(p<0.05)*	-	-	-	-
Energy Consumption	-	0.67	-	**0.82** *(p<0.05)*	-
Total Livestock	-	-	-	-	**1** *(p<0.05)*
No. of Vehicles	-	-	**0.96** *(p<0.05)*	-	-
Mineral & Coal Extraction	-	-	-	0.37	-
Aviation Route	-	-	0.63	-	-

The table 4 correlates the data presented by Pakistan Bureau of Statistics (PBS) and Edgar's data. The correlation between different sectors is high. The Edgar agriculture and PBS stats of crop give the value of R= 0.96. Similarly, transport sector and PBS vehicles stats return the R-value of 0.96. Edgar manure management and total livestock data by PBS return the value of R equals to 1. The correspondence between values suspects that the emission inventory has utilized the PBS data to estimate emissions. The poor correlation value between industrial emissions and mineral and coal extraction data by PBS shows that there are other industrial emissions that are responsible for nitrous oxide emissions not the mineral and coal extraction industry.

Table 7: R-values of Inventory data with multiple factors

	N_2O Emissions (Edgar)
Mean Temperature	0.54
Mean Precipitation	-0.14
GDP	**0.90** *(p<0.05)*
Population	**0.95** *(p<0.05)*

The inventory data was correlated with temperature, precipitation, GDP and population statistics. The temperature and precipitations' yearly mean gives very poor correlation with emissions. To draw their relationship, the monthly analysis might be needed to assess seasonal cycles. The GDP shows a good correlation value of 0.90. The population gives value of R equals to 0.95 with emissions. It is very interesting that the sum of sectors in emissions data is significantly explained by the population rise.

Chapter 5 : Conclusion & Recommendations

5.1. Conclusions

The conclusion of the study are as follows:

1. The carbon dioxide is increased ~8.2% from 2002 to 2016. It accounts for ~30.5 ppm increase in absolute concentrations over 15 years. The seasonal cycle of CO_2 shows the peak in spring season and decrease in fall season. The ARIMA forecast model showed that the concentrations will increase up to 549 ppm in 2100 with 95 % confidence interval, that is 38.8% increase from year 2013. Emission inventory, CEDS, showed the increasing trend of carbon dioxide emissions from ~110 Tg in 2000 to ~175 Tg in 2014. Carbon dioxide emissions mainly come from energy, industry, transport, and residential sector. There is a good correspondence between satellite dataset and CEDS emissions, with R^2 value of 0.847.

Loss of forest cover that act as a major sink has also caused rise in carbon dioxide atmospheric concentrations. The NDVI and CO_2 seasonal cycle showed the behavior of vegetation as a sink, but quantifying vegetation as a sink by using NDVI does not provide significant results.

2. The methane is increased ~6.2% from 2009 to 2020. It accounts for ~1.9 ppb increase in absolute concentrations over the period of 12 years. The concentrations peak in the months of June to August as a result of rice cultivation. The ARIMA forecast model showed that the concentrations will increase up to 2.47 ppb in 2100 with 95% confidence interval, that is 33% rise from 2018. Emission inventory, EDGAR, showed the increasing trend of methane emissions from 1.44 Tg in 1970 to 3.06 Tg in 2012. Agriculture, waste, fuel, and residential sectors are primarily responsible for methane emissions. The two datasets, satellite's and inventory emissions, do not correspond well with each other with R^2 value of 0.65. Quantifying NDVI as a measure of sink of methane is not significant as vegetation and forests' methane chemistry involves emissions and sinks both simultaneously making it more complex for quantification.

3. The emissions of nitrous oxide also show an increasing trend. The emissions were 0.04 Tg in 1970 that has reached up to 0.11 in 2008 that is 175% rise in nitrous oxide emissions since 1970. The absolute increase is 0.07 Tg in all these years. Nitrous oxide predominantly comes from agriculture, industry, residence, and waste sector.

The quantification of sinks can be complex as both processes simultaneously happen by the same environmental entities. The emissions cannot always show a causal relationship with atmospheric concentrations due to the chemistry involved in the behavior of these gases. The results showed the undeniable increase in the emissions and atmospheric concentrations of all three GHGs with the passage of time. This increase is alarming for a country like Pakistan. The population expansion and growing development activities have caused the rise in the GHG emissions.

5.2. Recommendations

The recommendations are as follows:

1. Normalized difference Soil Index (NDSI) should be calculated and checked as a measure of sink for methane.
2. Data should be kept consistent for such analysis; inclusion of multiple sensors increases the non-linearity of the data.
3. The shortcomings of the present study in terms of unavailability of data necessitate the urgent creation of a national level inventory for GHGs to collect and store reliable data for future analysis. The authenticity of available data, national and international, should also be examined and validated through local measurements.
4. The small-scale studies should be carried out for detailed analysis of sources, sinks, and atmospheric concentrations.
5. Preventive measures should be taken immediately for the mitigation of GHGs in order to prevent Pakistan from the catastrophic consequences of increased amounts of GHGs in the atmosphere in the future.
6. The development activities should be regulated in different sectors ensuring the minimum emissions of GHGs and maximum efficiency.
7. Forests should be protected on priority basis and should be expanded on the national scale.
8. This study should be extended further for the later years, and by including the remaining GHGs as well.

References

Al-Ghussain, L., 2019. Global warming: review on driving forces and mitigation. Environmental Progress & Sustainable Energy 38, 13–21.

Boden, T., Andres, R., Marland, G., 2015. Global, Regional, and National Fossil-Fuel CO2 Emissions (1751 - 2011) (V. 2015). https://doi.org/10.3334/CDIAC/00001_V2015

Brimblecombe, P., 1996. Air Composition and Chemistry. Cambridge University Press.

Chandra, N., Hayashida, S., Saeki, T., Patra, P.K., 2017. What controls the seasonal cycle of columnar methane observed by GOSAT over different regions in India? Atmospheric Chemistry and Physics 17, 12633–12643.

Chaudhry, Q.U.Z., 2017. Climate Change Profile of Pakistan. Asian Development Bank. http://dx.doi.org/10.22617/TCS178761

Choi, J.H., Joo, S.M., Um, J.S., 2013. Evaluating Cross-correlation of GOSAT CO 2 Concentration with MODIS NDVI Patterns in North-East Asia. Spatial Information Research 21, 15–22.

Climate Risk Profile: Pakistan [WWW Document], n.d. . Climatelinks. URL https://www.climatelinks.org/resources/climate-change-risk-profile-pakistan (accessed 4.7.20).

Crippa, M., Guizzardi, D., Muntean, M., Schaaf, E., Dentener, F., van Aardenne, J.A., Monni, S., Doering, U., Olivier, J.G., Pagliari, V., 2018. Gridded emissions of air pollutants for the period 1970–2012 within EDGAR v4. 3.2. Earth Syst. Sci. Data 10, 1987–2013.

Field, C.B., Raupach, M.R., 2012. The Global Carbon Cycle: Integrating Humans, Climate, and the Natural World. Island Press.

Gao, Z., Yuan, H., Ma, W., Li, J., Liu, X., Desjardins, R., 2011. Diurnal and Seasonal Patterns of Methane Emissions from a Dairy Operation in North China Plain. Advances in Meteorology 2011. https://doi.org/10.1155/2011/190234

Greenhouse Gas Emissions Factsheet: Pakistan [WWW Document], n.d. . Climatelinks. URL https://www.climatelinks.org/resources/greenhouse-gas-emissions-factsheet-pakistan (accessed 4.7.20).

Guo, M., Wang, X.-F., Li, J., Yi, K.-P., Zhong, G.-S., Wang, H.-M., Tani, H., 2013. Spatial distribution of greenhouse gas concentrations in arid and semi-arid regions: A case study in East Asia. Journal of Arid Environments 91, 119–128. https://doi.org/10.1016/j.jaridenv.2013.01.001

Heiden, P., 2011. Pakistan. ABDO.

Heilig, G.K., 1994. The greenhouse gas methane (CH 4): Sources and sinks, the impact of population growth, possible interventions. Population and environment 16, 109–137.

Hoesly, R.M., Smith, S.J., Feng, L., Klimont, Z., Janssens-Maenhout, G., Pitkanen, T., Seibert, J.J., Vu, L., Andres, R.J., Bolt, R.M., 2018. Historical (1750-2014) anthropogenic emissions of reactive gases and aerosols from the Community Emission Data System (CEDS). Geoscientific Model Development 11, 369–408.

Hopali, E., Cakmak, A., 2020. PREDICTION OF DAILY CO2 EMISSIONS OF A FACTORY USING ARIMA AND HOLT-WINTERS SEASONAL METHODS. Business and Management 12.

Hu, H., Landgraf, J., Detmers, R., Borsdorff, T., Aan de Brugh, J., Aben, I., Butz, A., Hasekamp, O., 2018. Toward global mapping of methane with TROPOMI: First results and intersatellite comparison to GOSAT. Geophysical Research Letters 45, 3682–3689.

Hussain, M., Butt, A.R., Uzma, F., Ahmed, R., Islam, T., Yousaf, B., 2019. A comprehensive review of sectorial contribution towards greenhouse gas emissions and progress in carbon capture and storage in Pakistan. Greenhouse Gases: Science and Technology 9, 617–636.

INDC PAKISTAN mocc, n.d.

IPCC, 2014, n.d. . IPCC, 2014: Climate Change 2014: Synthesis Report. Contribution of Working Groups I, II and III to the Fifth Assessment Report of the Intergovernmental Panel on Climate Change [Core Writing Team, R.K. Pachauri and L.A. Meyer (eds.)]. IPCC, Geneva, Switzerland, 151 pp. URL https://www.ipcc.ch/report/ar5/syr/ (accessed 1.28.20).

Javadinejad, S., Eslamian, S., Ostad-Ali-Askari, K., 2019. Investigation of monthly and seasonal changes of methane gas with respect to climate change using satellite data. Applied Water Science 9. https://doi.org/10.1007/s13201-019-1067-9

Jonai, H., Takeuchi, W., 2014. Comparison between global rice paddy field mapping and methane flux data from GOSAT, in: 2014 IEEE Geoscience and Remote Sensing Symposium. Presented at the 2014 IEEE Geoscience and Remote Sensing Symposium, pp. 2098–2101. https://doi.org/10.1109/IGARSS.2014.6946879

Keenan, T.F., Williams, C.A., 2018. The terrestrial carbon sink. Annual Review of Environment and Resources 43, 219–243.

Kirk-Davidoff, D., 2018. Chapter 3.4 - The Greenhouse Effect, Aerosols, and Climate Change, in: Török, B., Dransfield, T. (Eds.), Green Chemistry. Elsevier, pp. 211–234. https://doi.org/10.1016/B978-0-12-809270-5.00009-1

Kivimäki, E., Lindqvist, H., Hakkarainen, J., Laine, M., Sussmann, R., Tsuruta, A., Detmers, R., Deutscher, N.M., Dlugokencky, E.J., Hase, F., 2019. Evaluation and analysis of the seasonal cycle and variability of the trend from gosat methane retrievals. Remote Sensing 11, 882.

Lamb, W.F., Wiedmann, T., Pongratz, J., Andrew, R., Crippa, M., Olivier, J.G., Wiedenhofer, D., Mattioli, G., Al Khourdajie, A., House, J., 2021. A review of trends and drivers of greenhouse gas emissions by sector from 1990 to 2018. Environmental Research Letters.

Lorente, A., Borsdorff, T., Butz, A., Hasekamp, O., Schneider, A., Wu, L., Hase, F., Kivi, R., Wunch, D., Pollard, D.F., 2021. Methane retrieved from TROPOMI: improvement of the data product and validation of the first 2 years of measurements. Atmospheric Measurement Techniques 14, 665–684.

Lv, Z., Shi, Y., Zang, S., Sun, L., 2020. Spatial and Temporal Variations of Atmospheric CO2 Concentration in China and Its Influencing Factors. Atmosphere 11, 231.

Mahmood, I., Iqbal, M.F., Shahzad, M.I., Waqas, A., Atique, L., 2016. Spatiotemporal monitoring of CO2 and CH4 over Pakistan using Atmospheric Infrared Sounder (AIRS). International Letters of Natural Sciences 58.

Malik, A., Hussain, E., Baig, S., Khokhar, M.F., 2020. Forecasting CO2 emissions from energy consumption in Pakistan under different scenarios: The China–Pakistan economic corridor. Greenhouse Gases: Science and Technology 10, 380–389.

Mir, K.A., Ijaz, M., 2016. Greenhouse Gas Emission Inventory of Pakistan for the Year 2011-2012 GCISC-RR-19, 150.

Mir, K.A., Purohit, P., Mehmood, S., 2017. Sectoral assessment of greenhouse gas emissions in Pakistan. Environmental Science and pollution research 24, 27345–27355.

Mossa, H.A., Ahmed, H.S., Rajab, J.M., 2012. Analysis of Troposphere Carbon Dioxide in IRAQ from Atmosphere Infrared Sounder (AIRS) data: 2010-2011. Journal of University of Babylon 22, 524–531.

Mousavi, S.M., Falahatkar, S., 2020. Spatiotemporal distribution patterns of atmospheric methane using GOSAT data in Iran. Environ Dev Sustain 22, 4191–4207. https://doi.org/10.1007/s10668-019-00378-5

NASA GISS: NASA Goddard Institute for Space Studies [WWW Document], n.d. URL https://www.giss.nasa.gov/ (accessed 1.28.20).

Nyoni, T., Bonga, W.G., 2019. Prediction of co2 emissions in india using arima models. DRJ-Journal of Economics & Finance 4, 01–10.

Ozturk, S., Ozturk, F., 2018. Forecasting energy consumption of Turkey by Arima model. Journal of Asian Scientific Research 8, 52.

Pakistan Bureau of Statistics [WWW Document], n.d. URL http://www.pbs.gov.pk/ (accessed 1.30.20).

Pakistan Meteorological Department [WWW Document], n.d. URL http://www.pmd.gov.pk/en/ (accessed 4.13.20).

Parker, R., Boesch, H., Cogan, A., Fraser, A., Feng, L., Palmer, P.I., Messerschmidt, J., Deutscher, N., Griffith, D.W., Notholt, J., 2011. Methane observations from the Greenhouse Gases Observing SATellite: Comparison to ground-based TCCON data and model calculations. Geophysical Research Letters 38.

Qin, X., Lei, L., He, Z., Zeng, Z.-C., Kawasaki, M., Ohashi, M., Matsumi, Y., 2015. Preliminary assessment of methane concentration variation observed by GOSAT in China. Advances in Meteorology 2015.

Rajab, J.M., MatJafri, M.Z., Lim, H.S., Abdullah, K., 2009. Satellite mapping of CO2 emission from forest fires in indonesia using AIRS measurements. Modern Applied Science 3, 68–75.

Reay, D., Smith, P., Amstel, A. van, 2010. Methane and Climate Change. Earthscan.

Schneising, O., Buchwitz, M., Reuter, M., Bovensmann, H., Burrows, J.P., Borsdorff, T., Deutscher, N.M., Feist, D.G., Griffith, D.W., Hase, F., 2019. A scientific algorithm to simultaneously retrieve carbon monoxide and methane from TROPOMI onboard Sentinel-5 Precursor. Atmospheric Measurement Techniques 12, 6771–6802.

Sen, P., Roy, M., Pal, P., 2016. Application of ARIMA for forecasting energy consumption and GHG emission: A case study of an Indian pig iron manufacturing organization. Energy 116, 1031–1038.

Smith, K.A., 2010. Nitrous Oxide and Climate Change. Earthscan.

Tan, K.C., Lim, H.S., Mat Jafri, M.Z., 2012. Carbon dioxide distribution over Peninsular Malaysia from Scanning Imaging Absorption Spectrometer for Atmospheric Cartography (SCIAMACHY), in: 2012 International Conference on Computer and Communication Engineering (ICCCE). Presented at the 2012 International Conference on Computer and Communication Engineering (ICCCE), pp. 354–357. https://doi.org/10.1109/ICCCE.2012.6271210

TAR Climate Change 2001: Impacts, Adaptation, and Vulnerability — IPCC, n.d. URL https://www.ipcc.ch/report/ar3/wg2/ (accessed 1.30.20).

ul-Haq, Z., Tariq, S., Ali, M., 2017. Spatiotemporal assessment of CO2 emissions and its satellite remote sensing over Pakistan and neighboring regions. Journal of Atmospheric and Solar-Terrestrial Physics 152–153, 11–19. https://doi.org/10.1016/j.jastp.2016.11.001

Varon, D.J., Jervis, D., McKeever, J., Spence, I., Gains, D., Jacob, D.J., 2021. High-frequency monitoring of anomalous methane point sources with multispectral Sentinel-2 satellite observations. Atmospheric Measurement Techniques 14, 2771–2785.

Wang, K., Jiang, H., Zhang, X., Zhou, G., 2011. Analysis of spatial and temporal variations of carbon dioxide over China using SCIAMACHY satellite observations during 2003–2005. International Journal of Remote Sensing 32, 815–832. https://doi.org/10.1080/01431161.2010.517805

WDCGG (World Data Centre for Greenhous Gases) [WWW Document], n.d. URL https://gaw.kishou.go.jp/publications/global_mean_mole_fractions (accessed 1.30.20).

World Bank Open Data | Data [WWW Document], n.d. URL https://data.worldbank.org/ (accessed 4.7.20).

Zeng, Z.-C., Byrne, B., Gong, F.-Y., He, Z., Lei, L., 2021. Correlation between paddy rice growth and satellite-observed methane column abundance does not imply causation. Nature communications 12, 1–4.

Zhang, L., Jiang, H., Zhang, X., 2015. Comparison analysis of the global carbon dioxide concentration column derived from SCIAMACHY, AIRS, and GOSAT with surface station measurements. International Journal of Remote Sensing 36, 1406–1423. https://doi.org/10.1080/01431161.2015.1009656